2021-03

DOCTORAL DISSERTATION ON THE RELATIONSHIP BETWEEN SAMPLED-DATA MODELS, NUMERICAL INTEGRATION AND INTERPOLATIO

SÁNCHEZ QUINTERO, CLAUDIA

UNIVERSIDAD TÉCNICA FEDERICO SANTA MARÍA
DEPARTMENT OF ELECTRONIC ENGINEERING

DOCTORAL DISSERTATION
ON THE RELATIONSHIP BETWEEN SAMPLED-DATA MODELS, NUMERICAL INTEGRATION AND INTERPOLATION

CLAUDIA SÁNCHEZ QUINTERO

DOCTORATE PROGRAM
DOCTORATE IN ELECTRONIC ENGINEERING

THESIS SUPERVISOR	:	PROF. JUAN YUZ EISSMANN
EVALUATION COMMITTEE	:	PROF. JUAN YUZ EISSMANN
	:	PROF. JUAN CARLOS AGÜERO
	:	PROF. DANIEL SBARBARO

MARCH 2021

VALPARAÍSO-CHILE

A Levi y Augusto

"El tamaño de una satisfacción no lo puede medir sino el que la alcanza"

Arturo Uslar Pietri

RESUMEN

En general, la representación de sistemas de tiempo continuo se realiza mediante ecuaciones diferenciales lineales o no lineales. Actualmente, los dispositivos digitales, que solo operan en tiempo discreto, son los encargados de interactuar con los sistemas de tiempo continuo. Por lo tanto, los modelos muestreados son necesarios. La precisión de estos modelos depende, entre otras cosas, del método numérico utilizado para resolver la ecuación diferencial. Entonces, siguiendo la idea anterior, el interés es estudiar el efecto del comportamiento entre muestras de las señales y del método de integración numérica aplicado sobre el modelo de tiempo discreto resultante.

Las suposiciones hechas o el conocimiento que se tiene sobre las señales juega un papel esencial en el modelo de datos muestreados obtenido. En particular, la entrada al sistema generalmente se considera constante entre muestras, es decir, que es generada por un retentor de orden cero. Sin embargo, se pueden emplear dispositivos de orden superior para definir la entrada. Por ejemplo, las funciones B-spline se pueden usar en el retentor como una función de interpolación para modelar la suavidad de la entrada del sistema.

Por otro lado, la representación exacta de modelos de datos muestreados para sistemas de tiempo continuo no siempre está disponible. Por lo tanto, se desarrollan modelos aproximados, considerando que la estrategia de integración aplicada impacta directamente en el modelo de datos muestreados obtenido. En el caso lineal, aparecen ceros adicionales debido al proceso de muestreo. La ubicación de estos ceros de muestreo se puede caracterizar cuando el período de muestreo tiende a cero. Además, el interés es extender estos resultados a una clase de sistemas no lineales escritos en forma normal.

En esta tesis establece la relación entre la interpolación, la estrategía de integración numérica y los modelos de datos muestreados para sistemas lineales y no lineales. Específicamente, se estudia el impacto del retentor basado en funciones B-spline y los métodos numéricos, tales como Runge-Kutta o series de Taylor truncadas, en la caracterización asintótica de los ceros de muestreo, para el caso lineal, y las dinámicas cero para sistemas no lineales. La precisión de los modelos aproximados obtenidos se mide utilizando el error relativo y el error de truncamiento local para sistemas lineales y no lineales, respectivamente. Además, exploramos cómo explotar los modelos de datos muestreados aproximados para el diseño de una ley de control de tiempo discreto universal para sistemas lineales estables.

ABSTRACT

In general, the representation of continuous-time systems is made through linear or nonlinear differential equations. Nowadays, digital devices, which can only operate in the discrete-time domain, perform the interaction with continuous-time systems. Therefore, sampled-data models are needed. The accuracy of these models depends, among other things, on the numerical method applied to solve the equation. Following the above idea, the interest is to study the effect of the signals' intersample behavior and the numerical integration on the resulting discrete-time model.

Knowledge or assumptions made on the signals play an essential role in the obtained sampled-data model. In particular, the input to the system is usually considered to be piecewise constant, i.e., generated by a zero-order hold. However, higher-order devices can be used to define the input. For example, B-spline functions can also be used in the hold device as an interpolating function to model the smoothness of the system input.

On the other hand, the exact representation of sampled-data models for continuous-time systems is not always available. Hence, approximate models are developed, considering that the applied integration strategy directly impacts the obtained sampled-data model. In the linear case, extra zeros appear due to the sampling process. The location of these sampling zeros can be characterized as the sampling period approaches zero. Furthermore, the interest is to extend these results to a class of nonlinear systems written in normal form.

This thesis establishes the relationship between interpolation, numerical integration, and sampled-data models for linear and nonlinear systems. To be specific, we study the impact of the B-spline generalized hold and numerical methods such as Runge-Kutta or Truncated Taylor Series expansion on the asymptotic characterization of the sampling zero polynomial for the linear case and the sampling zero dynamics for nonlinear systems. The accuracy of the approximate models obtained is measured by using the relative error and the local truncation error for linear and nonlinear systems, respectively. Moreover, we explore how to exploit the approximate sampled-data models for the design of a universal discrete-time control law for stably linear systems.

Contents

1 INTRODUCTION

1.1 Sampling and Sampled-Data Models

Most of real processes evolve in continuous-time. In practice, for control or system identification, it may be useful to discretize them. Therefore, sampling and sampled-data models have been investigated for linear and nonlinear deterministic systems [1–10] and linear and nonlinear stochastic representations [2, 11–16].

A sampled-data model is assembled by a continuous-time system interfaced by a digital/analog converter and an analog/digital sensor. Typically, the sampling process is represented, as shown in Figure 1.1 [17]. This kind of hybrid system and the associated discrete-time model are used in control, parameter estimation and simulation [2].

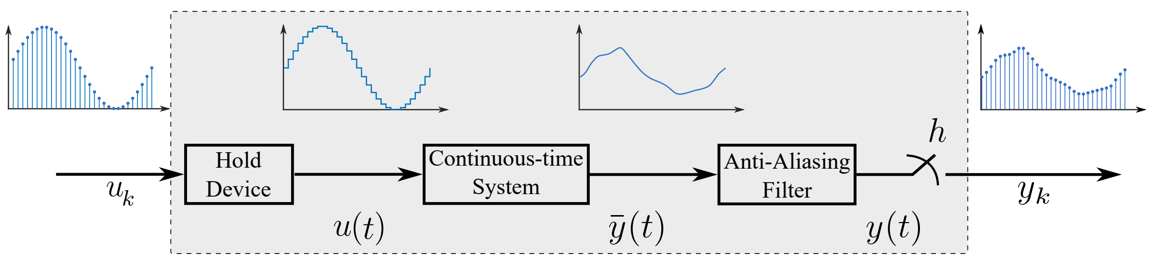

Figure 1.1: Scheme of a sampled-data system

The elements of a sampled-data systems are shown in Figure 1.1: the hold device, which is used to convert the discrete-time sequence $\{u_k\}$ into a continuous-time input $u(t)$. The plant, which defines the real system through a set of linear or nonlinear differential equations. Then, the output $\bar{y}(t)$ is processed, before taking samples, by an anti-aliasing filter. Finally, the sampler device, that creates a discrete-time sequence $\{y_k\}$ by instantaneous sampling at specific time instants $\{t_k\}$ with sampling period h [2, 17].

Typically, discrete-time systems are represented in the z-domain using the shift operator q, given by

$$qu_k = u_{k+1}. \tag{1.1}$$

and the poles p_i of the continuous-time are mapped to the discrete-time domain as follows,

$$z_i = e^{hp_i} \tag{1.2}$$

The above idea reflects that, for a small sampling period, the poles of the sampled-data model tends to the marginal location $z = 1$. Besides, for continuous-time systems with relative degree greater than or equal to two, the zeros that appear due to the sampling process converge, as the sampling rate approaches zero, to either marginally stable or unstable locations, i.e., for the fast sampling case, shift operator models cannot be directly related to the continuous-time model.

As a consequence, one could be interested in studying representations in the γ-domain, using the delta operator δ [1, 18–20] defined in (1.3) because for high sampling periods, there is a close relation to the continuous-time domain (1.4). This alternative representation presents convergence and numerical advantages over shift operator models [19, 21, 22].

$$\delta = \frac{q-1}{h} \implies \gamma = \frac{z-1}{h} \tag{1.3}$$

$$\delta u_k = \frac{u_{k+1} - u_k}{h} \tag{1.4}$$

$$\delta u_k \approx \left.\frac{du(t)}{dt}\right|_{u(t)=u_k}; \quad h \approx 0 \tag{1.5}$$

Based on (1.4), models in z-domain and γ-domain are related as follows:

$$Y_q(z) = \left.\frac{1}{h} Y_\delta(\gamma)\right|_{\gamma = \frac{z-1}{h}}, \tag{1.6}$$

$$Y_\delta(\gamma) = \left. hY_q(z)\right|_{z = h\gamma+1}. \tag{1.7}$$

The stability region of models in the shift operator is a circle of radius 1, whilst the stability region corresponding to δ-operator models is a circle of radius $1/h$ as shown in Figure 1.2. In addition, the poles in the δ-operator are given by

$$\gamma_i = \frac{e^{hp_i} - 1}{h}. \tag{1.8}$$

The above idea implies that when using incremental models in the γ-domain, the discrete-time poles converge to locations that depend on h and, as the sampling period approaches to zero, they converge to the corresponding continuous-time poles. Since incremental models provide a close connection between continuous and discrete-time domains, this kind of representation may be useful in applications such as control [21–26].

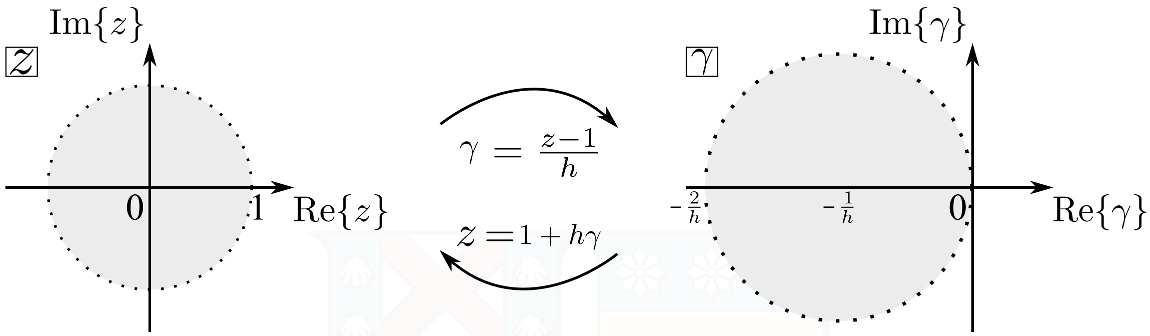

Figure 1.2: Comparison of the stability regions when using the shift operator q and the incremental operator δ.

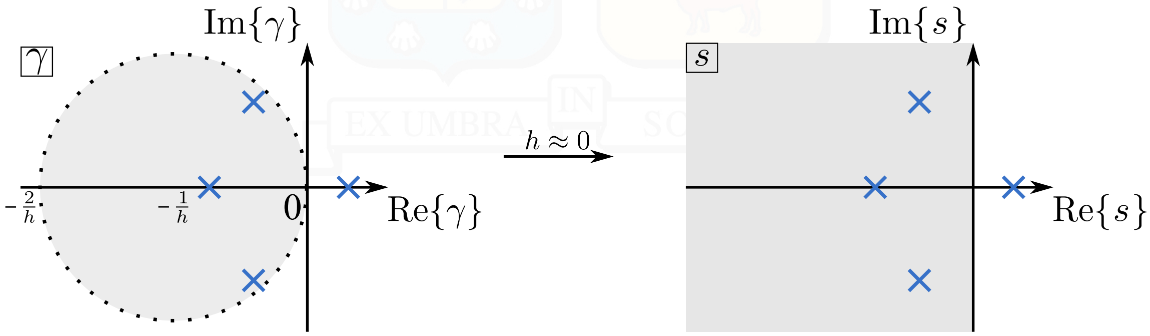

Figure 1.3: Comparison of the stability regions for discrete-time models and continuous-time models.

Notice that there is a direct transformation between the continuous-time poles p_i and their discrete-time counterpart (1.2)-(1.8). However, for the continuous-time zeros, we only have a simple transformation when the sampling period approaches zero [27]. Hence, in [28], a novel relationship between real and sampled-data zeros, independent of the sampling period, is proposed. On the other hand, non-uniform sampling has been considered in [29–31]. In addition, poles and zeros can be transformed into the z-domain using the matched pole-zero method (MPZ) [32, 33]. The MPZ mapped all the poles and zeros as shown in (1.2). The later technique turns out to be simpler than other methods frequently applied, and it is preferred for the discrete-time approximation of continuous-time controllers [34, 35].

The sampling process naturally implies loss of information. For linear systems, it is possible to obtain the exact sampled-data model as long as one makes appropriate assumptions on the nature of the signals. The usual assumption about the input to the system is that, between samples, it behaves piecewise constant, i.e., it is generated by a zero-order hold (ZOH).

On the other hand, approximate models may be preferred because they are related more directly to the parameters of the real system, they can be easier to obtain than the exact sampled-data model, they may require fewer computations and they are a consequence of the applied integration strategy [36]. Thus, approximate models may give further insights about the discretization process. As a consequence, the analysis of the accuracy of approximate discrete-time models is needed. In particular, for the linear case,it is measured using the relative error in frequency domain [36–38].

The nonlinear sampled-data theory is less developed compared to the linear case since it implies difficulties in solving nonlinear differential equations. The exact model typically cannot be developed. Thus, the goal is to obtain approximate models that are accurate in some sense. Then, the accuracy of such models depends on the applied integration strategy, which can be affected by the assumptions made on the smoothness of the input. Similarly to the linear case, there is an interest in quantifying the accuracy of these models using the local truncation error in the time domain [39–43].

Besides, the intersample behavior of the input can be modeled by higher-order hold devices. For example, B-splines functions can be used in a generalized hold with this aim. Therefore, it is possible to analyze the impact of such selection in the resulting sampled-data model. In particular, we expect to provide further insights into the discretization process: how the smoothness of the input signal and the applied integration strategy could impact in the asymptotic sampling zero polynomials, for the linear case, and in the asymptotic zero dynamics, for nonlinear systems.

1.2 Problem Statement

In the current thesis, we focus on developing sampled-data models for linear and nonlinear systems. The aim is to study issues such as the link between the corresponding discrete-time model, the smoothness of the signals, and the applied numerical integration method. The accuracy of the obtained approximate models and the asymptotic relation between linear and nonlinear sampled-data models is also studied. Besides, we explore the use of discrete-time linear models for the design of a simple control law.

This thesis addresses the following hypotheses:

- Accurate sampled-data models can be obtained for continuous-time dynamical systems, under assumptions or knowledge about the signals.
- Extra zeros and zero dynamics that appear in the discrete-time model as a consequence of the sampling process can be interpreted due to the plant's characteristics, the interpolation assumptions, and the applied numerical integration techniques.
- It is possible to establish a relationship between the hold used to generate the continuous-time input and the integration strategy proposed.
- It is possible to design a wide-bandwidth control law for stably invertible linear system based only on the continuous-time relative degree and high-frequency gain.

1.3 Objectives

This project's primary goal is to study the relationship between sampled-data models, numerical integration, and interpolation. The specific objectives are the following:

1. To express the generalized hold in terms of B-splines functions.

   We consider the case when only the discrete-time input sequence is known. Thus, the smoothness of the continuous-time system input is, in principle, unknown. In this case, B-spline functions can be used in the generalized hold to model the input or to describe an assumption about its intersample behavior.

2. To establish the connection between the interpolation assumption and the presence of sampling zeros and sampling zero dynamics.

   The interest is to characterize the sampling zeros (for linear systems) and the zero dynamics (in the case of nonlinear systems), as the sampling period approaches zero, for different interpolation assumptions.

3. To establish the link between numerical integration techniques and the obtained approximate sampled-data models.

   The interest is to evaluate the impact of the numerical integration in the discrete-time model. In this context, time-discretization when using numerical methods such as Runge-Kutta or Truncated Taylor series expansion allows to gain further insights into the sampling process, and both can be applied for linear and nonlinear systems.

4. To explore how to exploit approximate sampled-data models in the design of a linear discrete-time control law.

   Our interest here is to design a control law that stabilizes the real system by knowing only the relative degree and the continuous-time system's high-frequency gain. Moreover, we expect to analyze the impact of including, or not, knowledge about the asymptotic sampling zeros in the feedback law.

1.4 Thesis Organization and Contributions

Following the ideas presented above, the current thesis gives further insights about the discretization process for linear and nonlinear systems. It can be separated into two parts: the former covers sampled-data models for linear systems, while the latter extends the nonlinear case results. The structure of the thesis is as follows:

Chapter 1: In this chapter, we present the thesis overview: motivation, hypothesis and objectives. Also, a brief description of the main contribution is given.

Chapter 2: In this chapter, a literature review is presented. We first introduce different hold devices frequently used to model the continuous-time input to the system. Then, a background on B-Spline Functions and their relationship with the well-known Euler-Frobenius polynomials is given. Then, based on the holders previously defined, we present the most common representations of discrete-time models under different input signal assumptions. Moreover, for the linear case, the exact sampled-data model is given. In particular, we study the zeros (linear case) and zero dynamics (nonlinear case) of the corresponding sampled-data models for fast sampling rates.

Chapter 3: We begin this chapter by presenting **a novel equivalence for a B-spline generalized hold**, which will be used to model the input to the system for linear and nonlinear models. One of the advantages is that this hold provides different assumptions about the input smoothness since it is defined based on B-spline functions. In fact, it can be interpreted, for example, as zero, first or second-order hold when varying the order of the spline. Moreover, this hold is shown to be related to the well-known Euler-Frobenius polynomials, which will be useful in the asymptotic characterization of sampling zeros and zero dynamics.

Then, **we develop exact and approximate (linear) discrete-time models when using Runge-Kutta methods as an integration strategy.** We first consider the case when the expansion order is greater than or equal to the continuous-time relative degree r and hold order ℓ. Then, the exact sampled-data model turns out to be obtained. On the other hand, we consider the case when the expansion order is lower than $r+\ell$, leading to an approximate model. **For both models, the polynomial of the sampling zeros are asymptotically characterized for fast sampling rates**. Finally, a simulation study is presented to quantify the relative error in the frequency domain between the exact and the approximate model.

Chapter 4: In this chapter we propose **a simple sampled-data control law based only on the continuous-time relative degree and high-frequency gain**. We first analyze the continuous-time case to set ideas. Then, we extend the results to the discrete-time domain where two approximate models are studied: the first model is designed considering that the closed-loop bandwidth is chosen to be significantly less than the Nyquist rate. In contrast, the second model covers the case when the closed-loop bandwidth is near the Nyquist frequency.

Chapter 5: In this chapter, we study a class of nonlinear systems that can be written in normal form. Thus, **we develop an approximate sampled-data model based on the B-Spline generalized hold and using truncated Taylor series expansions as a numerical method**. The corresponding discrete-time system includes extra zero dynamics that can be characterized as the sampling period approaches zero. **In fact, it is shown that for fast sampling rates, the asymptotic zero dynamics converge to the asymptotic sampling zeros found in the linear case. Moreover, we study the model's accuracy through the local truncation error associated with the state vector**.

Chapter 6: This chapter details the conclusion of the current research work, summarizes the contributions of the thesis and present some possible ideas for future work.

1.5 Associated Publications

The results presented in this thesis have been published in journal and conference papers as listed bellow:

- Journal Papers:

  1. C. Sánchez and J.I. Yuz, «On the relationship between spline interpolation, sampling zeros and numerical integration in sampled-data models,» Control & System Letters, vol. 128, pp. 1-8, 2019.
     `doi:10.1016/j.sysconle.2019.04.006`.
  2. C. Sánchez and J.I. Yuz, «Approximate Nonlinear Discrete-Time Models Based on B-Spline Functions», IEEE Access, vol. 8, pp. 143366-143374, 2020.
     `doi:10.1109/ACCESS.2020.3013829`

- Conference Papers:

  1. C. Sánchez y J.I. Yuz, «B-spline Generalized Hold for Nonlinear Sampled-Data Systems,» 58th IEEE Conference on Decision and Control (CDC), 2019.
  2. C. Sánchez, G.C. Godwin, J.I. Yuz, M. Serón y D. Carrasco, «Towards a Simple Sampled-Data Control Law for Stably Invertible Linear Systems,» IFAC World Congress, 2020.

2 | LITERATURE REVIEW

2.1 Continuous-Time Linear Systems

We are interested in obtaining the sampled-data version of the linear single-input single-output (SISO) system given in (2.1).

$$G(s) = \frac{B(s)}{A(s)} = b\frac{(s-z_1)\cdots(s-z_m)}{(s-p_1)\cdots(s-p_n)}; \quad n > m, \tag{2.1}$$

where the roots of z_i and p_j are the continuous-time zeros and poles, respectively, and $r = n - m$ is the relative degree. The system (2.1) can be written in state-space from as

$$\dot{x}(t) = Ax(t) + Bu(t) \tag{2.2a}$$
$$y(t) = Cx(t), \tag{2.2b}$$

where $x(t)$ denotes the system state vector and the matrices are of appropriate dimensions. Thus, the system transfer function is given by

$$G(s) = \frac{\mathcal{L}\{y(t)\}}{\mathcal{L}\{u(t)\}} = \frac{Y(s)}{U(s)}, \tag{2.3}$$

where $\mathcal{L}\{\cdot\}$ is the Laplace transform defined as follows [44, 45]:

$$\mathcal{L}\{f(t)\} = \int_0^\infty f(t)e^{-st}dt = F(s) \tag{2.4}$$

and the inverse Laplace transform is given by

$$\mathcal{L}^{-1}\{F(s)\} = \frac{1}{2\pi j}\int_{\sigma-j\infty}^{\sigma+j\infty} F(s)e^{st}ds \tag{2.5}$$

Then, the system transfer function (2.3) can also be represented as:

$$G(s) = C(sI-A)^{-1}B \tag{2.6}$$
$$= \frac{C\text{adj}(sI-A)B}{\det(sI-A)}. \tag{2.7}$$

The zeros of (2.7) can also be written as [46, 47]

$$N(s) = \det \begin{bmatrix} sI - A & -B \\ C & 0 \end{bmatrix}. \tag{2.8}$$

Equation (2.8) will be a key tool in the following chapters.

2.2 The Hold Device

The process of discretization depends on knowledge or assumptions about the intersample behavior of the signals, because these are in principle unknown. In particular, the interpolating function chosen to model the system input plays a key role in the discrete-time model. On the other hand, the corresponding sampled-data model includes extra zeros (linear systems) or zero dynamics (nonlinear case) with no counterpart in the continuous-time domain. Thus, there is an interest in studying the impact of the hold device in the location of these sampling zeros and sampling zero dynamics.

The usual assumption is that, between samples, the signal is piecewise constant, i.e., is generated by a zero-order hold (ZOH) (see Figure 2.1), defined by

$$u(t) = u_k; \qquad t \in [kh, kh + h[\tag{2.9}$$

where $t_k = kh$ is the sampling instant, h is the sampling period and we have used the notation $u(kh) = u_k$.

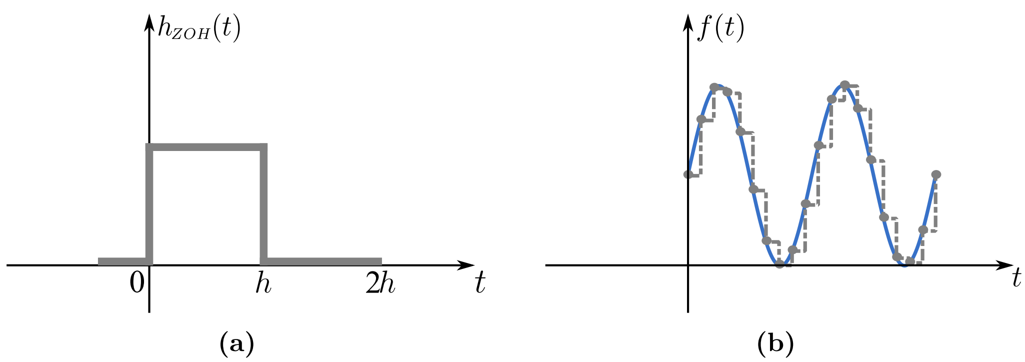

Figure 2.1: Impulse response for a Zero-Order Hold (Figure 2.1a) and a piecewise constant signal (Figure 2.1b).

Under the ZOH assumption, the discrete-time zeros may converge to either marginally stable or unstable locations. Thus, one can be interested in studying the effect of higher-order hold devices, such as first-order hold (FOH) and fractional-order hold (FROH). The FOH is defined by:

$$u(t) = u_k + \frac{u_k - u_{k-1}}{h}(t - kh); \qquad t \in [kh, kh + h[\tag{2.10}$$

$$u(t) = u_{k-1} + \frac{u_k - u_{k-1}}{h}(t - kh); \qquad t \in [kh, kh + h[\tag{2.11}$$

where the first device is based on a linear *extrapolation* and the second on a linear *interpolation* [48, 49]. According to [48], when using second or higher-order systems, the interpolating FOH provides a smoother output than the extrapolating FOH and the ZOH. Otherwise, both FOHs have shown to improve the ZOH since the output is smooth and has a frequency response without phase error.

A FROH [50, 51] is given by

$$u(t) = u_k + \beta\frac{u_k - u_{k-1}}{h}(t - kh); \qquad t \in [kh, kh + h[\tag{2.12}$$

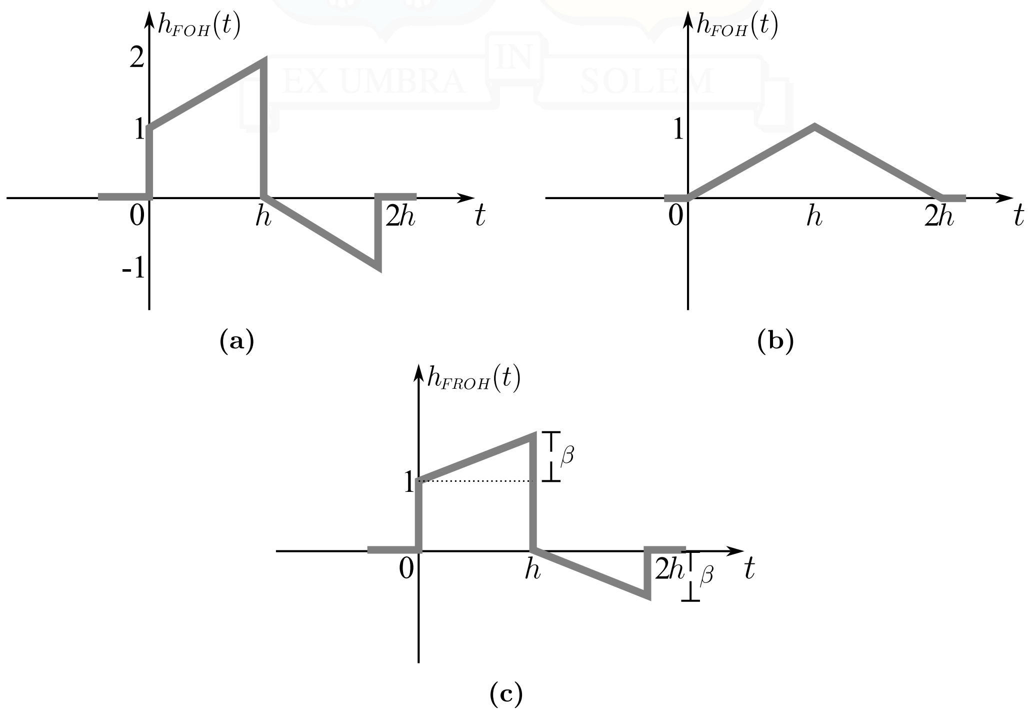

Figure 2.2: Impulse response for: Extrapolating First Order Hold (Figure 2.2a), Interpolating First Order Hold (Figure 2.2b) and Fractional-Order Hold (Figure 2.2c).

Notice that if the parameter β is chosen to be 0, $u(t)$ corresponds to the ZOH and for $\beta = 1$ it turns out to be the extrapolating FOH. It is also of interest to consider the Laplace transform (2.4) of the hold devices (2.9),(2.10) and (2.12):

$$H_{\text{ZOH}}(s) = \frac{1 - e^{-sh}}{s} \tag{2.13a}$$

$$H_{\text{FOH}}(s) = (1 - e^{-sh})^2 \frac{(1 + sh)}{hs^2} \tag{2.13b}$$

$$H_{\text{FROH}}(s) = (1 - \beta e^{-sh})\frac{1 - e^{-sh}}{s} + \frac{\beta}{hs^2}\left(1 - e^{-sh}\right)^2 \tag{2.13c}$$

Other hold devices are based on the traditional holds previously defined to improve the sampled-data model's stability or accuracy. For example, in [52], a mixed fractional order (MFROH) is defined as a combination of FROH and ZOH given by

$$u(t) = \begin{cases} u_k + \alpha \dfrac{u_k - u_{k-1}}{h}(t - kh); & t \in [kh, kh + \Delta h] \\ u_k + \alpha \dfrac{u_k - u_{k-1}}{h}(\Delta h); & t \in [kh + \Delta h, kh + h], \quad 0 \leq \Delta \leq 1, \end{cases} \tag{2.14}$$

where α is a parameter of the hold slope in the interval $[kh, hk + \Delta h]$ and Δ is a parameter describing the position of slope variation over the interval $[kh, kh+\Delta h]$ [52]. Also, its Laplace transform is given by

$$H_{MFROH}(s) = \frac{(1 - e^{-sh})(1 - \alpha\Delta e^{-sh})}{s} + \alpha \frac{(1 - e^{-sh})(1 - e^{-s\Delta h})}{hs^2} \tag{2.15}$$

Notice that for $\Delta = 0$, $u(t)$ corresponds to the ZOH and for $\Delta = 1$ it corresponds to the FROH. In [53, 54] the input is considered to be generated by a backward triangle sample and hold (BTSH), which is a modification of the ZOH and is defined as follows

$$u(t) = \begin{cases} \dfrac{\bar{u}(t)}{fh}(t - kh); & t \in]kh, kh + fh] \\ 0; & t \in]kh + fh, kh + h], \end{cases} \tag{2.16}$$

where $\bar{u}(t)$ is the ZOH (2.9) and $f \in]0, 1]$. Then, the Laplace transform of (2.16) is given by

$$H_{BTSH}(s) = \frac{1 - e^{-shf}}{s}\left(\frac{1}{shf} - \frac{k}{f}\right) - \frac{e^{-shf}}{s} \tag{2.17}$$

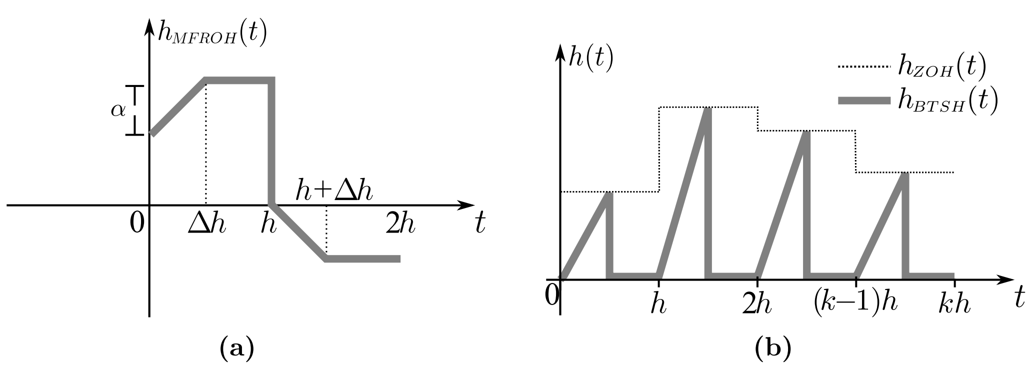

Figure 2.3: Impulse response for: Mixed Fractional Order Hold (Figure 2.3a) and Backward Triangle Sampled and Hold (Figure 2.2c).

To conclude this section we present a more general hold device than the one previous described, namely, a Generalized Hold Functions (GHF) [55–63]. A generalized hold can be characterized by its impulse response, which is the continuous-time output obtained when the discrete-time input is the Kronecker delta $\delta_K[k]$ [1,55].

$$\delta_K[k] = \begin{cases} 1 & k = 0 \\ 0 & \text{Otherwise.} \end{cases} \tag{2.18}$$

Then, the continuous-time signal generated by this hold device is given by [2]

$$u(t) = \sum_{k=-\infty}^{\infty} h_g(t - kh)u_k, \tag{2.19}$$

where $h_g(t)$ is the impulse response, given by [2,60]

$$h_g(t) = \begin{cases} 1 & t \in [0, h[\\ 0 & \text{Otherwise.} \end{cases} \tag{2.20}$$

In fact, ZOH and FOH can be thought of as a particular cases of this hold [2]. As mentioned before, the sampling zeros are function of the hold used to model the input system and they may converge to unstable locations. Thus, GHF can be used to assign these zeros to stable locations whether or not the continuous-time system has non-minimum phase zeros [61].

In [57] a GHF that places sampling zeros to the origin is proposed. Moreover, in [60] a GHF is used to protect cyber-physical system from the zero dynamics attack which remains effective if the system in non-minimum phase. However, changing the location of the zeros can imply an excessively large amplitude of the hold device [61]. In addition, using GHF can lead to sensitivity and robustness difficulties [59,64].

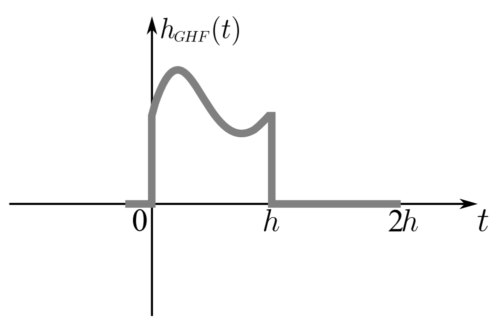

Figure 2.4: Impulse response for a Generalized Hold Functions.

Following the ideas above, one could be interested in designing a generalized hold to represent assumptions or additional knowledge about the input's smoothness. B-splines have been used with this aim (see, for example, [58,65]). In this thesis, we are interested in studying the impact of B-spline generalized hold in the corresponding sampled-data model. Firstly, we introduce the Euler-Frobenius Polynomials, which are defined in the z-domain through the $\mathcal{Z}$- transform (see, for example, [5,66]):

$$\mathcal{Z}\{f(t)\} = \sum_{t=0}^{\infty} f(t)z^{-t} = F(z), \tag{2.21}$$

while the inverse $\mathcal{Z}$-transform is given by

$$\mathcal{Z}^{-1}\{F(z)\} = \frac{1}{2\pi j}\oint_{\Gamma} F(z)z^{t-1}dz. \tag{2.22}$$

2.2.1 Euler-Frobenius Polynomials

The Euler-Frobenius polynomials are defined as follows

$$B_p(z) = b_1^p z^{p-1} + b_2^p z^{p-2} + \cdots + b_p^p;\ p \geq 1 \tag{2.23}$$

$$b_k^p = \sum_{l=1}^{k} (-1)^{k-l} l^p \binom{p+1}{k-l};\ k = 1, \ldots, p \tag{2.24}$$

Moreover, they satisfy several properties [2,27,58,67], as listed below

- The coefficients can be calculated recursively. In fact, $b_1^p = b_k^p = 1$ and

$$b_k^p = k b_k^{p-1} + (n-k+1) b_{k-1}^{p-1}; \quad k \geq 2. \tag{2.25}$$

- They satisfy the following differential relation

$$B_{p+1}(z) = z(1-z)\frac{dB_r(z)}{dz} + (1+pz)B_p(z); \quad r > 1. \tag{2.26}$$

- They coefficients are symmetrical

$$b_k^p = b_{p+1-k}^p, \tag{2.27}$$

and they satisfy

$$B_p(z_0) = 0 \implies B_p(z_0^{-1}) = 0 \tag{2.28}$$

$$B_p(z) = z^{p-1} B_p(z^{-1}). \tag{2.29}$$

We next list the first Euler-Frobenius polynomials

$$B_1(z) = 1 \tag{2.30a}$$

$$B_2(z) = z + 1 \tag{2.30b}$$

$$B_3(z) = z^2 + 4z + 1 \tag{2.30c}$$

$$B_4(z) = z^3 + 11z^2 + 11z + 1. \tag{2.30d}$$

From (2.30) we can notice that $B_p(z)$ has marginally stable and unstable zeros for $p \geq 2$. This polynomials will be useful in the characterization of the asymptotic sampling zeros and asymptotic zero dynamics in Chapters 3 and 5.

2.2.2 Background on B-Spline Functions

B-splines [68–70] are piecewise polynomials functions that are usually smooth, well-behaved, and continuous everywhere [71]. Moreover, they have minimal support, i.e., they vanish outside the interval $[t_i, t_{i+k}[$, and they are positive on the interior of such interval [69].

B-splines are defined for the nondecreasing *knot sequence* $\{t_1, t_2, \dots\}$ at the sampling instants $\{kh\}$. These functions have been used for interpolation, signal processing, and image reconstruction [71] to identify continuous-time systems based on non-uniform sampled data [30]. In fact, in [72] a relationship between B-splines and control theory is established.

An ℓ-th order B-spline is defined as follows

$$\beta_\ell(t) = \sum_{p=0}^{\ell+1} \frac{(-1)^p}{\ell!} \binom{\ell+1}{p} (t-ph)^\ell \mu(t-ph). \tag{2.31}$$

where $\mu(t)$ is the unit step function:

$$\mu(t) = \begin{cases} 0 & t < 0 \\ 1 & t \geq 0. \end{cases} \tag{2.32}$$

In order to prevent the ℓ-th order B-spline to go 0 as the sampling period is reduced, a scaling factor $1/h^\ell$ is included. Thus, we define $\tilde{\beta}_\ell(kh) = \frac{1}{h^\ell}\beta_\ell(kh)$. Then, the first B-splines are given by

$$\tilde{\beta}_0(t) = \mu(t) - \mu(t-h) \tag{2.33a}$$

$$\tilde{\beta}_1(t) = \frac{1}{h}\Big(t\mu(t) - 2(t-h)\mu(t-h) + (t-2h)\mu(t-2h)\Big) \tag{2.33b}$$

$$\tilde{\beta}_2(t) = \frac{1}{h^2}\Big(\frac{1}{2}t^2\mu(t) - \frac{3}{2}(t-h)^2\mu(t-h) + \frac{3}{2}(t-2h)^2\mu(t-2h) - \frac{1}{2}(t-3h)^2\mu(t-3h)\Big) \tag{2.33c}$$

Figure 2.5 shows the B-splines functions defined above. Moreover, in [30, 73] it is shown that B-spline functions are related to the Euler-Frobenius polynomials, i.e.,

$$\mathcal{Z}\left\{\beta_\ell(kh)\right\} = \frac{h^\ell}{\ell!}\frac{B_\ell(z^{-1})}{z} \tag{2.34}$$

where $B_\ell(z)$ is the Euler-Frobenius polynomial of order ℓ, given by (2.23)–(2.24).

Lemma 2.1 *[105]: Consider the B-spline of order ℓ defined in* (2.31)*. The i-th derivative is given by*

$$\frac{d^i}{dt^i}\tilde{\beta}_\ell(t) = \frac{1}{h^i}\sum_{j=0}^{i}(-1)^j\binom{i}{j}\tilde{\beta}_{(\ell-i)}(t-jh);\ i \leq \ell. \tag{2.35}$$

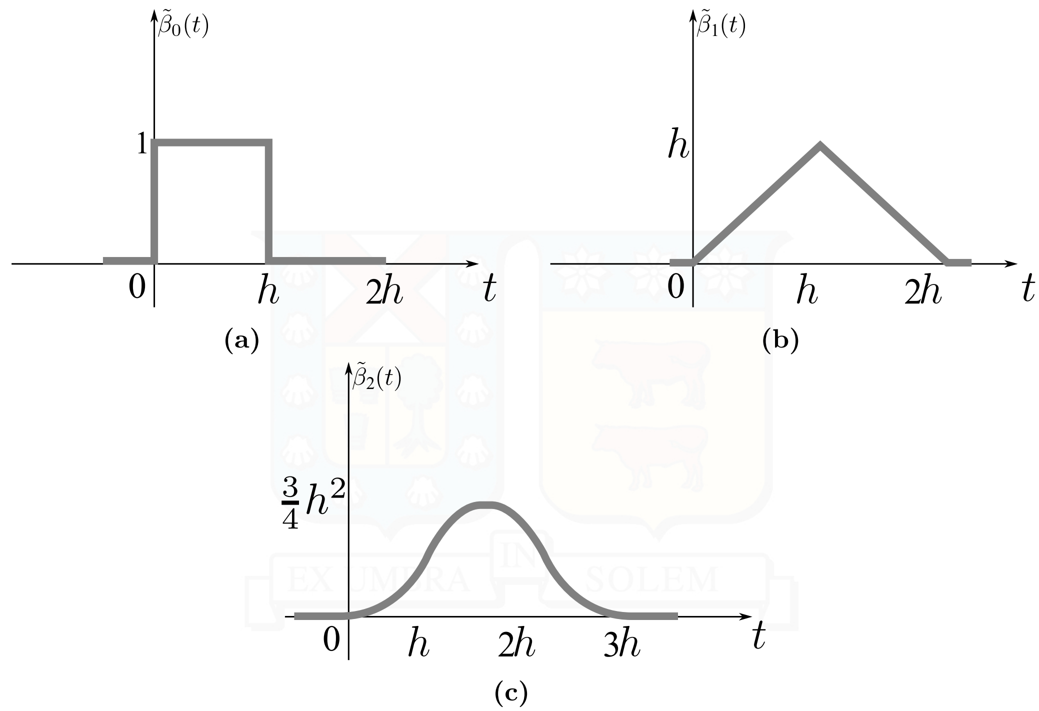

Figure 2.5: Some B-splines functions: Zero-order B-spline (Figure 2.5a) First-order B-spline (Figure 2.5b) and Second-order B-spline (Figure 2.5c).

Proof: Firstly, we consider the following definition:

$$\mathcal{B}_\ell(s) = \mathcal{L}\left\{\tilde{\beta}_\ell(t)\right\} = \frac{1}{h^\ell}\left(\mathcal{B}_0(s)\right)^{\ell+1}, \tag{2.36}$$

where $\mathcal{B}_0(s)$ is the Laplace transform of (2.33a), i.e., the Laplace transform in (2.13a). Then, we consider the convolution property [58, 65]:

$$\tilde{\beta}_\ell(t) = \frac{1}{h}\tilde{\beta}_{\ell-1}(t) * \tilde{\beta}_0(t). \tag{2.37}$$

We establish the proof by induction. For $i = 0$ the result is trivial. Then, for $i = 1$ we have that the Laplace transform of the first derivative can be written as,

$$s\mathcal{B}_\ell(s) = \frac{1}{h}\mathcal{B}_{\ell-1}(s)(1 - e^{-sh}). \tag{2.38}$$

Applying the inverse Laplace transform to (2.38), we have

$$\frac{d}{dt}\tilde{\beta}_\ell(t) = \frac{1}{h}\left(\tilde{\beta}_{\ell-1}(t) - \tilde{\beta}_{\ell-1}(t-h)\right). \tag{2.39}$$

We now assume that (2.35) holds for i and we will prove that it also holds for

$i+1$. Using (2.35), we obtain

$$\frac{d^{i+1}}{dt^{i+1}}\tilde{\beta}_\ell(t) = \frac{1}{h^{i+1}}\sum_{j=0}^{i}(-1)^j\binom{i}{j}\tilde{\beta}_{(\ell-(i+1))}(t-jh) - \frac{1}{h^{i+1}}\sum_{j=0}^{i}(-1)^j\binom{i}{j}\tilde{\beta}_{\ell-(i+1)}(t-(j+1)h) \tag{2.40}$$

$$= \frac{1}{h^{i+1}}\sum_{j=0}^{i}(-1)^j\binom{i}{j}\tilde{\beta}_{(\ell-(i+1))}(t-jh) + \frac{1}{h^{i+1}}\sum_{j=1}^{i+1}(-1)^j\binom{i}{j-1}\tilde{\beta}_{(\ell-(i+1))}(t-jh) \tag{2.41}$$

$$\frac{d^{i+1}}{dt^{i+1}}\tilde{\beta}_\ell(t) = \frac{1}{h^{i+1}}\left(\tilde{\beta}_{(\ell-(i+1))}(t) + \tilde{\beta}_{(\ell-(i+1))}(t-(i+1)h)\right) + \frac{1}{h^{i+1}}\sum_{j=1}^{i+1}(-1)^j\left(\binom{i}{j}\tilde{\beta}_{(\ell-(i+1))}(t-jh) + \binom{i}{j-1}\tilde{\beta}_{(\ell-(i+1))}(t-jh)\right) \tag{2.42}$$

$$= \frac{1}{h^{i+1}}\sum_{j=0}^{i+1}\binom{i+1}{j}\tilde{\beta}_{(\ell-(i+1))}(t-jh), \tag{2.43}$$

which corresponds to the result in (2.35).

Lemma 2.2 *[58, 105]: Consider the derivatives defined in* (2.35)*, then the* $\mathcal{Z}$*-transform is given by*

$$\mathcal{Z}\left\{\frac{d^i}{dt^i}\left.\tilde{\beta}_\ell\right|_{t=kh}\right\} = \frac{1}{h^i}\frac{(z-1)^i}{z^\ell}\frac{B_{\ell-i}(z)}{(\ell-i)!};\quad i\leq\ell. \tag{2.44}$$

Proof: From (2.35), we have that

$$\mathcal{Z}\left\{\frac{d^i}{dt^i}\tilde{\beta}_\ell(kh)\right\} = \frac{1}{h^i}\sum_{k=0}^{\infty}\left[\sum_{j=0}^{i}(-1)^j\binom{i}{j}\tilde{\beta}_{\ell-i}\left(kh-jh\right)\right]z^{-k} \tag{2.45}$$

where we have used the definition of the $\mathcal{Z}$-transform. Then,

$$\mathcal{Z}\left\{\frac{d^i}{dt^i}\tilde{\beta}_\ell(kh)\right\} = \frac{1}{h^i}\sum_{j=0}^{i}\left[(-1)^j\binom{i}{j}\sum_{k=0}^{\infty}\tilde{\beta}_{\ell-i}\left(kh-jh\right)z^{-k}\right] \tag{2.46}$$

According to [30], the sum over k can be written as shown in (2.34). Then,

$$\mathcal{Z}\left\{\frac{d^i}{dt^i}\tilde{\beta}_\ell(kh)\right\} = \frac{1}{h^i}\frac{B_{\ell-i}(z)}{z^{\ell-i}(\ell-1)!}\sum_{j=0}^{i}(-1)^j\binom{i}{j}z^{-j}. \tag{2.47}$$

Finally, the result in (2.44) is obtained

$$\mathcal{Z}\left\{\frac{d^i}{dt^i}\tilde{\beta}_\ell(kh)\right\} = \frac{1}{h^i}\frac{(z-1)^i}{(\ell-i)!}\frac{B_{\ell-i}(z)}{z^\ell}. \tag{2.48}$$

2.3 Discrete-Time Linear Systems

This section presents a review of sampled-data models for linear systems under different hold device assumptions, i.e., ZOH, FOH, and FROH. In particular, we introduce some solutions and approaches made by other authors in both shift- and delta-operator. To conclude this section, we study the asymptotic behavior of the sampling zeros polynomials and their relationship with the Euler-Frobenius polynomials described in Subsection 2.2.1.

2.3.1 Shift Operator Models

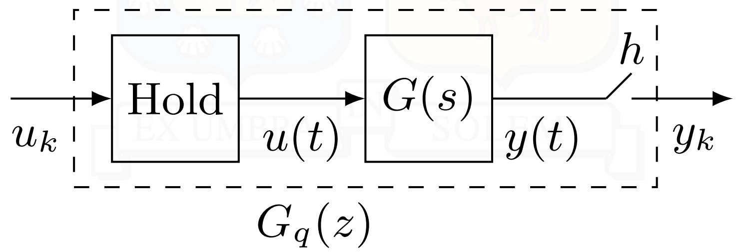

Figure 2.6: General scheme for a sampled-data model

Discrete-time models for linear systems can be obtained either from state-space representations or from transfer functions. The discrete-time function $G_q(z)$ that links the input samples $\{u_k\}$ with the output sequence $\{y_k\}$ is given by (see Figure 2.6)

$$G_q(z) = \frac{Y(z)}{U(z)} = \frac{\mathcal{Z}\{y_k\}}{\mathcal{Z}\{u_k\}}, \tag{2.49}$$

where $\mathcal{Z}\{\cdot\}$ denotes the transform in the z-domain.

We consider that $u(t)$ is generated by a ZOH. To compute the transfer function, we need the $\mathcal{Z}$-transform of $Y(s) = G(s)U(s)$. Thus, we apply the inverse Laplace transform ($\mathcal{L}^{-1}\{\cdot\}$) to $Y(s)$ and then the $\mathcal{Z}$-transform of the sequences $\{y(kh)\}$, $\{u(kh)\}$.

$$G_{ZOH}(z) = \frac{\mathcal{Z}\{y_k\}}{\mathcal{Z}\{u_k\}} = \frac{\mathcal{Z}\{\mathcal{L}^{-1}\{Y(s)\}\big|_{t_k}\}}{\frac{z}{z-1}} \tag{2.50}$$

$$= \frac{z-1}{z}\mathcal{Z}\left\{\mathcal{L}^{-1}\left\{\frac{G(s)}{s}\right\}\bigg|_{t_k}\right\}. \tag{2.51}$$

The model in (2.51) is *exact* because the output samples are exactly recovered, i.e., $y_k = y(kh)$. Moreover, this model has relative degree 1, which implies that it has sampling zeros.

Then, from the definitions of the inverse Laplace transform (2.5) and the $\mathcal{Z}-$transform (2.21), we have [8]

$$G_{ZOH}(z) = \frac{z-1}{z}\frac{1}{2\pi j}\int_{c-j\infty}^{c+j\infty}\frac{e^{sh}}{z-e^{sh}}\frac{G(s)}{s}ds. \tag{2.52}$$

Since $G(s)$ is strictly proper, the integration path can be closed and the integral can be evaluated using the Residue Theorem [44]. Thus, closing the complex integral to the left of the complex plain we obtain (2.53) and closing it to the right we get (2.54) [2, 27]:

$$G_q(z) = \frac{z-1}{z}\sum_{l=0}^{n}\mathrm{Res}_{s=p_l}\left\{\frac{G(s)}{s}\frac{e^{sh}}{z-e^{sh}}\right\}. \tag{2.53}$$

$$G_q(z) = \frac{z-1}{z}\sum_{l=-\infty}^{\infty}\frac{G[(\log(z)+2\pi jl)/h]}{\log(z)+2\pi jl}. \tag{2.54}$$

For the particular case of a pure r-th order integrator, i.e., $G(s) = s^{-r}$, the following relation holds [74]:

$$\sum_{k=-\infty}^{\infty}\frac{1}{(\log(z)+2\pi jl)^r} = \frac{zB_{r-1}(z)}{(r-1)!(z-1)^r}, \quad r \geq 2. \tag{2.55}$$

In addition, the discrete-transfer function when the input is generated by a FOH [75, 76] or a FROH [77, 78] are respectively given by:

$$G_{FOH}(z) = \left(\frac{z-1}{z}\right)^2\mathcal{Z}\left\{\frac{1+sh}{hs^2}G(s)\right\}. \tag{2.56}$$

$$G_{FROH}(z) = \frac{\beta(1-z^{-1})}{h}\mathcal{Z}\left\{\frac{1-e^{-sh}}{s}\frac{G(s)}{s}\right\} + (1-\beta z^{-1})\mathcal{Z}\left\{\frac{1-e^{-sh}}{s}G(s)\right\}. \tag{2.57}$$

Notice that when $\beta = 0$, we obtain the transfer function when using a ZOH (see (2.51)). On the other hand, if $\beta = 1$ the transfer function (2.56) is obtained.

In addition, we are interested in deriving the sampled-data model from the state-space representation. Thus, based on the ZOH assumption, the system (2.2) can be represented in the discrete-time domain as:

$$x_{k+1} = A_q x_k + B_q u_k \tag{2.58a}$$
$$y_k = Cx_k \tag{2.58b}$$

where we have used the notation $x_{k+1} = qx_k$, and where the matrices are given by [2]:

$$A_q = e^{Ah}, \quad B_q = \int_0^h e^{A\Delta}Bd\Delta. \tag{2.59}$$

Similarly to the result (2.6), the discrete-transfer function can be also written as

$$G_q(z) = C(zI_n - A_q)^{-1}B_q. \tag{2.60}$$

Moreover, we present the state-space representation when the continuous-time input is generated the FOH defined by (2.10) [2]

$$\begin{bmatrix} x_{k+1} \\ u_k \end{bmatrix} = \begin{bmatrix} A_q & B_q^1 \\ 0 & 0 \end{bmatrix}\begin{bmatrix} x_k \\ u_{k-1} \end{bmatrix} + \begin{bmatrix} B_q^2 \\ 1 \end{bmatrix} \tag{2.61a}$$

$$y_k = \begin{bmatrix} C & 0 \end{bmatrix}\begin{bmatrix} x_k \\ u_{k-1} \end{bmatrix}, \tag{2.61b}$$

where

$$A_q = e^{Ah} \tag{2.62a}$$

$$B_q^1 = \int_0^h \left(\frac{\Delta}{h} - 1\right) e^{A\Delta} B d\Delta \tag{2.62b}$$

$$B_q^2 = \int_0^h \left(2 - \frac{\Delta}{h}\right) e^{A\Delta} B d\Delta. \tag{2.62c}$$

Notice that the previous sample u_{k-1} is considered as an extra state. This will be a key tool to develop sampled-data models in Chapters 3 and 5.

We conclude this section with an example:

Example 1 *Consider the continuous-time system $G(s) = s^{-r}$, $r > 0$. We are interested in the corresponding exact sampled-data model when the input is modeled by a ZOH.*

We can rewrite the n-th order integrator in state space form:

$$y_1(t) = x_1(t) \tag{2.63}$$

$$\dot{x}_1 = x_2(t) \tag{2.64}$$

$$\vdots \tag{2.65}$$

$$\dot{x}_{r-1}(t) = x_r(t) \tag{2.66}$$

$$\dot{x}_r(t) = u(t) \tag{2.67}$$

Then, the model (2.63) can be represented as

$$\dot{x}(t) = Ax(t) + Bu(t) \tag{2.68a}$$

$$y = Cx(t), \tag{2.68b}$$

where the matrices $A \in \mathbb{R}^{r\times r}$, $B \in \mathbb{R}^{r\times 1}$ and $C \in \mathbb{R}^{1\times r}$ are expressed in the Brunovsky form [79]:

$$A = \left[\begin{array}{c|c} 0 & I_{r-1} \\ \hline 0 & 0 \end{array}\right], \quad B = \begin{bmatrix} 0_{(r-1)\times 1} \\ 1 \end{bmatrix} \tag{2.69a}$$

$$C = \begin{bmatrix} 1 & 0 & \cdots & 0 \end{bmatrix}. \tag{2.69b}$$

The associated sampled-data model, assuming a ZOH input, can be obtained using (2.59)*. Thus, we have:*

$$e^{Ah} = I + hA + \frac{h^2}{2}A^2 + \cdots + \frac{h^r}{r!}A^r + \cdots \tag{2.70}$$

Notice that the matrices can be exactly obtained noticing that A is nilpotent, i.e., $A^r = 0$. Thus, the exact sampled-data model of and r-th order integrator is given by

$$x_{k+1} = A_q x_k + B_q u_k \tag{2.71a}$$
$$y_k = Cx_k, \tag{2.71b}$$

where

$$A_q = \begin{bmatrix} 1 & h & \frac{h^2}{2!} & \cdots & \frac{h^{r-1}}{(r-1)!} \\ 0 & 1 & h & \cdots & \frac{h^{r-2}}{(r-2)!} \\ 0 & 0 & \ddots & \ddots & \vdots \\ \vdots & \vdots & & \ddots & h \\ 0 & 0 & 0 & \cdots & 1 \end{bmatrix}, \quad B_q = \begin{bmatrix} \frac{h^r}{r!} \\ \frac{h^{r-1}}{(r-1)!} \\ \vdots \\ \frac{h^2}{2!} \\ h \end{bmatrix} \tag{2.72a}$$

$$C_q = \begin{bmatrix} 1 & 0 & \cdots & 0 \end{bmatrix}. \tag{2.72b}$$

2.3.2 Delta Operator Models

The theory of sampled-data systems is usually represented in the z-domain associated with the shift operator q. However, one of the disadvantages of this representation is that it does not converge to a continuous-time differential operator, [18]. The latter implies that for small sampling period the corresponding continuous-time system is not recovered. In particular, from (2.58), it can be noticed that

$$\lim_{h\to 0} A_q = I, \qquad \lim_{h\to 0} B_q = 0. \tag{2.73}$$

Thus, one could be interested in using the δ-operator because the relation between the continuous-time system and the associated discrete-time model can be better expressed using incremental models. Also, it allows us to explicitly include the sampling period in the description. From (1.3), it can be noticed that

$$\delta x_k = \frac{q-1}{h} x_k = \frac{x_{k+1} - x_k}{h}. \tag{2.74}$$

Since the δ-operator is a difference, models expressed in the γ-domain are similar to models obtained with the (continuous-time) differential operator. Then, continuous-time insights can be used in the discrete-time representations [1].

Applying (2.74) to the state-space representation (2.58), we obtain

$$\delta x_k = A_\delta x_k + B_\delta u_k \tag{2.75a}$$
$$y_k = C x_k, \tag{2.75b}$$

where

$$A_\delta = \frac{e^{Ah} - I}{h}, \qquad B_\delta = \frac{B_q}{h}. \tag{2.76}$$

Notice that, for fast sampling rate, i.e., $h \to 0$, the matrices in (2.76) converge to the continuous-time counterpart [18]. In addition, the transfer function in γ-domain is given by

$$G_d(\gamma) = C(\gamma I - A_\delta)^{-1} B_\delta. \tag{2.77}$$

2.3.3 Exact Sampled-Data Models

A subject of interest is when the sampling period approaches zero because the polynomials of the sampling zeros can be asymptotically characterized in terms of continuous-time relative degree, the assumptions about the system input, and the sampling period. To study the asymptotic behavior of linear sampled-data models, we first consider the case when the continuous-time system is an r-th order pure integrator, i.e.,

$$G(s) = \frac{1}{s^r}, \quad r > 0. \tag{2.78}$$

The corresponding discrete-time transfer function arising for a ZOH can be obtained using (2.51). Furthermore, according to [27], $G_q(z)$ approaches the following model

$$G_q(z) = \frac{h^r}{r!} \frac{B_r(z)}{(z-1)^r}. \tag{2.79}$$

Notice that (2.79) only depends on the relative degree r and the sampling period h. The polynomial of the asymptotic sampling zeros is defined by $B_r(\cdot)$, which is the Euler-Frobenius polynomial of order r given by (2.23)–(2.24).

For the case of the general system (2.1) when the sampling period goes to 0 the associated sampled-data model is given by [27],

$$G_q(z) = b\frac{h^{n-m}}{(n-m)!} \frac{(z-1)^m B_{n-m}(z)}{(z-1)^n}. \tag{2.80}$$

According to [75], the corresponding discrete-time transfer function of (2.1) when using a FOH when $h \to 0$ is given by

$$G_q(z) = b\frac{h^{n-m}}{(n-m+1)!} \frac{(z-1)^m C_{n-m}(z)}{z(z-1)^n}, \tag{2.81}$$

where

$$C_p(z) = B_{p+1}(z) + (p+1)(z-1)B_p(z). \tag{2.82}$$

In addition, the transfer function $G_q(z)$ when using a FROH is given by [77, 80]

$$G_q(z) = b\frac{h^{n-m}}{(n-m+1)!}\frac{(z-1)^m D_{n-m}(z,\beta)}{z(z-1)^n}, \tag{2.83}$$

where,

$$D_p(z,\beta) = \beta B_{p+1}(z) + (1+p)(z-\beta)B_p(z). \tag{2.84}$$

This analysis can also be studied for representations expressed in δ-operator. Thus, based on the ZOH assumption and for an r-th order integrator, the corresponding sampled-data model in γ-domain is given by [2, 81]

$$G_d(\gamma) = \frac{P_r(h\gamma)}{\gamma^r}, \tag{2.85}$$

where the polynomial $P_r(h\gamma)$ can be related to the Euler-Frobenius polynomials as follows:

$$P_r(h\gamma) = \left.\frac{B_r(z)}{r!}\right|_{z=1+h\gamma} \tag{2.86}$$

The polynomials $P_r(h\gamma)$ can be computed recursively, (See [2, 81])

$$P_r(h\gamma) = \sum_{l=1}^{r}\frac{(h\gamma)^{l-1}}{l!}P_{r-l}(h\gamma), \quad r \geq 1, \tag{2.87}$$

$$P_0(h\gamma) = 1. \tag{2.88}$$

and, when the sampling period goes to 0,

$$\lim_{h\to 0} P_r(h\gamma) = 1, \quad r \geq 1. \tag{2.89}$$

The first $P_r(h\gamma)$ polynomials are listed below,

$$P_1(h\gamma) = 1 \tag{2.90a}$$

$$P_2(h\gamma) = 1 + \frac{h}{2}\gamma \tag{2.90b}$$

$$P_3(h\gamma) = 1 + h\gamma + \frac{h^2}{6}\gamma^2 \tag{2.90c}$$

$$P_4(h\gamma) = 1 + \frac{3h}{2}\gamma + \frac{7h^2}{12}\gamma^2 + \frac{h^3}{24}\gamma^3. \tag{2.90d}$$

From (2.90), it can be noticed that when using the δ-operator, the Euler-Frobenius polynomials are explicitly represented as a function of the sampling period and γ. Moreover, the discrete-time transfer function for the general system shown in (2.1) is given by

$$G_d(\gamma) = b\frac{\prod_{i=1}^{m}(\gamma - z_i)}{\prod_{i=1}^{n}(\gamma - p_i)}P_r(h\gamma). \tag{2.91}$$

2.4 Approximate Sampled-Data Models for Linear Systems

We have previously discussed that exact sampled-data representations can be developed for linear systems. However, approximate descriptions are preferred since they better preserve the real continuous-time system's parameters. They can also be easier to obtain than the exact model, and the methods can also be applied to nonlinear systems.

Ordinary differential equations (ODEs) arise in many contexts, for example, in physical problems. Thus, there is an interest in knowing the consequences of modeling these problems using specific numerical approximations [40]. Linear and nonlinear ODEs can be approximately solved, for example, using Euler integration, Runge-Kutta methods, or Taylor series expansions. In fact, these two first methods are based on Taylor series expansions.

2.4.1 Numerical Integration Strategies

Consider the Initial-Value Problem (IVP) written as [82, 83]:

$$\frac{dy(t)}{dt} = f(t, y(t)); \qquad y(t_0) = y_0, \tag{2.92}$$

that has a unique solution on some specific interval. Then, integrating both sides, we obtain:

$$\int_{t_n}^{t_{n+1}} dy = \int_{t_n}^{t_{n+1}} f(t, y(t))dt \tag{2.93}$$

$$y(t_{n+1}) - y(t_n) = \int_{t_n}^{t_{n+1}} f(t, y(t))dt \tag{2.94}$$

Therefore, when the integral (2.94) is hard or impossible to compute, numerical methods have to be used. Thus, in order to approximate a solution of (2.94), and therefore of (2.92), we use *Finite Difference Methods* [84, 85].

We suppose that the numerical solution of the integral is as shown in Figure 2.7. Then, the area below the curve between t_n and t_{n+1} is approximately given by

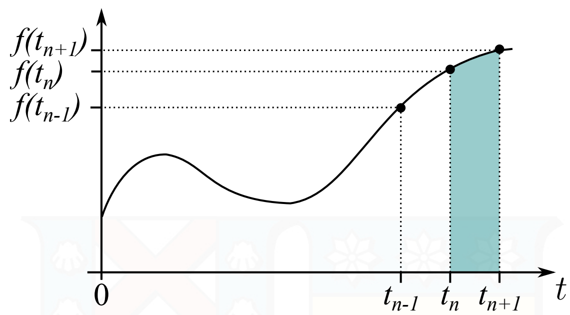

Figure 2.7: Finite Difference Method

$f(t_n, y_n)(t_{n+1} - t_n)$. Thus,

$$y(t_{n+1}) - y(t_n) = f(t_n, y_n)(t_{n+1} - t_n) \tag{2.95}$$

$$y(t_{n+1}) - y(t_n) = f(t_n, y_n)\Delta t \tag{2.96}$$

$$\frac{y(t_{n+1}) - y(t_n)}{\Delta t} = f(t_n, y_n) \tag{2.97}$$

Equation (2.97) is known as *Forward Difference Approximation* [84]. If we compute the area under the curve between t_{n-1} and t_n, we have the *Backward Difference Approximation* [84], which is given by

$$\frac{y(t_n) - y(t_{n-1})}{\Delta t} = f(t_n, y_n) \tag{2.98}$$

Notice that as Δt approaches zero, the approximations (2.97) and (2.98) recover the original ODE. On the other hand, we certainty know the value of $y(t)$ at the initial point $t = t_0$. Thus, we can approximate the solution of (2.92) near the initial condition, i.e., it is possible to estimate $y(t)$ by approximating $f(t, y(t)) \approx f(t_0, y(t_0))$ for $t \in [t_0, t_0 + \tau[$, where $\tau > 0$ is a real value sufficiently small [83]. Then, integrating both sides, we have:

$$\int_{t_0}^{t} dy = \int_{t_0}^{t} f(t', y(t'))dt' \tag{2.99}$$

$$y(t) - y_0 \approx (t - t_0) f(t_0, y_0), \tag{2.100}$$

where we have used the notation $y(t_n) = y_n$. Then, knowing the initial value, the sequence of next points will be

$$t_1 = t_0 + \tau \tag{2.101}$$

$$t_2 = t_1 + \tau = t_0 + 2\tau \tag{2.102}$$

$$t_3 = t_2 + \tau = t_0 + 3\tau \tag{2.103}$$

$$\vdots \tag{2.104}$$

$$t_{n+1} = t_n + n\tau. \tag{2.105}$$

Then, following (2.100), we have that:

$$\int_{t_0}^{t1} dy = \int_{t_0}^{t_1} f(t', y(t'))dt' \tag{2.106}$$

$$y_1 - y_0 \approx (t - t_0)f(t_0, y_0) \tag{2.107}$$

$$y_1 \approx y_0 + \tau f(t_0, y_0) \tag{2.108}$$

Thus, we obtain the recursive scheme

$$y_{n+1} = y_n + \tau f(t_n, y_n). \tag{2.109}$$

Equation (2.109) is called the *Forward Euler's Method* [40, 82, 83], which is basically the forward difference approximation defined in (2.97).

Now, it is reasonable to ask how good is Euler's approximation. In general, numerical methods are chosen for their convergence, the order of convergence, and stability characteristics. The first analyze whether the method approximates the solution, and the second how rapidly it converges. We will discuss both in Subsection 2.7.2.

On the other hand, we are also interested in knowing the error behavior between the numerical and the exact solution, i.e., whether the computed result remains bounded in cases when the exact solution is bounded. This criteria is known as stability and it may depend on the step size τ [40, 82].

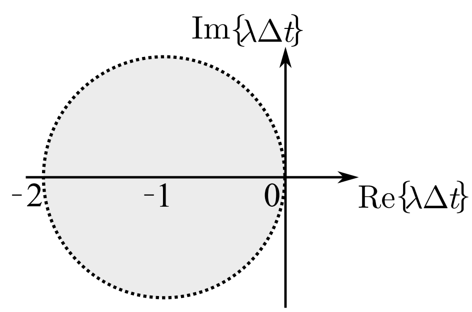

Figure 2.8: Forward Euler Method Stability Region

Thus, let us suppose that

$$\frac{dy(t)}{dt} = \lambda y(t); \qquad y(t_0) = y_0. \tag{2.110}$$

Then, using (2.109), we have that:

$$y_{n+1} = y_n + \tau f(t_n, y_n) \tag{2.111}$$

$$y_{n+1} = y_n + \tau (\lambda y_n) \tag{2.112}$$

$$y_{n+1} = (1 + \lambda \tau) y_n, \tag{2.113}$$

which implies that

$$y_1 = (1 + \lambda\,\tau)\,y_0 \tag{2.114}$$
$$y_2 = (1 + \lambda\,\tau)^2\,y_0 \tag{2.115}$$
$$\vdots \tag{2.116}$$
$$y_{n+1} = (1 + \lambda\,\tau)^{n+1}\,y_0 \tag{2.117}$$

The solution (2.117) is stable if and only if $|1 + \lambda\,\tau| \le 1$. Then, for λ negative and real, we have

$$-2 < \lambda\tau < 0 \implies \tau < -\frac{2}{\lambda}. \tag{2.118}$$

Thus explicit Euler method requires a small step size τ to ensure stability. As a consequence, it is necessary to apply methods that have better stability characteristics.

So far, we have dealt with one-step methods. When using them, we obtain a numerical solution from t_0 to t_1, starting from the initial value y_0. Then, we iterate from t_1 to t_2 using y_1 as the new initial value. However, a numerical approximation can be obtained considering 'the history' available, i.e., instead of computing y_n from just the value y_{n-1}, we could combine the values computed in past steps to generate an approximation at the next step. This is the idea behind multistep methods [82].

A general from of linear multistep methods is given by [83]:

$$\begin{aligned} y_n + a_1 y_{n-1} + a_2 y_{n-2} + \cdots + a_k y_{n-k} &= \\ \tau\left(b_0 f(t_n, y_n) + b_1 f(t_{n-1}, y_{n-1}) + \cdots + b_k f(t_{n-k}, y_{n-k})\right)&, \end{aligned} \tag{2.119}$$

where $a_0 = 1$ and a_i, b_i are give constants, independent of τ. Moreover, if $b_i = 0$, the method is called *explicit*, otherwise it is *implicit*.

When higher derivatives of $y(t)$ are available, then a common choice is to use the ***Taylor Series Method***. Thus, by repeating differentiation, it is possible to find functions $f_i(t, y(t))$, $i = 1, 2, \ldots, m$, which give values of $y^m(t)$, where m denotes the order of the derivative [40]. Then, we write an m-th order Taylor series method in the form

$$y_{n+1} = y_n + \tau f_1(t_n, y_n) + \frac{\tau^2}{2!} f_2(t_n, y_n) + \cdots + \frac{\tau^m}{m!} f_m(t_n, y_n) + R_m(t_n, y_n), \tag{2.120}$$

where we have used the notation $y_{n+1} = y(t_{n+1}) = y(t_n + \tau)$. The term $R_m(t_n, y_n)$ is called the remainder and is of the order of $\mathcal{O}(\tau^{m+1})$ [82]. Notice that the *big O notation* $\mathcal{O}\{\cdot\}$ is used to describe the asymptotic behavior of a specific function when the argument approaches a particular value or infinity.

Since the remainder term decays to zero rapidly, it can be neglected. Thus, (2.120) can be written as

$$y_{n+1} = y_n + \tau y_n^{(1)} + \frac{\tau^2}{2!} y_n^{(2)} + \cdots + \frac{\tau^m}{m!} y_n^{(m)} + \mathcal{O}(\tau^{m+1}). \tag{2.121}$$

Notice that the Euler's method corresponds to a special case of (2.121) when the first two terms are considered. Multistep methods are more accurate than one-step methods, however, they may impact the computational cost because multistep methods require additional memory for function values at previous steps. In comparison, multistage methods provides better efficiency since they generate values of the solution and its derivatives within a single time step [86].

Consider (2.94), this time we will use the trapezoidal rule [87] to approximate the integral. Thus, we obtain

$$y_{n+1} = y_n + \frac{\tau}{2}\left[f(t_n, y_n) + f(t_{n+1}, y_{n+1})\right] \tag{2.122}$$

However, (2.122) requires us to know the value of the function at the time step t_{n+1}. To overcome this difficulty, we can approximate the term y_{n+1} on the right-hand side using the forward Euler's method (2.109), yielding:

$$y_{n+1} = y_n + \frac{\tau}{2} f(t_n + \tau,\, y_n + \tau f(t_n, y_n)), \tag{2.123}$$

which is typically written as

$$y_{n+1} = y_n + \frac{\tau}{2}(k_1 + k_2) \tag{2.124a}$$

$$k_1 = f(t_n, y_n) \tag{2.124b}$$

$$k_2 = f(t_n + \tau,\, y_n + \tau f(t_n, y_n)) \tag{2.124c}$$

The method presented in (2.124) is an example of a second-order ***Runge-Kutta Method*** (RK2). Note that to generate a RK2, we need to approximate the integral by a quadrature rule of the same order and then approximate k_2 using (2.109). It is important to recall that, even when Euler's method have been proven to be inefficient, in scheme (2.124), k_2 is scaled by τ and therefore its error becomes smaller [41].

A general s-stage Runge-Kutta method is given by [82]:

$$y_{n+1} = y_n + h \sum_{i=1}^{s} b_i k_i \tag{2.125a}$$

$$k_i = f\left(t_n + h\, c_i, y_n \sum_{j=1}^{s} a_{i,j}\, k_1\right); \quad i = 1, \ldots, s, \tag{2.125b}$$

where $a_{i,j}$, b_i are real coefficients, where c_i satisfy the condition:

$$c_i = \sum_{j=1}^{i-1} a_{i,j}. \tag{2.126}$$

Thus, given a value of s, (2.125) depends on $s^2 + s$ parameters which are not unique. A common choice for them are found in the Butcher array for Runge-Kutta Methods (see, for example, [40, 82, 83]).

Example 2 *Consider the general form of an RK2 method*

$$y_{n+1} = y_n + \tau\left(b_1 k_1 + b_2 k_2\right) + \mathcal{O}(\tau^3) \tag{2.127a}$$
$$k_1 = f(t_n, y_n) \tag{2.127b}$$
$$k_2 = f\left(t_n + \tau c_2,\, y_n + \tau a_{2,1} k_1\right) \tag{2.127c}$$

We are interested in finding conditions over the coefficients $a_{2,1}, b_1, b_2, c_2$. Then, we will use the first order Taylor polynomial for k_2, around the point (t_n, y_n). This yields to

$$f\left(t_n + \tau c_2,\, y_n + \tau a_{2,1} k_1\right) \approx f(t_n, y_n) + \tau\left(c_2 \frac{\partial f(t_n, y_n)}{\partial t} + a_{2,1} \frac{\partial f(t_n, y_n)}{\partial y} f(t_n, y_n)\right) + \mathcal{O}(\tau^2). \tag{2.128}$$

Replacing in (2.127)*, we have*

$$y_{n+1} \approx y_n + \tau(b_1 + b_2) f(t_n, y_n) + \tau^2 b_2 \left[c_2 \frac{\partial f(t_n, y_n)}{\partial t} + a_{2,1} \frac{\partial f(t_n, y_n)}{\partial y} f(t_n, y_n)\right] + \mathcal{O}(\tau^3), \tag{2.129}$$

Then, we set

$$b_1 + b_2 = 1 \tag{2.130a}$$
$$b_2 c_2 = \frac{1}{2} \tag{2.130b}$$
$$b_2 a_{2,1} = \frac{1}{2}, \tag{2.130c}$$

where, considering condition (2.126)*, $c_2 = a_{2,1}$.*

Notice that (2.127) can be expressed as a second-order Taylor series expansion.

Definition 2.3 *[41, page 134] A Runge-Kutta method is of order κ if, for sufficiently smooth problems, the Taylor Series method coincides up to the term h^κ.*

2.5 Continuous-Time Nonlinear Systems

The majority of real processes have nonlinearities that cannot be ignored. Contrasted with linear systems, it is not always possible to find closed-form expressions for the solutions of nonlinear ODEs [88]. Thus, in order to simplify the problem, a standard option is to transform the nonlinear model into a linearized system and make predictions about its behavior into a known region.

There are several options to perform a linearization; some are based on approximating the nonlinear system, however such approximation is only valid around an equilibrium point. Besides, a control technique based on a linearized model can exhibit poor robustness [89].

On the other hand, there are control strategies such as *Feedback Linearization*, that allows to obtain a linear model that based on the representation of the nonlinear system. This approach's key idea is to obtain a fully or partially equivalent linear system through a coordinate transformation and a suitable control law. Then, the classical feedback techniques such as PID or pole placement could be applied [90]. Moreover, it is important to recall that feedback linearization does not depend on approximations such as Taylor series expansion [91].

Typically, feedback linearization can be achieved in two forms: *state-space linearization* (also known as full-state linearization) and *input-output linearization*. In the former, the goal is to cancel the nonlinearities between the transformed inputs and the transformed state variables, which results in a fully linearized state equation. In contrast, the latter aims to linearize the mapping between the transformed inputs and the original outputs. In this case, the state equation is only partially linearized [89]. However, when using state-space linearization, a control law's design is still challenging because the output remains nonlinear. Therefore, input-output feedback is preferable.

Moreover, it is not always possible to cancel nonlinearities in every system. Therefore, the system must have a particular structure that allows us to linearize it. Then, we consider a class of nonlinear single-input single-output (SISO) systems affine in the input, i.e.,

$$\dot{x}(t) = f(x(t)) + g(x(t))u(t) \tag{2.131a}$$

$$y(t) = h(x(t)), \tag{2.131b}$$

where $f(x(t))$, $g(x(t))$ and $h(x(t))$ are sufficiently smooth, i.e., that all the derivatives are well-defined and continuous, in a domain $\mathcal{M} \in \mathbb{R}$, containing the origin [39, 92].

2.5.1 Relative Degree

One of the basic properties of nonlinear systems is the notion of relative degree, which is related to the number of times that ones need to differentiate the output $y(t)$ to make the input $u(t)$ explicitly appear.

We explain this idea with the following example:

Example 3 *Consider the nonlinear system given by*

$$\dot{x}_1(t) = x_2(t) \tag{2.132a}$$
$$\dot{x}_2(t) = -x_1^2(t)x_2(t) + u(t) \tag{2.132b}$$
$$y(t) = x_1(t), \tag{2.132c}$$

we are interested in calculating the relative degree. Computing the derivatives of the output $y(t)$, we have,

$$\dot{y}(t) = \dot{x}_1(t) = x_2(t) \tag{2.133}$$
$$\ddot{y}(t) = \dot{x}_2(t) = -x_1^2(t)x_2(t) + u(t), \tag{2.134}$$

where we can notice that after the second derivative of $y(t)$, the input appears in the output equation. Thus, (2.132) *is said to have relative degree 2. Notice that if the $y(t) = x_2(t)$, the system is of relative degree 1.*

Formally, the definition of relative degree is as follows:

Definition 2.4 *[39, page 137] The nonlinear system 2.131 is said to have relative degree r at a point x_0 if*

(i) $L_g L_f^k h(x) = 0$ *for all x in a neighborhood of x_0 and for* $k = 0, \dots, r-2$

(ii) $L_g L_f^{r-1} h(x_0) \neq 0$,

where L_g and L_f correspond to Lie derivatives.

The new notation defined above is a useful tool when repeating the calculation of the output derivative. For example, if we consider that (2.131) has relative degree r, computing the derivatives of the output $y(t)$ we obtain

$$y^{(0)}(t) = h(x(t)) \tag{2.135a}$$
$$\begin{aligned} y^{(1)}(t) &= \frac{\partial h(x)}{\partial x}\frac{dx(t)}{dt} = \frac{\partial h(x)}{\partial x} f(x) + \frac{\partial h(x)}{\partial x} g(x(t))u(t) \\ &= L_f h(x) + L_g h(x) u(t). \end{aligned} \tag{2.135b}$$

Assuming relative degree $r > 1$, we have that $y^{(1)}(t)$ is independent of $u(t)$, therefore $L_g h(x) = 0$. This yields

$$y^{(2)}(t) = \frac{\partial(L_f h(x))}{\partial x}\left(f(x(t)) + g(x(t))u(t)\right) = L_f^2 h(x(t)) + L_g L_f h(x) u(t). \tag{2.136}$$

Again, assuming $r > 2$, then $L_g L_f h(x) = 0$. Repeating this calculation up to $k = r$, we have that

$$y^{(r)}(t) = L_f^r h(x) + L_g L_f^{r-1} h(x) u(t). \tag{2.137}$$

Notice that $u(t)$ can be chosen in such a way that it cancels the nonlinearities in (2.137). For example:

$$u(t) = \frac{1}{L_g L_f^{r-1} h(x)} \left[v(t) - L_f^r h(x) \right], \tag{2.138}$$

which exactly linearizes the map between the original output $y(t)$ and the transformed input $v(t)$ [89].

On the other hand, there are systems in which $L_g L_f^{r-1} h(x) = 0$ for all x in a neighborhood of x_0 and for $k \geq 0$. In this case, the relative degree is not well-defined. Nevertheless, it is possible to find a local coordinate transformation around x_0 that partially linearizes the nonlinear system (see, for example, [39, 92]). In what follows we explore this idea.

2.5.2 Normal Forms

The theory of normal forms has been studied for continuous and discrete-time nonlinear systems (see, for example [79, 93–96]). Normal forms allow us to rewrite the system as a chain of integrators followed by nonlinear dynamics. This particular structure is called prime form [94]. Thus, we are interested in expressing (2.131) in this form.

Firstly, we synthesize the results presented in Section 2.5.1 in the following lemmas:

Lemma 2.5 *[90, Page 231] Consider the nonlinear system* (2.131) *having relative degree $r = n$ (i.e., equal to the state dimension) at some point $x = x_0$ and the following coordinates transformation:*

$$z(t) = \Phi(x) = \begin{bmatrix} \phi_1(x) \\ \phi_2(x) \\ \vdots \\ \phi_r(x) \end{bmatrix} = \begin{bmatrix} h(x) \\ L_f h(x) \\ \vdots \\ L_f^{n-1} h(x) \end{bmatrix}, \tag{2.139}$$

then, there exists a nonlinear static feedback $u(t)$ such that the closed-loop system in the new coordinates is linear and controllable.

Since we are focused in a neighborhood of x_0, a transformation of the type (2.139) is called *local diffeomorphism* on $\mathbb{R}$. Moreover, $\Phi(x)$ is not unique and invertible, i.e., there exists a function $\Phi^{-1}(z)$ and both functions, $\Phi(x)$ and $\Phi^{-1}(z)$ have continuous partial derivatives of any order [39].

Thus, the new coordinates describe the system in **Normal Form** as

$$\dot{z}_1(t) = \frac{\partial \phi_1(x)}{\partial x}\frac{dx}{dt} = L_f h(x) = \phi_2(x) = z_2(t) \tag{2.140a}$$

$$\dot{z}_2(t) = \frac{\partial \phi_2(x)}{\partial x}\frac{dx}{dt} = L_f^2 h(x) = \phi_3(x) = z_3(t) \tag{2.140b}$$

$$\vdots \tag{2.140c}$$

$$\dot{z}_{r-1}(t) = \frac{\partial \phi_{r-1}(x)}{\partial x}\frac{dx}{dt} = L_f^{r-1} h(x) = \phi_r(x) = z_r(t) \tag{2.140d}$$

$$\dot{z}_r(t) = \frac{\partial \phi_r(x)}{\partial x}\frac{dx}{dt} = v(t), \tag{2.140e}$$

where

$$v(t) = \left[\underbrace{L_f^r h(x)}_{a(z)} + \underbrace{L_g L_f^{r-1} h(x)}_{b(z)} u(t)\right]\Bigg|_{x=\Phi^{-1}(z)} ;\, z(t) = (z_1(t), \ldots, z_r(t)). \tag{2.141}$$

Note that, according to Definition 2.4, $b(z) \neq 0$ for all z in the neighborhood of $z_0 = \Phi(x_0)$. Besides, the nonlinear state feedback (2.138) is given by

$$u(t) = \frac{1}{b(z)}(v(t) - a(z)). \tag{2.142}$$

On the other hand, if the relative degree is not well-defined at some point x_0, it is possible to find r functions that partially linearizes the nonlinear system (2.131), and $n - r$ functions fixed arbitrarily to describe the internal dynamics.

Lemma 2.6 *[39, Page 141] Consider the n-th order nonlinear system* (2.131) *having relative degree r at x_0, i.e., the relative degree is less than the state dimension. Then, it is possible to find $n - r$ functions $\phi_{r+1}(x), \ldots, \phi_n(x)$ such that a local coordinate transformation around x_0 is given by*

$$z(t) = \Phi(x) = \begin{bmatrix} h(x) \\ L_f h(x) \\ \vdots \\ L_f^{r-1} h(x) \\ \hdashline \phi_{r+1}(x) \\ \vdots \\ \phi_n(x) \end{bmatrix}, \tag{2.143}$$

where $\phi_{r+1}(x)$ to $\phi_n(x)$ are chosen in such a way that $\frac{\partial \phi_i}{\partial x} g(x) = L_g \phi_i(x) = 0$ for all x in the neighborhood of x_0 and for $r + 1 \leq i \leq n$.

In the new set of coordinates, the first r equations are given by (2.140). Then, the $n-r$ functions are defined as

$$\dot{z}_i(t) = \frac{\partial \phi_i(x)}{\partial x}\frac{dx}{dt} = L_f\phi_i(x) + L_g\phi_i(x)u(t); \quad r+1 \le i \le n, \tag{2.144}$$

setting $L_g\phi_i(x) = 0$, we have that

$$L_f\phi_i(\Phi^{-1}(x)) = q_i(z) = \dot{z}_i(t); \quad r+1 \le i \le n. \tag{2.145}$$

Thus, an n-th order nonlinear system of the form (2.131) can be expressed in normal form as follows

$$\dot{z}_1(t) = z_2(t) \tag{2.146a}$$
$$\vdots \tag{2.146b}$$
$$\dot{z}_{r-1}(t) = z_r(t) \tag{2.146c}$$
$$\dot{z}_r(t) = v(t) \tag{2.146d}$$
$$\dot{z}_{r+1}(t) = q_{r+1}(z) \tag{2.146e}$$
$$\vdots \tag{2.146f}$$
$$\dot{z}_n(t) = q_n(z) \tag{2.146g}$$
$$y(t) = z_1(t) = h(t), \tag{2.146h}$$

where $v(t)$ is given by (2.141). Notice that this system is decomposed into a linear subsystem of order r, which is a chain of r integrators, and a nonlinear subsystem of order $n-r$, which is not directly affected the input $u(t)$ and defines the zero dynamics of the system [90].

2.5.3 Zero Dynamics

As mentioned before, in the linear case, we define the relative degree as the difference between the number of poles and zeros in the transfer function. Therefore, if $r = n$ the system has no zeros; otherwise it has $n-r$ zeros. Following this idea, we have that $q_i(z)$ defines the system's zeros (or internal) dynamics of an n-th order nonlinear system relative having degree r.

In order to simplify the notation introduced in (2.143), we consider

$$z(t) = \Phi(x) = \begin{bmatrix} \zeta(t) \\ \hdashline \eta(t) \end{bmatrix}, \tag{2.147}$$

where $\zeta(t) = [z_1(t), \dots, z_r(t)]^T$ and $\eta(t) = [z_{r+1}(t), \dots, z_n(t)]^T$. Then, to characterize the zero dynamics, we choose an appropriate input $u(t)$ to maintain the output $y(t)$ at zero. Therefore, supposing that the output and all of its derivatives are equal to zero, we have that $y(t) = h(x) = 0$ for all t, it follows that

$$z_1(t) = \dot{z}_1(t) = \dot{z}_2(t) = \cdots = \dot{z}_r(t) \equiv 0 \tag{2.148}$$

Thus, the continuous-time zero dynamics are given by

$$\dot{\eta}(t) = q(0, \eta(0)), \tag{2.149}$$

for any initial condition $\phi(0, \eta(0))$, and for an input

$$u_{zd}(t) = -\frac{a(0, \eta)}{b(0, \eta)}. \tag{2.150}$$

2.6 Discrete-Time Nonlinear Systems

We consider a discrete-time nonlinear system affine in the input u_k, similar to (5.1), using the shift operator model:

$$x_{k+1} = F_q(x_k) + G_q(x_k)u_k \tag{2.151a}$$
$$y_k = H_q(x_k), \tag{2.151b}$$

where we have used the notation $x_k = x(kh)$ and h is the sampling period. Using the local coordinate transformation in (2.147), then (2.151) can be written as

$$\zeta_{k+1} = a(\zeta_k, \eta_k) + b(\zeta_k, \eta_k)u_k \tag{2.152a}$$
$$\eta_{k+1} = c(\zeta_k, \eta_k) \tag{2.152b}$$
$$y_k = \zeta_{1,k}. \tag{2.152c}$$

In addition, the necessary condition over the input u_k in order to characterize the internal zero dynamics of system (2.152) is given by [81]:

$$(u_{zd})_k = -\frac{a(0, \eta_k)}{b(0, \eta_k)}. \tag{2.153}$$

2.7 Sampled-Data Models for Nonlinear Systems

For nonlinear systems, the exact sampled-data model is usually unknown or impossible to compute [97]. Thus, the motivation has been to study the effect of numerical integration methods on the obtained approximate sampled-data model. To solve the differential equations, these models have been developed based on, for example, Runge-Kutta methods [98–100] or truncated series expansion, e.g., Taylor or Lie series methods [81, 101–104].

Moreover, when discretizing a continuous-time system, the corresponding sampled-data model includes extra zeros (linear case) or zero dynamics (nonlinear case), which depends on the hold device used to generate the system input [17]. Based on the ZOH assumption, in [101], the nonlinear sampling zero dynamics were described for the first time, while [81] proposed a truncated Taylor series expansion to discretize nonlinear systems, explicitly characterizing the sampling zero dynamics.

In [103, 104], a more accurate model than the proposed in [81] is presented for a continuous-time system of relative degree two.

Higher-order hold devices have also been used to model the input. For example, in [54], a discrete-time model is obtained considering that the input is generated by a backward triangle sample and hold. In addition, Generalized Hold Functions (GHF) can be used to arbitrarily place the zeros of the sampled-data model without restricting the sampling period to be small [56]. The properties of GHF have been used, for example, in [57] to shift the sampling zeros asymptotically to the origin for fast sampling rates. However, the use of this kind of holds can give misleading results [55]. On the other hand, non-uniform sampling has been considered in [29] and [30].

Besides, normal forms are useful to characterize the resulting sampled-data model under different assumptions on the system input (see, for example, [54, 81, 101, 103, 105–107]). In what follows, we will review the truncated Taylor series expansion since it can exploit the assumption used to model the system input.

2.7.1 Numerical Integration Strategies

Consider the nonlinear system (2.131) expressed in normal form as shown in (2.143). As mentioned before, the first r states are described by a chain of integrators. Thus, it is possible to obtain the corresponding sampled-data model when the applied integration strategy is a Taylor series expansion up to the first discontinuous term at the sampling instants $t = kh$. On the other hand, the remaining $n - r$ functions can be approximating using the Euler's Method.

Following the above idea, in [2, 81] an approximate sampled-data model was proposed by truncating the Taylor expansion based on the smoothness of system input. Thus, under the ZOH assumption, we have that the corresponding exact sampled-data model of (2.146) is given by

$$\zeta_1(kh+h) = \zeta_1(kh) + h\zeta_2(kh) + \cdots + \frac{h^r}{r!}\left[a(\zeta,\eta) + b(\zeta,\eta)u(t)\right]\Big|_{t=\alpha_1} \tag{2.154a}$$

$$\zeta_2(kh+h) = \zeta_2(kh) + \cdots + \frac{h^{r-1}}{(r-1)}\left[a(\zeta,\eta) + b(\zeta,\eta)u(t)\right]\Big|_{t=\alpha_2} \tag{2.154b}$$

$$\vdots \tag{2.154c}$$

$$\zeta_r(kh+h) = \zeta_r(kh) + h\left[a(\zeta,\eta) + b(\zeta,\eta)u(t)\right]\Big|_{t=\alpha_r} \tag{2.154d}$$

$$\eta(kh+h) = \eta(kh) + h\, q(\zeta,\eta)\Big|_{t=\alpha_{r+1}}. \tag{2.154e}$$

for some time instants $kh < \alpha_i < kh + h$, $i = 1, \ldots, r+1$. Note that replacing the unknown time instants by kh, we obtain an approximate discrete-time model. In Chapter 5 we show that the truncated Taylor series method can exploit the B-spline assumption on the system input to obtain a more accurate model than the usual one based on a ZOH assumption.

2.7.2 Local Truncation Error

In Subsection 2.4.1 it was mentioned that numerical methods were chosen based on their convergence and order of convergence. In general, a method is said to be convergent if, for all IVPs of the form (2.92)

$$\lim_{h \to 0} ||y(t_{n+1}) - \hat{y}(t_{n+1})|| = 0, \tag{2.155}$$

where $\hat{y}(t_{n+1})$ denotes the numerically computed solution and $y(t_{n+1})$ refers to the exact values.

Thus, *the Local Truncation Error* is defined to be the difference between the true and the approximate solution within a single iteration of the method. Since we are considering the local error, we assume that the current solution is exact, i.e., $\hat{y}(t_n) = y(t_n)$ [82]. Moreover, if the error $e_{n+1} = \hat{y}(t_{n+1} - y(t_{n+1})) \in \mathcal{O}(h^{\kappa+1})$ we say that the method is of order κ.

Consider the numerical integration strategy (2.154). Then, it is possible to estimate the local truncation error between the real and the approximate output assuming that, at $t = kh$, the state $\hat{\zeta}(kh)$ is equal to the true system state $\zeta(kh)$, i.e., [2, 81]

$$y(kh+h) = \zeta_1(kh+h) = \zeta_1(kh) + \cdots + \frac{h^r}{r!}\left[a(\zeta,\eta) + b(\zeta,\eta)u(t)\right]_{t=\alpha_1} \tag{2.156}$$

$$\hat{y}(kh+h) = \hat{\zeta}_1(kh+h) = \zeta_1(kh) + \cdots + \frac{h^r}{r!}\left[a(\zeta,\eta) + b(\zeta,\eta)u(t)\right]_{t=kh}. \tag{2.157}$$

Then, the error is given by

$$\hat{e} = |y(kh+h) - \hat{y}(kh+h)| \tag{2.158}$$

$$= \frac{h^r}{r!}\left|\left[a(\zeta,\eta) + b(\zeta,\eta)u(t)\right]_{t=\alpha_1} - \left[a(\zeta,\eta) + b(\zeta,\eta)u(t)\right]_{t=kh}\right| \tag{2.159}$$

$$\leq \frac{h^r}{r!} L\left|\zeta(\alpha_1) - \zeta(kh)\right|, \tag{2.160}$$

where $L > 0$ is the Lipschitz constant. Moreover, the state trajectory $\zeta(t)$ is bounded in the form [83]

$$|\zeta(\alpha_1) - \zeta(kh)| \leq C\frac{e^{Lh} - 1}{L} = \mathcal{O}(h) \tag{2.161}$$

Therefore, the local error truncation is of the order of h^{r+1}.

3 LINEAR SAMPLED-DATA MODELS BASED ON B-SPLINE FUNCTIONS

In Chapter 2, we discussed that discrete-time models depend on knowledge or assumptions about the input signal. Also, it was mentioned that exact sampled-data models for linear systems can be developed; however, extra zeros with no continuous-time counterparts appear in the resulting model. Such zeros are called sampling zeros and have been (asymptotically) characterized for different types of holds.

It is usually assumed that a zero-order hold generates the input to the continuous-time system. However, there are different options to interpolate the continuous-time input from the discrete-time sequence. When interpolating with high-order degree polynomials, one can have the Runge's phenomenon, which can be avoided using piecewise polynomials functions such as B-splines [30].

Besides, its intersample behavior and its accurate modeling in the associated discrete-time model may be of interest for system identification, state estimation or prediction, and also for high-performance digital control strategies such as Model Predictive Control (MPC) [108].

This chapter first explores the connections between the sampling zeros of discrete-time models and the smoothness of the continuous-time system input. In particular, we show that when a B-spline is used in a generalized hold then the order of the Euler-Frobenius polynomial that characterizes the asymptotic sampling zeros is increased by the order of the B-spline function used in the hold device.

In addition, we explore the connections between the sampling zeros and the applied numerical integration strategy. Thus, we characterize the sampling zeros for approximate sampled-data models using Runge-Kutta methods and truncated Taylor Series expansions. Moreover, we show that the smoothness of the input (described by spline interpolation) can also be exploited in these integration strategies, also playing a role in the characterization of the sampling zeros.

Finally, a key issue for approximate sampled-data models is their accuracy. No matter how fast the sampling rate is chosen, there will be a difference between the continuous-time and the corresponding discrete-time model. Thus, we will present a numerical example in order to quantify the error using the relative error in the frequency domain.

3.1 B-Spline Generalized Hold

In this section, we present one of the contributions in this thesis: a B-spline generalized hold expressed as shown in Figure 3.1. Firstly, we consider that a B-spline of order ℓ can be constructed from a weighted sum of shifted B-splines [71]

$$u(t) = \sum_{p=-\infty}^{\infty} u_p \tilde{\beta}_\ell(t - ph); \tag{3.1}$$

where u_p denotes de *weight* of the B-spline at $t_p = ph$ [58]. Notice that since $\tilde{\beta}_\ell(t)$ has minimal support, (3.1) can be rewritten as,

$$u(t) = \sum_{p=0}^{\ell} u_{k-p} \tilde{\beta}_\ell(t - kh + ph); \qquad t \in [kh, kh+h[\tag{3.2}$$

The objective is to represent the generalized hold in terms of known hold devices. Thus, in Theorem 3.1, we show that a B-spline hold can be expressed by a hybrid system composed by the interconnection of a digital filter followed by a ZOH and an ℓ-th order continuous-time integrator.

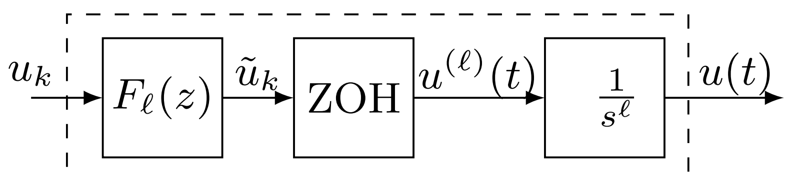

Figure 3.1: Generalized B-spline Hold

Theorem 3.1 *An ℓ-th order B-spline hold is equivalent to the hybrid system shown in Figure 3.1, where*

$$F_\ell(z) = \frac{1}{h^\ell}\left(\frac{z-1}{z}\right)^\ell. \tag{3.3}$$

Proof: From (2.36) in Lemma 2.1 we have that

$$\tilde{\beta}_\ell(t) = \frac{1}{h^\ell}\mathcal{L}^{-1}\left\{\left(\frac{1-e^{-sh}}{s}\right)^{\ell+1}\right\}. \tag{3.4}$$

Notice that (3.4) is the output of the generalized hold when the input sequence is a Kronecker delta $u_k = \delta_k$. In addition, note that the expression within brackets can be rewritten as

$$\left(\frac{1-e^{-sh}}{s}\right)^{\ell+1} = \left(1-e^{-sh}\right)^{\ell}\left(\frac{1-e^{-sh}}{s}\right)\left(\frac{1}{s^{\ell}}\right), \tag{3.5}$$

where the first term corresponds to pure time delays which are integer number of the sampling period, the middle term corresponds to the unit Kronecker delta response of a ZOH, and the last term corresponds to an ℓ-th order integrator. Also, the first term can be expressed in the z-domain as

$$\mathcal{Z}\left\{\mathcal{L}^{-1}\left\{(1-e^{-sh})^{\ell}\right\}\Big|_{t=kh}\right\} = (1-z^{-1})^{\ell} = \frac{(z-1)^{\ell}}{z^{\ell}}, \tag{3.6}$$

which corresponds to the result presented in (3.3). ■

Corollary 3.2 *From Theorem 3.1 we have that*

$$\tilde{U}(z) = F_{\ell}(z)U(z) \tag{3.7}$$

where $\tilde{U}(z) = \mathcal{Z}\{\tilde{u}_k\}$ and $U(z) = \mathcal{Z}\{u_k\}$.

Remark 3.3 *In Figure 3.2, we notice that the output signal of the ZOH corresponds to the ℓ-th derivative of $u(t)$ and it is piecewise constant. Therefore, derivatives greater than ℓ are equal to zero in each sampling interval, i.e.,*

$$u^{\ell+1}(t) = u^{\ell+2} = \cdots = 0. \tag{3.8}$$

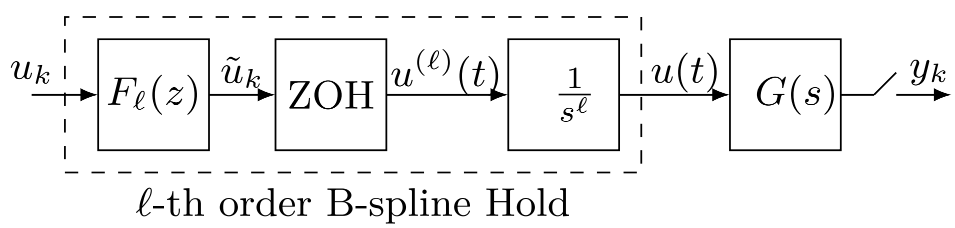

Figure 3.2: Generalized B-spline Hold and G(s)

3.2 Exact Sampled-Data Models Based on B-spline Functions

Following the ideas presented in Section 2.3, there is an interest in studying the impact of the B-spline holder in the corresponding sampled-data model. In particular, we show the connection between the B-spline order and the asymptotic sampling zeros polynomial. Firstly, in Theorem 3.4, we consider that the plant $G(s)$ is an r-th order pure integrator. Then, in Theorem 3.5 we analyze the general linear case.

Theorem 3.4 *Consider a sampled-data scheme, as shown in Figure 3.2, where the input sequence is $\{u_k\}$, the hold is an ℓ-th order B-spline hold defined in Lemma 3.1 and the continuous-time system is $G(s) = s^{-r}$, $r > 0$. The output sequence is $\{y_k = y(kh)\}$. Then the equivalent discrete-time transfer function is given by*

$$G_q(z) = \frac{h^r}{(r+\ell)!} \frac{B_{r+\ell}(z)}{z^\ell (z-1)^r}. \tag{3.9}$$

where $B_{r+\ell}(z)$ is the Euler-Frobenius polynomial defined in (2.23)–(2.24).

Proof: According to Lemma 3.1, an ℓ-th order B-spline hold can be equivalently represented as the system shown in Figure 3.1 Therefore, the corresponding discrete-time model $G_q(z)$ for the system in Figure 3.2 is

$$G_q(z) = F_\ell(z)\tilde{G}_q(z), \tag{3.10}$$

where $F_\ell(z)$ is given by (3.3) and $\tilde{G}_q(z)$ is the ZOH discretization of

$$\tilde{G}(s) = \frac{1}{s^\ell} G(s) = \frac{1}{s^{r+\ell}}. \tag{3.11}$$

Then, following the result in [27], the sampled-data model for (3.11) is given by

$$\tilde{G}_q(z) = \frac{h^{r+\ell}}{(r+\ell)!} \frac{B_{r+\ell}(z)}{(z-1)^{r+\ell}}. \tag{3.12}$$

where $B_{r+\ell}(z)$ is the Euler-Frobenius polynomial of order $r+\ell$. Then,

$$G_q(z) = \frac{1}{h^\ell} \frac{(z-1)^\ell}{z^\ell} \tilde{G}_q(z), \tag{3.13}$$

which completes the proof. ∎

From Theorem 3.4, we notice that the order of the sampling zeros polynomial corresponding to a system of relative degree r is increased exactly by the order of the hold, ℓ. In fact, this result is consistent with [27], given that a ZOH corresponds to $\ell = 0$. We next extend the previous results to a more general continuous-time linear system of relative degree r.

Theorem 3.5 *Consider the sampled-data system shown in Figure 3.2, where the input is generated by the ℓ-th order B-spline hold* (3.2) *and $G(s)$ is the continuous-time system defined in* (2.1). *For fast sampling rates, the associated discrete-time transfer function is given by*

$$G_q(z) = \frac{b\, h^r}{(\ell+r)!} \frac{B_{\ell+r}(z)}{z^\ell (z-1)^r}; \; r = n - m. \tag{3.14}$$

where $B_{r+\ell}(z)$ is the Euler-Frobenius polynomial of order $r+\ell$ defined in (2.23)–(2.24).

Proof: The ℓ-th order B-spline hold can be equivalently represented as shown in Figure 3.2, where $G(s)$ is the continuous-time system in (2.1). Then, $\tilde{G}(s)$ is given by

$$\tilde{G}(s) = \frac{b}{s^\ell} \frac{(s - z_1)(s - z_2) \dots (s - z_m)}{(s - p_1)(s - p_2) \dots (s - p_n)}. \tag{3.15}$$

Then, the discrete-time transfer function in (2.51) can be expressed as [8]:

$$\tilde{G}_q(z) = (1 - z^{-1}) \frac{1}{2\pi j} \int_{c-j\infty}^{c+j\infty} \frac{e^{sh}}{z - e^{sh}} \frac{\tilde{G}(s)}{s} ds. \tag{3.16}$$

Introducing the variable $s = \omega/h$, it follows that

$$\tilde{G}\left(\frac{\omega}{h}\right) = \left(\frac{h}{\omega}\right)^r \left(\frac{h}{\omega}\right)^\ell b \frac{(1 - \frac{hz_1}{\omega}) \cdots (1 - \frac{hz_m}{\omega})}{(1 - \frac{hp_1}{\omega}) \cdots (1 - \frac{hp_n}{\omega})}. \tag{3.17}$$

For fast sampling period, i.e., $h \approx 0$, we can characterize the asymptotic model by considering the following limit:

$$\lim_{h \to 0} h^{-r} \tilde{G}_q(z) = h^\ell \frac{b}{2\pi j} \frac{(z-1)}{z} \int_{c-j\infty}^{c+j\infty} \frac{e^\omega}{z - e^\omega} \frac{1}{w^{r+\ell}} \frac{d\omega}{\omega} \tag{3.18}$$

$$= h^\ell \frac{b\,(z-1)}{z(r+\ell)!} \frac{zB_{r+\ell}(z)}{(z-1)^{r+\ell+1}}. \tag{3.19}$$

where the last equation (3.18) follows by taking into account that the complex integral corresponds to the sampled-data model of an integrator of order $r + \ell$ (see equation (2.55)). Then, considering $G_q(z) = F_\ell(z)\tilde{G}_q(z)$:

$$G_q(z) = \frac{b}{h^\ell} \frac{(z-1)^{\ell+1}}{z^\ell} \frac{h^\ell B_{r+\ell}(z)}{(r+\ell)!(z-1)^{r+\ell+1}}. \tag{3.20}$$

■

Thus, we have shown that the Euler-Frobenius polynomial $B_{r+\ell}(z)$ characterizes the asymptotic sampling zeros for any linear system of (continuous-time) relative degree r, when an ℓ-th order B-spline hold models the input.

3.3 Approximate Sampled-Data Models Based on B-Spline Functions

In the previous sections, we have shown that the location of the (asymptotic) sampling zeros depends on the continuous-time relative degree and on the hold used. This section shows the impact of the numerical integration strategy applied to discretize the continuous-time system and the characterization of the sampling zeros that appear in the discrete-time model.

In our analysis, we apply a Runge-Kutta numerical integration strategy to the continuous-time system, also considering the smoothness of the input signal (modeled using spline interpolation) to obtain the sampling zeros polynomial that appears in the discrete-time model.

To develop the corresponding discrete-time model, we assume a system of relative degree r that is numerically solved by a κ-th order Runge-Kutta method. Then, assumptions on the input smoothness can also be introduced by including an ℓ-th order B-spline hold, as shown in Figure 3.2. Thus, in the following subsections we obtain the characterization of the asymptotic sampling zeros for high-order Runge-Kutta methods ($\kappa \geq r+\ell$) and for low-order Runge-Kutta methods ($\kappa < r+\ell$).

3.3.1 High-Order Runge-Kutta Methods

The first result shows that, for an r-th order integrator, when the order of the Runge-Kutta method is greater than or equal to $r+\ell$, then the exact sampled-data model is obtained.

Theorem 3.6 *Consider a sampled-data system, as shown in Figure 3.1, where the input sequence is $\{u_k\}$, the hold is an ℓ-th order B-spline hold* (3.5) *and the continuous-time system is $G(s) = s^{-r}$, $r > 0$. The output sequence is $\{y_k = y(kh)\}$. For a high-order Runge-Kutta method, i.e., $\kappa \geq r+\ell$, the equivalent discrete-time transfer function is given by the expression in* (3.9)*, i.e.,*

$$G_q(z) = \frac{h^r}{(r+\ell)!}\frac{B_{r+\ell}(z)}{z^\ell (z-1)^r}. \tag{3.21}$$

Proof: Consider that the normal form of the linear system in (3.11) given by

$$\begin{aligned}
y(t) &= x_1(t) && (3.22a)\\
\dot{x}_1(t) &= x_2(t) && (3.22b)\\
&\vdots \\
\dot{x}_{r-1}(t) &= x_r(t) && (3.22c)\\
\dot{x}_r(t) &= u(t) = x_{r+1}(t) && (3.22d)\\
\dot{x}_{r+1}(t) &= u^{(1)}(t) = x_{r+2}(t) && (3.22e)\\
&\vdots \\
\dot{x}_{r+\ell}(t) &= u^{(\ell)}(t) = x_{r+\ell+1}(t). && (3.22f)
\end{aligned}$$

where $x = [x_1(t), \cdots, x_{r+\ell+1}(t)]^T$ is the state vector, $y(t)$ is the system output and $u^{(\ell)}(t)$ corresponds to the ℓ-th derivative of $u(t)$. This derivative is generated by the ZOH in Figure 3.2, i.e. (see Lemma 3.1)

$$u^{(\ell)}(t) = \tilde{u}_k;\; kh \leq t < kh+h. \tag{3.23}$$

According to Definition 2.3, using a Runge-Kutta expansion of order κ, corresponds to perform a Taylor series expansion of the system in (3.22) up to the order κ, which yields:

$$x_1(kh+\tau) = x_1(kh) + \tau x_1^{(1)}(kh) + \cdots + \frac{\tau^\kappa}{\kappa!} x_1^{(\kappa)}(kh) \tag{3.24a}$$

$$x_2(kh+\tau) = x_2(kh) + \tau x_2^{(1)}(kh) + \cdots + \frac{\tau^{\kappa-1}}{(\kappa+1)!} x_2^{(\kappa)}(kh) \tag{3.24b}$$

$$\vdots$$

$$x_{r+\ell}(kh+\tau) = x_{r+\ell}(kh) + \tau x_{r+\ell}^{(1)}(kh) + \cdots + \frac{\tau^\kappa}{\kappa!} x_{r+\ell}^{(\kappa)}(kh), \tag{3.24c}$$

where $0 \leq \tau < h$. From Remark 3.3, higher-order derivatives are all equal to zero. Then, replacing the derivatives by the associated states, we obtain:

$$x_{1,k+1} = x_{1,k} + hx_{2,k} + \frac{h}{2!}x_{3,k} + \cdots + \frac{h^{r+\ell-1}}{(r+\ell-1)!}x_{r+\ell,k} + \frac{h^{r+\ell}}{(r+\ell)!}\tilde{u}_k \tag{3.25a}$$

$$x_{2,k+1} = x_{2,k} + hx_{3,k} + \frac{h}{2!}x_{4,k} + \cdots + \frac{h^{(r+\ell-1)}}{(r+\ell-1)!}\tilde{u}_k \tag{3.25b}$$

$$\vdots$$

$$x_{r+\ell,k+1} = x_{r+\ell,k} + h\tilde{u}_k, \tag{3.25c}$$

where we have used the notation $x_{i,k} = x_i(kh)$. Then, using Corollary 3.2, we can rewrite (3.25) in the following state-space form:

$$zX(z) = A_q X(z) + B_q F_\ell(z) U(z). \tag{3.26a}$$

$$Y(z) = C_q X(z). \tag{3.26b}$$

where the matrices $A_q \in \mathbb{R}^{(r+\ell)\times(r+\ell)}$, $B_q \in \mathbb{R}^{(r+\ell)\times 1}$ and $C_q \in \mathbb{R}^{1\times(r+\ell)}$ are given by,

$$A_q = \begin{bmatrix} 1 & h & \frac{h^2}{2!} & \cdots & \frac{h^{r+\ell-1}}{(r+\ell-1)!} \\ 0 & 1 & h & \cdots & \frac{h^{r+\ell-2}}{(r+\ell-2)!} \\ 0 & 0 & \ddots & \ddots & \vdots \\ \vdots & \vdots & & \ddots & h \\ 0 & 0 & 0 & \cdots & 1 \end{bmatrix}, \quad B_q = \begin{bmatrix} \frac{h^{r+\ell}}{(r+\ell)!} \\ \frac{h^{r+\ell-1}}{(r+\ell-1)!} \\ \vdots \\ \frac{h^2}{2!} \\ h \end{bmatrix} \tag{3.27a}$$

$$C_q = \begin{bmatrix} 1 & 0 & 0 & \cdots & 0 \end{bmatrix}. \tag{3.27b}$$

The matrices in (3.27) correspond to the exact sampled-data model of the $(r+\ell)$-th order integrator in (3.11) (see Example 1). Then, the discrete-time transfer function is given by

$$G_q(z) = C_q(zI - A_q)^{-1} B_q \, F_\ell(z). \tag{3.28}$$

$$G_q(z) = \frac{h^{r+\ell}}{(z-1)^{r+\ell}} \frac{B_{r+\ell}(z)}{(r+\ell)!} \frac{1}{h^\ell} \frac{(z-1)^\ell}{z^\ell}. \tag{3.29}$$

Thus, the result in (3.9) is readily obtained. ■

Corollary 3.7 *Similar to Theorem 3.5, if we consider a fast sampling rate and a B-spline hold, the associated sampled-data model for the continuous-time system* (2.1)*, having relative degree r, can be asymptotically characterized by* (3.14)*.*

3.3.2 Low-Order Runge-Kutta Methods

We define a Runge-Kutta method to be of low order if $\kappa < r + \ell$. In this case, the order of the method (i.e., the Taylor series expansion) is not sufficient to exactly represent $u(t)$ and its derivatives. As a consequence, in the following result, we obtain an approximate sampled-data model for an r-th order integrator, whose sampling zeros depend on the order of the Runge-Kutta method κ.

Theorem 3.8 *Consider a sampled-data system, where the input sequence is $\{u_k\}$, the hold is an ℓ-th order B-spline hold* (3.2) *and the continuous-time system is $G(s) = s^{-r}$, $r > 0$. The output sequence is $\{y_k = y(kh)\}$. For a low-order Runge-Kutta method, i.e., $\kappa < r + \ell$, the equivalent discrete-time transfer function is given by*

$$\tilde{G}_q(z) = C_q(zI - A_q)^{-1}\tilde{B}_q\, V(z)F_\ell(z). \tag{3.30}$$

where A_q and C_q are given in (3.27)*, $\tilde{B}_q$ is given by* (3.35)-(3.36) *and $V(z)$ is given by* (3.34)*.*

Proof: As in the proof of Theorem 3.6, a (low-order) Runge-Kutta method of order κ corresponds to a truncated Taylor serie expansion of order κ, as given in (3.24). Replacing the derivatives by the associated states (see equation (3.22)), we have that:

$$x_{1,k+1} = x_{1,k} + hx_{2,k} + \cdots + \frac{h^{\kappa-1}}{(\kappa-1)!}x_{\kappa,k} + \frac{h^\kappa}{\kappa!}x_{\kappa+1,k} \tag{3.31a}$$

$$\vdots$$

$$x_{r+\ell-\kappa,k+1} = x_{r+\ell-\kappa,k} + \cdots + \frac{h^{\kappa-1}}{(\kappa-1)!}x_{r+\ell+1,k} + \frac{h^\kappa}{\kappa!}x_{r+\ell,k} \tag{3.31b}$$

$$x_{r+\ell-\kappa+1,k+1} = x_{r+\ell-\kappa+1,k} + \cdots + \frac{h^{\kappa-1}}{(\kappa-1)!}x_{r+\ell,k} + \frac{h^\kappa}{\kappa!}\tilde{u}_k \tag{3.31c}$$

$$\vdots$$

$$x_{r+\ell,k+1} = x_{r+\ell,k} + h\tilde{u}_k. \tag{3.31d}$$

Notice that (3.31a)-(3.31b) correspond to the κ-th order truncation of the Taylor Series expansions and, thus, they are only an approximation of the exact (finite order) expansion. On the other hand, equations (3.31c)-(3.31d) are exact since the remaining terms of the Taylor Series expansion are equal to zero (see Remark 3.3).

The expressions in (3.31) can be written in the z-domain. It can be noticed that, for the last κ states in (3.31c)-(3.31d), the exact sampled-data model of a κ-th order integrator is obtained (see Theorem 3.6). The last κ states can be expressed in transfer function form which explicitly shows the presence of the Euler-Frobenius polynomials, i.e.,

$$X_1(z) = \frac{h}{(z-1)}X_2(z) + \frac{h^2}{2!(z-1)}X_3(z) + \cdots + \frac{h^\kappa}{\kappa!(z-1)}X_{\kappa+1}(z) \tag{3.32a}$$

$$X_2(z) = \frac{h}{(z-1)}X_3(z) + \frac{h^2}{2!(z-1)}X_4(z) + \cdots + \frac{h^\kappa}{\kappa!(z-1)}X_{\kappa+2}(z) \tag{3.32b}$$

$$\vdots$$

$$X_{r+\ell-\kappa}(z) = \left[\frac{h^\kappa B_\kappa(z)}{\kappa!(z-1)^\kappa} + \cdots + \frac{h^\kappa B_2(z)}{2!(\kappa-1)!(z-1)^2} + \frac{h^\kappa B_1(z)}{\kappa!(z-1)}\right] F_\ell(z)U(z) \tag{3.32c}$$

$$X_{r+\ell-\kappa+1}(z) = \frac{h^\kappa}{\kappa!}\frac{B_\kappa(z)}{(z-1)^\kappa}F_\ell(z)U(z) \tag{3.32d}$$

$$\vdots$$

$$X_{r+\ell}(z) = \frac{hB_1(z)}{(z-1)}F_\ell(z)U(z). \tag{3.32e}$$

A state-space representation of the model (3.32) is given by

$$z\tilde{X}(z) = A_q\tilde{X}(z) + \tilde{B}_q V(z)F_\ell(z)U(z) \tag{3.33a}$$

$$\tilde{Y}(z) = C_q\tilde{X}(z) \tag{3.33b}$$

where $\tilde{X}(z) = [X_1(z), X_2(z)\cdots, X_{r+\ell-\kappa}(z)]^T$, $\tilde{Y}(z)$ is the system output, the matrices $A_q \in \mathbb{R}^{(r+\ell-\kappa)\times(r+\ell-\kappa)}$ and $C_q \in \mathbb{R}^{1\times(r+\ell-\kappa)}$ are as defined in (3.27), $V(z) \in \mathbb{R}^{\kappa\times 1}$ is given by

$$V(z) = \begin{bmatrix} \frac{h^\kappa B_\kappa(z)}{\kappa!(z-1)^\kappa} \\ \frac{h^{\kappa-1}B_{\kappa-1}(z)}{(\kappa-1)!(z-1)^{\kappa-1}} \\ \vdots \\ \frac{h^2 B_2(z)}{2!(z-1)^2} \\ \frac{hB_1(z)}{(z-1)} \end{bmatrix}, \tag{3.34}$$

and the matrix $\tilde{B}_q \in \mathbb{R}^{(r+\ell-\kappa)\times\kappa}$ depends on $r+\ell$ and κ. When $r+\ell-\kappa \leq \kappa$, then

$$\tilde{B}_q = \begin{bmatrix} \frac{h^{r+\ell-\kappa}}{(r+\ell-\kappa)!} & \cdots & \frac{h^k}{k!} & 0 & \cdots & 0 \\ \frac{h^{r+\ell-\kappa-1}}{(r+\ell-\kappa-1)!} & \frac{h^{r+\ell-\kappa}}{(r+\ell-\kappa)!} & \cdots & \frac{h^k}{k!} & & \vdots \\ \vdots & \vdots & & & \ddots & 0 \\ h & \frac{h^2}{2!} & \frac{h^3}{3!} & \cdots & \cdots & \frac{h^\kappa}{\kappa!} \end{bmatrix}. \tag{3.35}$$

On the other hand, if $r + \ell - \kappa > \kappa$, then $\tilde{B}_q$ is given by

$$\tilde{B}_q = \left[\begin{array}{ccccc} 0 & & \cdots & & 0 \\ 0 & & \cdots & & 0 \\ \hline \frac{h^\kappa}{\kappa} & 0 & 0 & \cdots & 0 \\ \frac{h^{\kappa-1}}{(\kappa-1)!} & \frac{h^\kappa}{\kappa!} & 0 & & \vdots \\ \vdots & \vdots & & \ddots & \vdots \\ \frac{h^2}{2!} & \frac{h^3}{3!} & \cdots & \frac{h^\kappa}{\kappa!} & 0 \\ h & \frac{h^2}{2!} & \frac{h^3}{3!} & \cdots & \frac{h^\kappa}{\kappa!} \end{array}\right] = \left[\begin{array}{cccc} & 0_{(r+\ell-2\kappa)\times\kappa} & & \\ \hline \frac{h^\kappa}{\kappa!} & 0 & \cdots & 0 \\ \vdots & \ddots & & \vdots \\ \frac{h^2}{2!} & \cdots & \frac{h^\kappa}{\kappa!} & 0 \\ h & \frac{h^2}{2!} & \cdots & \frac{h^\kappa}{\kappa!} \end{array}\right]. \tag{3.36}$$

Finally, the discrete transfer function corresponding to (3.32) is as defined in (3.30). ■

Corollary 3.9 *Similarly as in Section 3.3.1, the sampled-data model corresponding to the continuous-time linear system* (2.1)*, having relative degree r, when using an ℓ-th order B-spline hold and for a given Runge-Kutta order $\kappa < r + \ell$ can be asymptotically characterized for fast sampling rates by the model* (3.30)*, where the sampling zeros are defined by the Euler-Frobenius polynomials that appear in $V(z)$.*

Remark 3.10 *The results in Theorems 3.6 and 3.8 shows that, for a given order κ of the Runge-Kutta method, the sampling zeros polynomials depend only on $r + \ell$. Table 3.1 and Table 3.2 show the sampling zeros polynomials for Runge-Kutta methods of order $\kappa = 2$ and $\kappa = 3$, respectively, and for different values of the relative degree r and hold order ℓ. Notice that when the high-order condition for the Runge-Kutta method is satisfied ($\kappa \geq r + \ell$) the sampling zeros are explicitly given by the Euler-Frobenius polynomials (see equation* (3.21)*). On the other hand, if κ is lower than $r + \ell$, then the sampling zeros polynomials are given by the transfer function* (3.30) *in Theorem 3.8. Tables 3.1 and 3.2 also show that the sampling zeros polynomial depend only on $r + \ell$, i.e., they are the same along the (anti) diagonals of the tables.*

ℓ \ r	1	2	3	4
0	1	$z+1$	z	z^2+4z-1
1	$z+1$	z	z^2+4z-1	$3z^2+2z-1$
2	z	z^2+4z-1	$3z^2+2z-1$	z^3+9z^2-z-1

Table 3.1: Sampling zeros for Runge-Kutta order $\kappa = 2$

In what follows, we present a numerical example to illustrate the results in Theorem 3.6 and Theorem 3.8. In addition, we analyze the relative error associated with the frequency response of the exact discrete-time model $R^{Ex}(\omega)$ and the approximate model $R^{RK}(\omega)$ with respect to the continuous-time system. We consider the

ℓ \ r	1	2	3	4
0	1	$z+1$	z^2+4z+1	$7z^2+4z+1$
1	$z+1$	z^2+4z+1	$7z^2+4z+1$	$2z^3+9z^2+1$
2	z^2+4z+1	$7z^2+4z+1$	$2z^3+9z^2+1$	$2z^4+37z^3+33z^2-5z+5$
3	$7z^2+4z+1$	$2z^3+9z^2+1$	$2z^4+37z^3+33z^2-5z+5$	$5z^4+16z^3+2z^2+1$

Table 3.2: Sampling zeros for Runge-Kutta order $\kappa = 3$

following relative error measures:

$$R^{Ex}(\omega) = \left| \frac{G(j\omega) - G_q(e^{j\omega h})}{G(j\omega)} \right| \tag{3.37}$$

$$R^{RK}(\omega) = \left| \frac{G(j\omega) - \tilde{G}_q(e^{j\omega h})}{G(j\omega)} \right|, \tag{3.38}$$

where $G(j\omega)$ is continuous-time system, $G_q(e^{j\omega h})$ and $\tilde{G}_q(e^{j\omega h})$ are the exact and approximate discrete-time models, respectively.

Example 4 *In this example we consider a continuous-time system of relative degree $r = 2$, given by*

$$G(s) = \frac{\omega_n^2}{s^2 + 2\xi\omega_n s + \omega_n^2}, \tag{3.39}$$

where $\xi = 0.5$, $\omega_n = 2$. We consider the case where the continuous-time input $u(t)$ is generated by a second order B-spline hold, i.e., $\ell = 2$. Our interest is to obtain the discrete-time function $\tilde{G}_q(z)$ when using a Runge-Kutta method of order $\kappa = 3$.

According to (3.3), the digital filter corresponding to a second order B-spline hold can be written as

$$F_2(z) = \frac{(z-1)^2}{h^2 z^2}. \tag{3.40}$$

From Theorem 3.8, the approximate discrete-time transfer function $\tilde{G}_q(z)$ when using a Runge-Kutta method of order $\kappa = 3$ and sampling period $h = 0.1$ is given by

$$\tilde{G}_q(z) = \frac{0.0073(6.32z^2 + 2.59z + 1)}{z^2(z^2 - 1.58z + 0.657)}. \tag{3.41}$$

Notice that, the asymptotic zeros of $\tilde{G}_q(z)$ are given by Theorem 3.8 and they are shown in Table 3.2, i.e., they are given by the polynomial $7z^2 + 4z + 1$. On the other hand, according to equation (3.21), the exact discrete-time transfer function $G_q(z)$ is given by

$$G_q(z) = \frac{0.0643(1.286z^3 + 13.0z^2 + 11.95z + 1)}{24z^2(z^2 - 1.58z + 0.657)}. \tag{3.42}$$

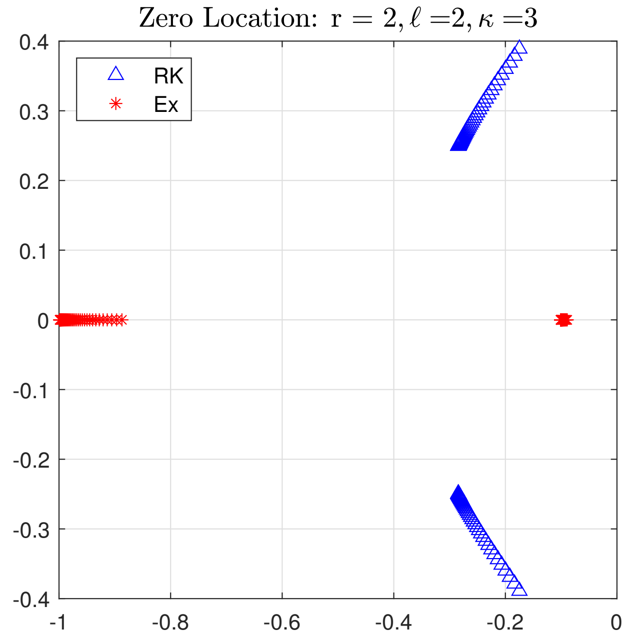

Figure 3.3: Sampling zero locations for the exact and the approximate discrete-time models for different sampling periods.

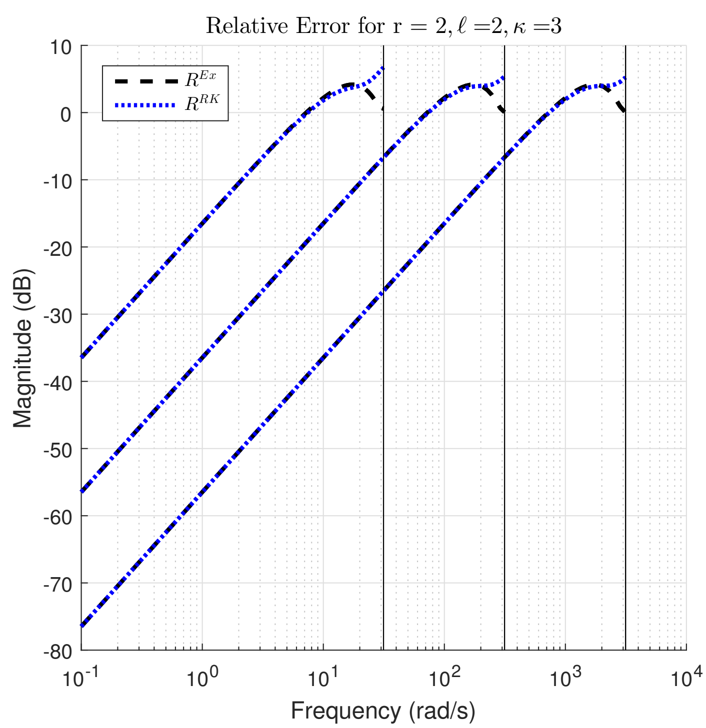

Figure 3.4: Relative errors $R^{Ex}(\omega)$ and $R^{RK}(\omega)$ for sampling periods $h \in [0.001, 0.1]$.

According to Theorem 3.6, the asymptotic sampling zeros of $G_q(z)$ are given by *the Euler-Frobenius polynomial of order* $r + \ell = 4$*, i.e,.* $z^3 + 11z^2 + 11z + 1$.

Figure 3.3 shows the movement of the zeros of the discrete-time models when the sampling period $h \in [\,0.001,\, 0.1\,]$*. Note that due to the scale of the figure only two of the three sampling zeros of* $G_q(z)$ *appear in the plot. Also, notice that the zeros of the approximate discrete-time function converge to the zeros of the exact model as* h *goes to* 0.

Notice that (3.41) *and* (3.42) *have the same poles. However, the approximate discrete-time system has fewer zeros than the exact discrete-time model due to the order of the Runge-Kutta method* ($\kappa = 3$) *compared to the continuous-time relative degree plus the order of the hold* ($r + \ell = 4$).

In order to compare the accuracy of the discrete-time models with respect to the continuous-time system, Figure 3.4 shows the relative errors in (3.37) *and* (3.38) *for three different sampling periods* $h = 0.1$, $h = 0.01$ *and* $h = 0.001$*. We notice that the exact and approximate discrete-time models provide similar accuracy for low and high frequencies. However, near the Nyquist frequency the exact discrete-time model provides higher accuracy. Moreover, as the sampling period goes to* 0*, the error between both models is reduced.*

3.4 Summary

We have modeled the smoothness of the system input using a generalized hold device based on B-Spline functions. It was previously established that the order of the Euler-Frobenius polynomial, which characterizes the asymptotic sampling zeros, depends on the continuous-time system relative degree. This chapter shows that the order of the hold device increases the order of the sampling zeros polynomial.

We also characterized the asymptotic sampling zeros of (approximate) sampled-data models using a Runge-Kutta method. Moreover, we have shown that the order of the Runge-Kutta method applied to the continuous-time system directly impacts the location of the zeros of the corresponding discrete-time model. In fact, we obtained novel polynomials that characterize the sampling zeros when the order of the integration strategy is low compared to the continuous-time system relative degree and hold order.

In summary, we have shown that the presence of asymptotic sampling zeros can be explained as a consequence of the integration strategy underlying the discretization process and on (the assumptions on) how the continuous-time input is generated. These results explicitly show that the sampling zeros are a consequence of how the system is discretized: how the continuous-time input is generated and how the differential equation description is translated into the discrete-time domain.

In Chapter 5, we extend these results to the sampling zero dynamics that appear in approximate nonlinear discrete-time models.

4 CONTROL LAW FOR LINEAR SYSTEMS

In this chapter our interest is on exploring how to design a discrete-time control law based on approximate models. For this thesis we will use polynomial pole-assignment (see, for example, [109]). We first analyze the continuous-time case to set ideas.

The heuristic idea is that, at high frequencies, a continuous-time system of relative degree r behaves similarly to an r-th order integrator. The latter approximation has been applied, for example, in [65, 110, 111]. Thus, one should be able to design a wide-bandwidth control law for stably invertible linear system by knowing only the relative degree and high frequency gain.

The extension of the above idea to the discrete-time domain faces extra difficulty. For continuous-time systems having relative degree two, the asymptotic sampling zero is on the stability boundary, and for relative degree larger than two, the asymptotic zeros lie outside the stability region. The presence of such non-minimum phase zeros represent a significant complication, in particular for wide-bandwidth control when the closed-loop bandwidth approaches the Nyquist rate for the given sampling period [112].

Therefore, to address the sampling zero issue, two approximate models are proposed: the former covers the case where the closed-loop bandwidth is significantly less than the Nyquist frequency, while the second includes the asymptotic sampling zero, i.e., this covers the case when the closed-loop bandwidth is near the Nyquist frequency. Then, it is shown that the robustness properties of these two models differ due to the presence of sampling zeros.

Besides, we study whether, under some conditions, the roots of the nominal and true closed-loop polynomials are close in some sense. The latter is one of the core problems in perturbation theory, and a useful result in this context is the Ostrowski's Theorem [113, page 276]. Thus, a preliminary theoretical analysis is provided for degree two, showing that the design based on the approximate model stabilizes the true system for the continuous and sampled-data cases.

4.1 Continuous-Time Control Law

In this section, we start considering an r-th order continuous-time system having transfer function

$$G_c(s) = \frac{B_c(s)}{A_c(s)} = \frac{b}{s^r + a_1 s^{r-1} + \dots a_r}. \tag{4.1}$$

We are interested in designing a continuous-time control law based on the following approximate model:

$$G_0(s) = \frac{B_0(s)}{A_0(s)} = \frac{b}{s^r}. \tag{4.2}$$

Several designs are possible, however, we are focused in polynomial pole-assignment. Thus, a biproper controller of order $r-1$ can be designed such that:

$$C(s) = \frac{p_0 s^{r-1} + \dots + p_{r-1}}{s^{r-1} + \dots + l_{r-1}} \tag{4.3}$$

with a target closed-loop polynomial of the form:

$$A^*_{cl}(s) = A_0(s)L(s) + B_0(s)P(s) = (s + \alpha^*)^{2r-1}. \tag{4.4}$$

Note that the closed-loop poles are all assigned to $s = -\alpha^*$. Then, using (4.2), we have that the closed-loop polynomial is given by

$$\begin{aligned} s^r\left(s^{r-1} + l_1 s^{r-2} + \cdots + l_{r-1}\right) + K\left(p_0 s^{r-1} + \cdots + p_{r-1}\right) &= (s+\alpha^*)^{2r-1} \\ &= \sum_{k=0}^{2r-1} \binom{2r-1}{k} s^{2r-1-k} (\alpha^*)^k \end{aligned} \tag{4.5}$$

Then, by equating coefficients, the controller parameters can be obtained as follows:

$$l_1 = \binom{2r-1}{1}\alpha^* \tag{4.6a}$$

$$l_2 = \binom{2r-1}{2}(\alpha^*)^2 \tag{4.6b}$$

$$\vdots \tag{4.6c}$$

$$p_0 = \binom{2r-1}{r-1}\frac{(\alpha^*)^r}{b} \tag{4.6d}$$

$$\vdots \tag{4.6e}$$

$$p_{r-1} = \binom{2r-1}{2r-1}\frac{(\alpha^*)^{2r-1}}{b} \tag{4.6f}$$

On the other hand, the true closed-loop polynomial is given by

$$A_{cl}(s) = A_c(s)L(s) + B_c(s)P(s), \tag{4.7}$$

where $A_c(s)$ and $B_c(s)$ are given in (4.1) and $L(s)$ and $P(s)$ are given by (4.6). Once the controller is designed based on the approximate model (4.2), it is necessary to check if the true closed-loop stability is guaranteed, i.e., we need to check the robust stability. A first attempt to measure the performance of $C(s)$ is through the Robust Stability Theorem (see, for example, [109, 114]), namely

$$|T_0(s)G_\Delta(s)| < 1; \qquad \forall \quad s = jw, \tag{4.8}$$

where $T_0(s)$ is the nominal closed-loop complementary sensitivity function given by

$$T_0(s) = \frac{G_0(s)C(s)}{1 + G_0(s)C(s)}, \tag{4.9}$$

and $G_\Delta(s)$ is the relative model error, i.e.,

$$G_\Delta(s) = \left| \frac{G(s) - G_0(s)}{G_0(s)} \right|. \tag{4.10}$$

The core hypothesis is that for α^* positive and sufficiently large, the controller (4.3) based on (4.2) will stabilize all systems of the form (4.1) provided that the open-loop poles lie in a restricted region. Moreover, the true and nominal closed-loop performance will be nearly indistinguishable.

On the other hand, the true closed-loop complementary function is defined as

$$T(s) = \frac{G_c(s)C(s)}{1 + G_c(s)C(s)}, \tag{4.11}$$

We introduce the following assumptions on the location of the open loop poles of the true system.

Assumption 4.1 *We assume that the poles, α_i, $i = 1, \ldots, r$ of $G(s)$, i.e., the roots of the polynomial $A(s)$ in* (4.1)*, belong to a bounded region in the complex plane, such that $|\alpha_i| < M$.*

Assumption 4.2 *We assume a high-bandwidth control loop, i.e., $|\alpha^*| \gg M$.*

Motivating by Assumption 4.2, we recall that at high-frequencies, for sampled-data models, the role of the sampling zeros become important, since they because the sampling impact the discrete-time response near the Nyquist frequency.

In what follows, we study the second order case in detail. Thus, we consider the system

$$G_c(s) = \frac{b}{(s + \alpha_1)(s + \alpha_2)}, \tag{4.12}$$

which leads to the model (4.2), with $r = 2$, i.e.,

$$G_0(s) = \frac{b}{s^2}. \tag{4.13}$$

Then, based on the approximate model above, we design a suitable biproper controller of the form

$$C(s) = \frac{p_0 s + p_1}{s + l_1}, \tag{4.14}$$

where the parameters are given by

$$p_1 = \frac{(\alpha^*)^3}{b}, \qquad p_0 = \frac{3(\alpha^*)^2}{b}, \qquad l_1 = 3\alpha^*. \tag{4.15}$$

Example 5 *As a specific numerical example, we consider $b = 1$, $\alpha_1 = 1$, $\alpha_2 = -1$. Based on the above discussion and Assumption 4.1, we consider several values of α^* satisfying $\alpha^* > M > |\alpha_{1,2}|$.*

Figure 4.1a shows the resulting normalized step responses of the closed-loop transfer function, i.e.,

$$T_0(s) = \frac{G_0(s)C(s)}{1 + G_0(s)C(s)}, \tag{4.16}$$

achieved when using the nominal model (4.13). *On the other hand, Figure 4.1b shows the normalized step responses of the true closed-loop system, i.e.,*

$$\frac{T(s)}{T(0)} = \frac{G_c(s)C(s)}{T(0)\left(1 + G_c(s)C(s)\right)}, \tag{4.17}$$

when the same controller is applied to the true plant (4.12).

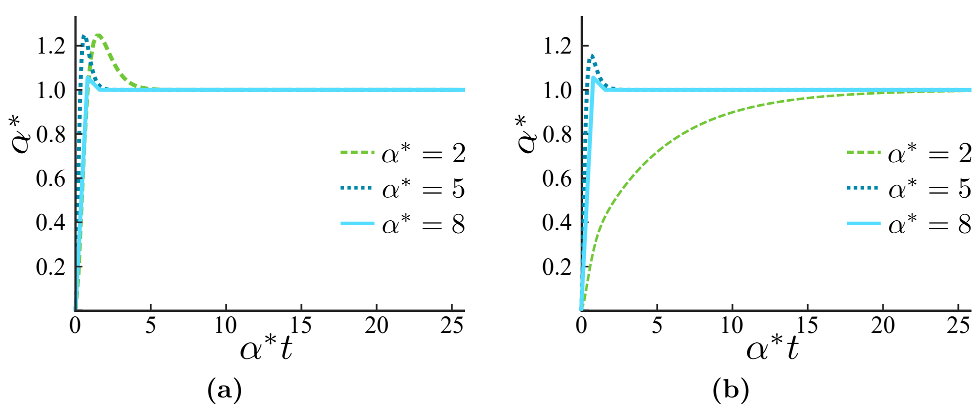

Figure 4.1: Step response for (a) nominal and (b) true closed-loop.

Notice that the nominal and the true closed-loop responses (Figures 4.1a and 4.1b, respectively), are very similar except for the case when $\alpha^* = 2$. On the other *hand, particularizing to the above problem, we have that*

$$T_0(s) = \frac{B_0(s)P(s)}{A_{cl}^*(s)}, \tag{4.18}$$

$$G_\Delta(s) = -\frac{(\alpha_1+\alpha_2)s+\alpha_1\alpha_2}{(s+\alpha_1)(s+\alpha_2)} \tag{4.19}$$

Taking $s = jw$ and considering $w = 0$, yields to

$$T_0(j0) = 1, \qquad G_\Delta(j0) = -1. \tag{4.20}$$

Hence, condition (4.8) *is not satisfied and robust stability cannot be guaranteed using this approach.*

The remainder of this chapter is focused on deriving a relationship between the bound M defined in Assumption 4.1 and the target closed-loop pole location α^*, such that for the controller (4.14)–(4.15) is able to stabilize both, the approximate model (4.13) and the true system (4.12).

4.2 Ostrowski's Theorem

In this section, our interest is to find a bound between the roots of the nominal and true closed-loop polynomials. We apply the Ostrowski's Theorem, which is described below.

Theorem 4.3 *Consider two polynomials*

$$f(s) = a_0 s^n + a_1 s^{n-1} + \cdots + a_n = \prod_{i=1}^{n}(s-\theta_i^f) \tag{4.21}$$

$$g(s) = b_0 s^n + b_1 s^{n-1} + \cdots + b_n = \prod_{i=1}^{n}(s-\theta_i^g), \tag{4.22}$$

where $a_0 = b_0 = 1$. Let

$$T = 2 \max_{1\le k\le n}\left(|a_k|^{1/k}, |b_k|^{1/k}\right). \tag{4.23}$$

Then the roots θ_i^f and θ_i^g of $f(s)$ and $g(s)$ can be enumerated in such a way that

$$\max_i |\theta_i^f - \theta_i^g| \le (2n-1)\left\{\sum_{k=1}^{n}|a_k - b_k|T^{n-k}\right\}^{1/n}. \tag{4.24}$$

Proof: See [113]. ■

Remark 4.4 *The above result provides a mean of estimating the differences between the roots θ_i^f and θ_i^g in terms of the coefficients a_i and b_i. The result was embellished by [115], where the factor $(2n-1)$ is replaced by $(n-1)$ if n is even, and by n when is odd.*

Theorem 4.3 provides a sufficient condition for asymptotic stability of the closed-loop system given by the true system (4.12) and the controller defined by (4.14)–(4.15), which is based on the approximate system (4.13). We study again the second order case, however, a similar strategy is anticipated to apply for the general case (4.1).

Theorem 4.5 *Subject to Assumption 4.1, a sufficient condition for closed-loop stability of the true plant $G_c(s)$, given in* (4.12)*, under controller* (4.14)-(4.15)*, is $\alpha^* \geq \kappa M$, for some sufficiently large positive real number κ.*

Proof: The numerator gain b cancels in the controller, so without loss of generality, we consider $b = 1$. Thus, the system (4.12) can by rewritten as follows

$$G_c(s) = \frac{1}{s^2 + t_1 s + t_2} = \frac{B(s)}{A(s)}, \tag{4.25}$$

where $t_1 = \alpha_1 + \alpha_2$ and $t_2 = \alpha_1\alpha_2$. Also, we notice that the polynomials (4.21)-(4.22) for this particular problem are given by

$$\begin{aligned} f(s) &= s^3 + 3(\alpha^*)s^2 + 3(\alpha^*)^2 s + (\alpha^*)^3 && (4.26)\\ g(s) &= A(s)L(s) + B(s)P(s) \\ &= s^3 + (l_1 + t_1)s^2 + (t_1 l_1 + t_2 + p_0)s + (t_2 l_1 + p_1). && (4.27)\end{aligned}$$

Replacing the parameters in (4.15), considering Assumption 4.1, and defining $S = \alpha^*/M$. Then, the bounds for the coefficients in (4.26) and (4.27) are given by

$$\begin{aligned} |a_1| &\leq 3SM, & |b_1| &\leq 2M + 3SM, && (4.28a)\\ |a_2| &\leq 3S^2M^2, & |b_2| &\leq 6SM^2 + M^2 + 3S^2M^2, && (4.28b)\\ |a_3| &\leq S^3M^3, & |b_3| &\leq 3SM^3 + S^3M^3. && (4.28c)\end{aligned}$$

Therefore, based on Remark 4.4 and using (4.24), we have

$$\max_i |\theta_i^f - \theta_i^g| \leq 3\left\{\sum_{k=1}^{3} |a_k - b_k| T^{n-k}\right\}^{1/3}, \tag{4.29}$$

where

$$\begin{aligned} T \leq & 2\max\Big(3SM, \sqrt{3}SM, SM, 3SM + 2M, \\ & (6SM^2 + M^2 + 3S^2M^2)^{1/2}, (3SM^3 + S^3M^3)^{1/3}\Big). \end{aligned} \tag{4.30}$$

The first 3 elements do not contribute to the maximization since they are smaller than the fourth element, yielding:

$$\begin{aligned} T &\leq 2\max\left((3S+2)M, ((3S^2 + 6S + 1)M^2)^{1/2}, ((S^3 + 3S)M^3)^{1/3}\right) \\ T &\leq 2(3S + 2)M. && (4.31)\end{aligned}$$

where the last inequality holds true for any $S \geq 0$. Replacing T in (4.29) and bounding each term $|a_k - b_k|$, we obtain

$$\begin{aligned}
&\max_i |\theta_i^f - \theta_i^g| \leq 3\Big\{(2M)T^2 + (6SM^2 + M^2)T + (3SM^3)\Big\}^{1/3} \\
&\leq 3M\left\{8(3S+2)^2 + 2(6S+1)(3S+2) + 3S\right\}^{1/3} \\
&\leq 3M\left\{108S^2 + 129S + 36\right\}^{1/3} \qquad (4.32)
\end{aligned}$$

Thus, closed-loop stability is ensured if the right hand side of the above inequality is less than $|\alpha^*| = SM$. This yields

$$\begin{aligned}
&\max_i |\theta_i^f - \theta_i^g| < |\alpha^*| \\
\iff\quad & 3M\left(108S^2 + 129S + 36\right)^{1/3} < SM \\
\iff\quad & S^3 - 27(36 + 129S + 108S^2) > 0 \qquad (4.33)
\end{aligned}$$

which holds true for $S = \kappa \geq 2918$. ■

4.3 Stably Invertible Continuous-Time Systems

In Sections 4.1 and 4.2, we considered continuous-time systems with no zeros. This section considers more general linear systems provided that the polynomial $B(s)$ is Hurwitz, i.e., all its roots are located in the open left-half of the complex plane [116].

We illustrate via a numerical study based on the following third order system

$$G_c(s) = \frac{b\,(s+\beta_1)}{(s+\alpha_1)(s+\alpha_2)(s+\alpha_3)} \qquad (4.34)$$

where $\beta_1 > 0$. Note that the system has relative degree $r = n - m = 2$. Thus, design a control law to place all the closed-loop poles at $s = -\alpha^*$ using the approximate model (4.13), which yields to the control law (4.14)- (4.15). Particularizing the system (4.34), we choose $b = 2$ $\beta_1 = 4$, $\alpha_1 = -2$, $\alpha_2 = 2$, $\alpha_3 = 3$. Figure 4.2 shows the normalized true closed-loop response for different values of α^*. Notice that, similarly to Example 5, as long as α^* is sufficiently large the true closed-loop system is stable (see Figure 4.2a), whilst, when α^* is not sufficiently large, then the system can be unstable (see Figure 4.2b).

4.4 Discrete-Time Control Law

Following the ideas presented in Section 2.3.3, in this section we propose a controller based on an approximate model in shift or delta operator. For simplicity,

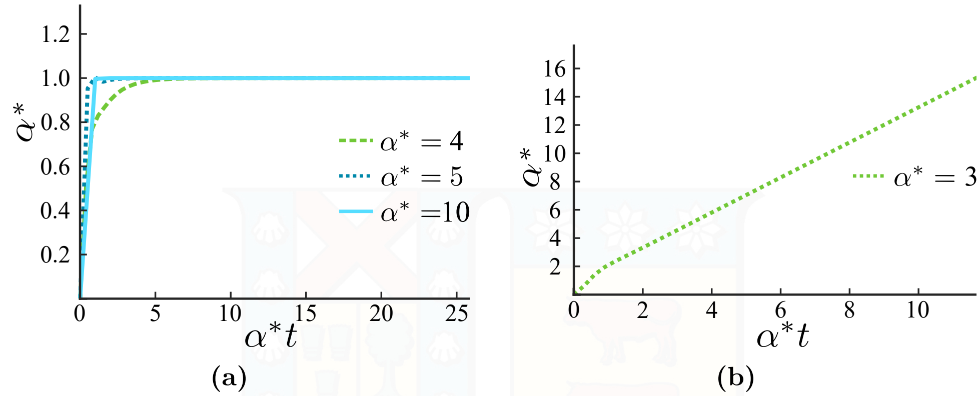

Figure 4.2: Step response for normalized true closed-loop.

we express the time discretization in the δ-domain. However, the results can be easily extended to the z-domain using (1.3).

Considering a sampling period h and assuming that a ZOH generates the system input, we obtain the exact discrete-time model of the form:

$$G(\gamma) = \frac{A_c(\gamma)}{B_c(\gamma)} = b' \, \frac{\bar{P}_r(h\gamma)\,(\gamma^m + c_{m-1}\gamma^{m-1} + \cdots + c_0)}{\gamma^n + d_{n-1}\gamma^{n-1} + \cdots + d_0}, \quad n > m \tag{4.35}$$

where $\bar{P}_r(h\gamma)$ is the sampling zeros polynomial. As mentioned before, for small h, $\bar{P}_r(h\gamma)$ converges to the asymptotic sampling zeros polynomial $P_r(h\gamma)$ defined in (2.87)-(2.90).

Once the sampled-data model is obtained, it is possible to design a discrete-time control law based on the following approximate model:

$$G_0(\gamma) = \frac{A_0(\gamma)}{B_0(\gamma)}. \tag{4.36}$$

We again use polynomial pole assignment to design the controller of order $r-1$,

$$C(\gamma) = \frac{P'(\gamma)}{L'(\gamma)} = \frac{p'_0\gamma^{r-1} + \cdots + p'_{r-1}}{\gamma^{r-1} + \cdots + l'_{r-1}}, \tag{4.37}$$

where the parameters of the controller depend on the approximate model chosen, for example, it is possible to study two cases:

$$G_d^1(\gamma) = \frac{b'}{\gamma^r} \tag{4.38}$$

$$G_d^2(\gamma) = b' \, \frac{P_r(h\gamma)}{\gamma^r}. \tag{4.39}$$

The first model covers the case where the closed-loop bandwidth is significantly less than the Nyquist frequency $\frac{\pi}{T_s}$. The second model includes the asymptotic sampling zeros and, thus, model (4.39) covers the case when the closed-loop bandwidth is near the Nyquist frequency. The nominal target closed-loop polynomial is

$$A^*_{cl}(\gamma) = A_0(\gamma)L'(\gamma) + B_0(\gamma)P'(\gamma) = (\gamma + \alpha^*)^{2r-1}\,, \tag{4.40}$$

where all the closed-loop poles are placed at $\gamma = -\alpha^*$.

Using (4.36), the closed-loop polynomial is given by (4.5) with s replaced by γ. Then, the parameters of the controller are as shown in (4.6). On the other hand, using (4.39), we have

$$\gamma^r\left(\gamma^{r-1} + \cdots + l'_{r-1}\right) + b'\,P_r(h\gamma)\left(p'_0\gamma^{r-1} + \cdots + p'_{r-1}\right) = (\gamma + \alpha^*)^{2r-1}\,. \tag{4.41}$$

Note that, the controller parameters depend on h. On the other hand, the real closed-loop polynomial is given by

$$A_{cl}(\gamma) = A_c(\gamma)P'(\gamma) + B_c(\gamma)L'(\gamma). \tag{4.42}$$

4.5 Second Order Systems with no Finite Zeros

Following the ideas presented in Section 4.1, we are interested in extending the results to a simple sampled-data control law. Thus, we consider that the poles and the zeros of the discrete-time system be $\alpha_1, \ldots, \alpha_n$ and $\beta_1, \ldots, \beta_m$, respectively. The following assumption which a region where the open loop poles and zeros lie.

Assumption 4.6 *The poles and zeros of the discretized system* (4.35) *belong to a bounded region in the complex plane, such that* $|\alpha_i, \beta_i| < R < \frac{1}{h}$.

Analogously to the continuous-time case, we consider a true second-order discrete-time system given by

$$G_d(\gamma) = \frac{b'\,P_r(h\gamma)}{\gamma^2 + t'_1\gamma + t'_2} = \frac{b'\,(1 + \nu\frac{h}{2}\gamma)}{\gamma^2 + t'_1\gamma + t'_2} \tag{4.43}$$

Note that ν tends to 1 as h approaches zero. For the system (4.43), the proposed controller is given by

$$C(\gamma) = \frac{p'_0\gamma + p'_1}{\gamma + l'_1}. \tag{4.44}$$

Therefore, for relative degree $r = 2$, based on the approximate model $G^1_d(\gamma)$, the parameters of the controller are as in (4.15) with s replaced by γ. On the other hand, for the approximate model $G^2_d(\gamma)$, with $\bar{P}_2(h\gamma) = (1 + \gamma\frac{h}{2})$, the parameters are

$$p'_1 = \frac{(\alpha^*)^3}{b'}, \qquad p'_0 = \frac{3(\alpha^*)^2}{b'} - \frac{h}{2}\frac{(\alpha^*)^3}{b'}, \qquad l'_1 = 3\alpha^* - 3\frac{h}{2}(\alpha^*)^2 + \frac{h^2}{4}(\alpha^*)^3. \tag{4.45}$$

In what follows we often use the approximation $\nu \approx 1$, which is valid as the sampling period approaches zero. We have the following result regarding the closed-loop stability of the true and approximates systems:

Theorem 4.7 *Consider the discrete-time model of the form* (4.43)*. Then, for the control law design based on* $G_d^1(\gamma)$ *in* (4.38) *and subject to Assumption 4.6, a sufficient condition for closed-loop stability of the true closed-loop is that the nominal closed-loop poles at* $\gamma = -\alpha^*$ *satisfy* $\frac{1}{h} \gg \alpha^* \gg |\alpha_{1,2}|$*, i.e.,* $\frac{1}{h} \gg \alpha^* > \kappa' R$ *for some sufficiently large positive real number* κ'*.*

Proof: As before, we consider $b' = 1$ and a controller designed for the approximate model given by

$$G_d^1(\gamma) = \frac{1}{\gamma^2}. \tag{4.46}$$

We apply the controller to the true system (4.43), and we use again Theorem 4.3 (Ostrowski's Theorem), where the polynomials are

$$f(\gamma) = \gamma^3 + 3(\alpha^*)\gamma^2 + 3(\alpha^*)^2\gamma + (\alpha^*)^3 \tag{4.47}$$

$$g(\gamma) = \gamma^3 + (l_1' + t_1' + p_0'\frac{\nu h}{2})\gamma^2 + (t_1' l_1' + t_2' + p_0' + p_1'\frac{\nu h}{2})\gamma + (t_2' l_1' + p_1'), \tag{4.48}$$

where the parameters p_i'; $i = 0, 1, 2$ are given by (4.15). We consider Assumption 4.6 and define $K = \alpha^*/R$. Then,

$$|a_1| \leq 3KR, \qquad |b_1| \leq 2R + 3KR + 3\tfrac{\nu h}{2}K^2R^2, \tag{4.49a}$$

$$|a_2| \leq 3K^2R^2, \qquad |b_2| \leq 6KR^2 + R^2 + 3K^2R^2 + \tfrac{\nu h}{2}K^3R^3 \tag{4.49b}$$

$$|a_3| \leq K^3R^3, \qquad |b_3| \leq 3KR^3 + K^3R^3. \tag{4.49c}$$

Thus, proceeding as in the proof of Theorem 4.5, we have that

$$\begin{aligned} T \leq 2\max\Big(&3KR + 2R + 3\tfrac{\nu h}{2}(KR)^2, (3KR^3 + K^3R^3)^{1/3}, \\ &(6KR^2 + R^2 + 3K^2R^2 + \tfrac{\nu h}{2}(KR)^3)^{1/2}\Big) \end{aligned} \tag{4.50}$$

where, as mentioned in (4.30), the first 3 terms in the maximization have been discarded. Moreover, we have that $\nu \approx 1$, for small h, and hence $\nu hKR \approx hKR = h\alpha^* \ll 1$. Thus,

$$T \leq 2\max\Big((4.5K + 2)R, (3K + K^3)^{1/3}R, (6K + 1 + 3K^2 + 0.5K^2)^{1/2}R\Big)$$

$$T \leq 2(4.5K + 2)R, \tag{4.51}$$

where the last inequality holds true for any $K \geq 0$. Thus, the distance between the roots of the polynomials is bounded as

$$\begin{aligned} \max_i |\theta_i^f - \theta_i^g| &\leq 3\left\{(2R + 3\tfrac{\nu h}{2}K^2R^2)T^2 + (6KR^2 + R^2 + \tfrac{\nu h}{2}K^3R^3)T + 3KR^3\right\}^{1/3} \\ &\leq 3\left\{(2R + \tfrac{3}{2}R)(9K + 4)^2R^2 + (6KR^2 + R^2 + \tfrac{1}{2}KR^2)(9K + 4)R + 3KR^3\right\}^{1/3} \\ &\leq 3R\left\{60 + 290K + 342K^2\right\}^{1/3}. \end{aligned} \tag{4.52}$$

where we have used that, since $\frac{1}{h} \gg KR$, then we have that

$$hKR \ll 1 \implies hK^2R < 1 \implies \nu hK^2R < 1 \tag{4.53}$$

since $\nu \approx 1$ as $h \to 0$. Then, closed-loop stability is guaranteed if the right hand side is less than $|\alpha^*| = KR$. This yields

$$\begin{aligned} &\max_i |\theta_i^f - \theta_i^g| < |\alpha^*| \\ \iff\ & 3R\left(60 + 290K + 342K^2\right)^{1/3} < KR \\ \iff\ & K^3 - 27(342K^2 + 290K + 60) > 0 \end{aligned} \tag{4.54}$$

Thus, taking $K = \kappa' \geq 9235$ the theorem is proved. ■

Theorem 4.8 *Consider the discrete-time model of the form* (4.43)*. Then, for a control law design based on* (4.39) *and subject to Assumption 4.6, a sufficient condition for closed-loop stability of the corresponding sampled-data model is that the closed-loop poles satisfy* $\frac{1}{h} \geq \alpha^* > \kappa' R$ *for some sufficiently large positive real number* κ'.

Proof: Again, without loss of generality, we take $b' = 1$. We are interested in designing a controller based on the approximate model that includes the asymptotic sampling zeros. For relative degree $r = 2$, we have

$$G_d^2(\gamma) = \frac{\bar{P}_2(h\gamma)}{\gamma^2} = \frac{1 + \gamma\frac{h}{2}}{\gamma^2}. \tag{4.55}$$

We apply Theorem 4.3, where the polynomials are the same as shown in (4.47)-(4.48), but with the parameters defined in (4.45). Then, considering Assumption 4.6, defining $K = \alpha^*/R$ and using the triangle inequality, we have that the bounds for a_i; $i = 1, 2, 3$ are given by (4.49) and

$$|b_1| \leq 2R + 3KR + \frac{3}{2}h(KR)^2|\nu - 1| + \frac{h^2}{4}(KR)^3|1 - \nu| \tag{4.56a}$$

$$|b_2| \leq 6KR^2 + R^2 + \frac{h}{2}(KR)^3|1 - \nu| + 3(KR)^2 + \frac{h^2}{2}K^3R^4 + 3hK^2R^3 \tag{4.56b}$$

$$|b_3| \leq 3KR^3 + (KR)^3 + \frac{3}{2}hK^2R^4 + \frac{h^2}{4}K^3R^5. \tag{4.56c}$$

As before, we find a bound on T defined in (4.23). We then consider

$$T \leq 2\max\left(3KR,\ \sqrt{3}KR, KR, |b_1|, |b_2|^{1/2}, |b_3|^{1/3}\right). \tag{4.57}$$

In order to find the maximum, we consider that

$$KR < 1/h \implies hKR < 1 \tag{4.58}$$

$$\nu \to 1 \implies |1 - v|K < 1. \tag{4.59}$$

Then, we have that

$$T \leq 2\max\left(R\left(2+3K+\frac{3}{2}+\frac{1}{4}\right), R\left(6K+1+\frac{1}{2}K+3K^2+\frac{1}{2}K+3K\right)^{1/2},\right.$$
$$\left. R\left(3K+K^3+\tfrac{3}{2}K+\frac{1}{4}K\right)^{1/3}\right)$$
$$T \leq 2\left(3K+\frac{15}{4}\right)R, \tag{4.60}$$

where the last inequality holds true for any $K \geq 0$. Replacing T in (4.24) and using Remark 4.4, the distance between the roots of the polynomials can be bounded as

$$\begin{aligned}\max_i |\theta_i^f - \theta_i^g| \leq 3\Bigg\{&\left(2R+\frac{3}{2}hK^2R^2|\nu-1|+\frac{h^2}{4}K^3R^3|1-\nu|\right)T^2+\\ &\left(R^2+6KR^2+3hK^2R^3+\frac{h^2}{2}K^3R^4+\frac{h}{2}K^3R^3|1-\nu|\right)T\\ &+\left(3KR^3+\frac{3}{2}hK^2R^4+\frac{h^2}{4}K^3R^5\right)\Bigg\}^{1/3}\\ \leq 3\Bigg\{&\left(2R+\frac{3}{2}R+\frac{1}{4}R\right)4\left(3K+\frac{15}{4}\right)^2R^2+\\ &\left(R^2+6KR^2+3KR^2+\frac{1}{2}KR^2+\frac{1}{2}KR^2\right)2\left(3K+\frac{15}{4}\right)R+\\ &\left(3KR^3+\frac{3}{2}KR^3+\frac{1}{4}KR^3\right)\Bigg\}^{1/3}\\ \leq 3R\Bigg\{&\frac{3495}{16}+\frac{1693}{4}K+195K^2\Bigg\}^{1/3}\end{aligned} \tag{4.61}$$

Thus, closed-loop stability is guaranteed if the right hand side is less than $|\alpha^*| = KR$. This yields

$$\begin{aligned}&\max_i |\theta_i^f - \theta_i^g| < |\alpha^*|\\ \iff\ & 3R\left(\frac{3495}{16}+\frac{1693}{4}K+195K^2\right)^{1/3} < KR\\ \iff\ & K^3 - 27\left(\frac{3495}{16}+\frac{1693}{4}K+195K^2\right) > 0.\end{aligned} \tag{4.62}$$

Therefore, taking $K = \kappa' \geq 5268$ the theorem is proved. ■

Example 6 *We consider a second-order plant of the form* (4.12)*. For a specific numerical example we choose $b = -6$, $\alpha_1 = 3$, $\alpha_2 = -2$, i.e.,*

$$G_c(s) = \frac{-6}{(s+3)(s-2)}. \tag{4.63}$$

Then, its discrete-time model depends on the sampling period chosen. Table 4.1 shows the nature of the closed-loop response of the true system when the controller designed based on the approximation $G_d^1(\gamma) = -6/\gamma^2$*. Note that the blank entries are not relevant since we consider only the case where* $\alpha^* \leq 1/h$*.*

α^* \ $1/h$	10	20	100	1000	10000
5	Stable	Stable	Stable	Stable	Stable
10	**Unstable**	Stable	Stable	Stable	Stable
16		**Unstable**	Stable	Stable	Stable
20		**Unstable**	Stable	Stable	Stable
50			Stable	Stable	Stable
70			**Unstable**	Stable	Stable
100			**Unstable**	Stable	Stable
500				Stable	Stable
800				**Unstable**	Stable
1000				**Unstable**	Stable
5000					Stable
10000					**Unstable**

Table 4.1: Robustness of the discrete-time model without considering sampling zeros

On the other hand, the closed-loop performance when the controller design is based on the model (4.39) *is shown in Table 4.2.*

α^* \ $1/h$	10	20	100	1000	10000
5	Stable	Stable	Stable	Stable	Stable
10	Stable	Stable	Stable	Stable	Stable
16		Stable	Stable	Stable	Stable
20		Stable	Stable	Stable	Stable
50			Stable	Stable	Stable
70			Stable	Stable	Stable
100			Stable	Stable	Stable
500				Stable	Stable
800				Stable	Stable
1000				Stable	Stable
5000					Stable
10000					Stable

Table 4.2: Robustness of the discrete-time model considering sampling zeros

Therefore, for h *small enough and for* $\frac{1}{h} \gg \alpha^* > R$*, the design based on* $G_d^1(\gamma)$ *stabilizes the true system. However, when* α^* *tends to* $\frac{1}{h}$*, the closed-loop stability is not achieved. Hence, to ensure stability of the true closed-loop system when* α^* *approaches* $\frac{1}{h}$ *it becomes necessary to use the controller designed using* $G_d^2(\gamma)$*, i.e., the asymptotic sampling zeros must be added in the approximate model.*

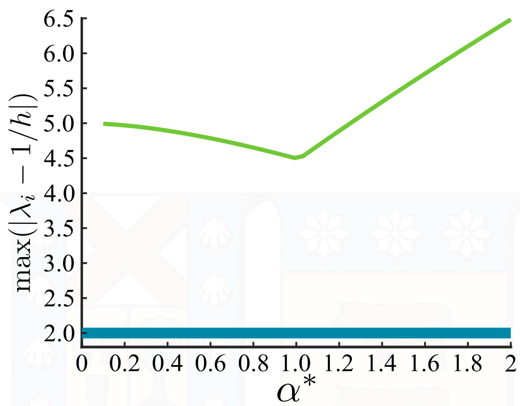

Figure 4.3: Illustration of instability for $h = 0.5$.

Besides, the results are only suitable for h sufficiently small. For example, considering $h = 0.5$ and varying α^*, the closed-loop response is unstable, even when the asymptotic sampling zeros are included in the control law. This is illustrated in Figure 4.3, where the maximum distance from the closed-loop eigenvalues from the point $-\frac{1}{h}$ is plotted as a function of $\alpha^* \in (0, \frac{1}{h})$. Note that this distance is larger than $\frac{1}{h} = 2$ in all cases, which implies that the closed-loop system is unstable.

4.6 Summary

In this chapter a high-gain control law was proposed for stably invertible linear systems that depends only on the continuous-time relative degree and high-frequency gain. In the first instance, the continuous-time case has been analyzed to establish ideas. Thus, a preliminary theoretical analysis based on Ostrowski's Theorem has been provided for relative degree two, showing that the approximate model's design stabilizes the true system.

The results were extended to the discrete-time domain when the sampling period is small, which is more challenging due to the presence of (asymptotic) sampling zeros. Therefore, a methodology that specifically addresses the sampling zero issue is developed. The methodology study two approximate models: the first model covers the case where the closed-loop bandwidth is significantly less than the Nyquist frequency, while the second includes the asymptotic sampling zeros, and, as a consequence, the closed-loop bandwidth is near the Nyquist frequency.

The results show that when the nominal closed-loop poles approach the inverse of the sampling period, it is necessary for the closed-loop stability of the true system that the control design is based on an approximate model that includes the asymptotic sampling zeros.

5 NONLINEAR SAMPLED-DATA MODELS BASED ON B-SPLINE FUNCTIONS

As mentioned in Chapter 2, the exact sampled-data model is not usually available for nonlinear systems. In this chapter our interest is on studying the effect of the numerical integration strategy applied to solve the (nonlinear) differential equation. Analogous to the linear case, approximate sampled-data models can be obtained that include extra zero dynamics that depend on the system input smoothness modeled using B-spline functions as in Chapter 3.

The usual assumption is that a ZOH generates the input. However, spline interpolation can represent a different assumption to introduce knowledge about the continuous-time input smoothness.

This chapter first propose an approximate sampled-data model for an n-th order nonlinear system having relative degree r when the input is generated by an ℓ-th order B-spline hold. We show how a truncated Taylor series expansion can discretize the continuous-time system taking into account the smoothness of the input. It is shown that the corresponding sampled-data model depends on the nonlinear relative degree of the continuous-time system and on the order of the hold device.

Moreover, an explicit characterization of the sampling zero dynamics is given, showing that these zero dynamics are asymptotically equal to the asymptotic sampling zeros of the linear case when the sampling period goes to zero. Finally, we study the accuracy of the applied integration strategy by analyzing the local truncation error associated with the state vector.

5.1 Approximate Sampled-Data Models for Nonlinear Systems

Consider the class of nonlinear systems affine in the input, i.e.,

$$\dot{x}(t) = f(x(t)) + g(x(t))u(t) \tag{5.1a}$$
$$y(t) = h(x(t)), \tag{5.1b}$$

where $x(t)$ is the state vector, the vector fields $f(x(t))$ and $g(x(t))$, and the output function $h(x(t))$ are analytic in an open set $\mathcal{M} \in \mathbb{R}$ containing the origin [39].

Assumption 5.1 *The system* (5.1) *has an equilibrium point* $x_0 = 0$. *Then, note that* $f(0) = 0$ *and* $g(0) \neq 0$, *otherwise* $\dot{x}(t) = 0$ *for any* $u(t)$ *[94, 95].*

Moreover, there exists a local coordinate transformation $\Phi(x) = [\zeta(t);\ \eta(t)]^T$, such that the nonlinear system (5.1) can be represented in normal form (see Subsection 2.5.2):

$$\dot{\zeta}(t) = \left[\begin{array}{c|ccc} 0 & & & \\ \vdots & & I_{r-1} & \\ 0 & & & \\ \hline 0 & 0 & \cdots & 0 \end{array}\right] \zeta(t) + \begin{bmatrix} 0 \\ \vdots \\ 0 \\ 1 \end{bmatrix} (a(\zeta,\eta) + b(\zeta,\eta)u(t)) \tag{5.2a}$$
$$\dot{\eta}(t) = q(\zeta,\eta) \tag{5.2b}$$
$$y(t) = \zeta_1(t). \tag{5.2c}$$

where $\zeta(t) = [\phi_1(x), \ldots, \phi_r(x)]^T$ and $\eta(t) = [\phi_{r+1}(x), \ldots, \phi_n(x)]^T$.

Remark 5.2 *The local coordinate transformation* $\Phi(x)$ *does not (locally) change the equilibrium point. Thus, the proposed model* (5.2) *evolves in the neighborhood of* $\phi_0 = 0$. *Thus, fundamental properties such as the controllability of the system remain invariant [79, 95].*

Considering that $\Phi(x)$ is close to the origin, we have that

$$a(\phi) = a(0) + a_1\vec{\phi} + \frac{1}{2}\vec{\phi}^T a_2 \vec{\phi} + \ldots \tag{5.3a}$$
$$b(\phi) = b(0) + b_1\vec{\phi} + \frac{1}{2}\vec{\phi}^T b_2 \vec{\phi} + \ldots \tag{5.3b}$$

Remark 5.3 *Considering Assumption 5.1 and Remark 5.2, we have that* $a(0) = 0$ *and* $b(0) \neq 0$. *Thus,*

$$a(\phi) = \bar{a}(\phi) = a_1\vec{\phi} + \frac{1}{2}\vec{\phi}^T a_2 \vec{\phi} + \ldots \tag{5.4a}$$
$$b(\phi) = b_0 + \bar{b}(\phi) \tag{5.4b}$$

We now focus in obtaining a sampled-data model for the continuous-time system (5.1) when the input is generated by a B-spline hold. In particular, we are interested in the characterization of the extra discrete-time zero dynamics that appear due to the sampling process.

Firstly, we present the sampled-data model for an n-th order integrator when the input is generated by a B-spline generalized hold to set ideas. Then, we extend the results to the nonlinear case.

Theorem 5.4 *Consider the continuous-time system $G(s) = s^{-n}$, where $n > 0$, and consider that the input to the system is generated by a B-spline ℓ-th order hold, as shown in Fig. 3.2. The corresponding sampled-data model is given by*

$$\bar{x}_{k+1} = A_q \bar{x}_k + B_q u_k \tag{5.5a}$$
$$y_k = C_q \bar{x}_k \tag{5.5b}$$

where matrices A_q, B_q and C_q are given in (5.13).

Proof: An n-th order integrator whose input is generated by an ℓ-th order hold can be written in normal form as shown in (3.22), i.e.,

$$y(t) = x_1(t) \tag{5.6a}$$
$$\dot{x}_1(t) = x_2(t) \tag{5.6b}$$
$$\vdots$$
$$\dot{x}_n(t) = u(t) \tag{5.6c}$$
$$\vdots$$
$$\dot{x}_{n+\ell}(t) = u^{(\ell)}(t). \tag{5.6d}$$

We recall that, according to Remark 3.3, $(\ell + 1)$-th and higher order derivatives of the input $u(t)$ are all equal to zero. Thus, the corresponding discrete-time model corresponds to a truncated Taylor series expansion (2.121) up to the order $(n + \ell)$ of the system (5.6), i.e.,

$$x_1(kh + \tau) = x_1(kh) + \tau x_1^{(1)}(kh) + \cdots + \frac{\tau^{(n+\ell)}}{(n+\ell)!} x_1^{(n+\ell)}(kh) \tag{5.7a}$$
$$x_2(kh + \tau) = x_2(kh) + \cdots + \frac{\tau^{n+\ell-1}}{(n+\ell-1)} x_2^{(n+\ell-1)}(kh) \tag{5.7b}$$
$$\vdots \tag{5.7c}$$
$$x_{n+\ell}(kh + \tau) = x_{n+\ell}(kh) + \tau x_{n+\ell}^{(1)}(kh), \tag{5.7d}$$

where $0 \leq \tau < h$. Then, model (5.7) can be expressed in state-space as

$$x_{k+1} = A_q^1 x_k + B_q^1 \bar{u}(kh) \tag{5.8a}$$
$$y_k = C_q x_k, \tag{5.8b}$$

where we have used the notation $x_k = x(kh)$. The matrices are

$$A_q^1 = \begin{bmatrix} 1 & h & \cdots & \frac{h^{n-1}}{(n-1)!} \\ 0 & 1 & \cdots & \vdots \\ \vdots & & \ddots & \vdots \\ 0 & \cdots & 0 & 1 \end{bmatrix}, B_q^1 = \begin{bmatrix} \frac{h^n}{n!} & \frac{h^{n+1}}{(n+1)!} & \cdots & \frac{h^{n+\ell}}{(n+\ell)!} \\ \frac{h^{n-1}}{(n-1)!} & \frac{h^n}{n!} & \cdots & \frac{h^{n+\ell-1}}{(n+\ell-1)!} \\ \vdots & \vdots & \vdots & \vdots \\ h & \frac{h^2}{2} & \cdots & \frac{h^{\ell+1}}{(\ell+1)!} \end{bmatrix} \tag{5.9a}$$

$$C_q = \begin{bmatrix} 1 & 0 & \cdots & 0 \end{bmatrix}. \tag{5.9b}$$

Then, using (2.34) and (2.44) we can compute $u(kh)$ and its ℓ-th derivatives. Thus, $\bar{u}(kh)$ is given by

$$\bar{u}_k(kh) = \begin{bmatrix} u(kh) \\ u^{(1)}(kh) \\ \vdots \\ u^{(\ell)}(kh) \end{bmatrix} = \underbrace{\left.\begin{bmatrix} \tilde{\beta}_\ell(t) \\ \frac{d}{dt}\tilde{\beta}_\ell(t) \\ \vdots \\ \frac{d^\ell}{dt^\ell}\tilde{\beta}_\ell(t) \end{bmatrix}\right|_{t=kh}}_{M} \begin{bmatrix} u_k \\ u_{k-1} \\ \vdots \\ u_{k-\ell} \end{bmatrix}. \tag{5.10}$$

Note that $u(kh)$ and $u^{(i)}(kh)$, for $i = 1, \ldots, \ell$ depend on u_k and previous input samples. These samples can be thought as auxiliary states for the previous sample, i.e., $(\xi_1)_{k+1} = u_k$ and $(\xi_j)_k = u_{k-j}$. The additional ℓ states can be represented as follows:

$$\begin{bmatrix} \xi_1 \\ \xi_2 \\ \vdots \\ \xi_\ell \end{bmatrix}_{k+1} = \underbrace{\begin{bmatrix} 0 & 0 & \cdots & 0 \\ 1 & 0 & \cdots & 0 \\ 0 & 1 & \ddots & 0 \\ \vdots & & & \vdots \\ 0 & \cdots & 1 & 0 \end{bmatrix}}_{E} \begin{bmatrix} \xi_1 \\ \xi_2 \\ \vdots \\ \xi_\ell \end{bmatrix}_k + \begin{bmatrix} 1 \\ 0 \\ \vdots \\ 0 \end{bmatrix} u_k \tag{5.11}$$

Matrix E allows us to include all the information available about $u(t)$. The augmented state vector is then defined as $\bar{x}_k = [x;\ \xi]_k^T$ and the state-space representation is given by

$$\bar{x}_{k+1} = A_q \bar{x}_k + B_q u_k \tag{5.12a}$$
$$y_k = C_q \bar{x}_k. \tag{5.12b}$$

where C_q is defined in (5.9b), the matrices

$$A_q = \left[\begin{array}{c|c} A_q^1 & B_q^1 M_1 \\ \hline 0_{\ell\times n} & E_{\ell\times\ell} \end{array}\right], \ B_q = \left[\begin{array}{c} B_q^1 M_0 \\ \hline 1 \\ 0 \\ \vdots \\ 0 \end{array}\right] \tag{5.13}$$

and $M_0 = M_{1:\ell+1,1}$ (i.e., the first column of M), and $M_1 = M_{1:\ell+1,2:\ell+1}$. Moreover, due to the matrix M structure, we have that

$$B_q^1 M_0 = \frac{h^n}{(n+\ell)!}. \tag{5.14}$$

■

As mentioned in Chapter 3, the discrete-time transfer function associated with (5.8) is given by

$$G_q(z) = \frac{h^n}{(n+\ell)!}\frac{B_{n+\ell}(z)}{z^\ell (z-1)^n}. \tag{5.15}$$

We are interested in characterizing the asymptotic sampling zeros that appear in the sampled-data model. Moreover, this result will be a useful tool for analyzing the zero dynamics of the nonlinear case. Thus, the following theorem provides the discrete-time normal form representation of (5.15).

Theorem 5.5 *The discrete-time model for an n-th order integrator defined in* (5.8) *(and, therefore in* (5.15)*) can be written in normal form as:*

$$w_{1,k+1} = q_{11} w_{1,k} + Q_{12}\chi_k + \frac{h^n}{(n+\ell)!} u_k \tag{5.16a}$$

$$\chi_{k+1} = Q_{21} w_{1,k} + Q_{22}\chi_k, \tag{5.16b}$$

where χ_k represents the $(w_{2:n+\ell})_k$ states, and where the eigenvalues of matrix Q_{22} are the sampling zeros of (5.15)*, i.e.,*

$$B_{n+\ell}(z) = det(zI - Q_{22}). \tag{5.17}$$

Proof: Consider the similarity transformation $w_k = T\bar{x}_k$, where

$$T = \left[\begin{array}{c|c} 1 & 0 \\ \hline T_{21} & I_{n+\ell-1} \end{array}\right] \tag{5.18}$$

and

$$T_{21} = -\frac{(B_q)_{2:n+\ell,1}}{(B_q^1 M_0)_{1,1}} = -\frac{(n+\ell)!}{h^n}(B_q)_{2:n+\ell,1}. \tag{5.19}$$

Applying T to (5.12), the following state-space representation is obtained:

$$\tilde{A}_q = T A_q T^{-1} = Q = \left[\begin{array}{c|c} q_{11} & Q_{12} \\ \hline Q_{21} & Q_{22} \end{array}\right] \tag{5.20}$$

$$= \left[\begin{array}{c|c} -A_{12}T_{21} & A_{12} \\ \hline -(T_{21}A_{12} + A_{22})T_{21} & T_{21}A_{12} + A_{22} \end{array}\right]. \tag{5.21}$$

Using matrix A_q in (5.13), we have that

$$A_{12} = \begin{bmatrix} h & \frac{h^2}{2} & \cdots & \frac{h^{n-1}}{(n-1)!} & (B_q^1 M_1)_{1,1:\ell} \end{bmatrix} \tag{5.22}$$

$$A_{22} = \begin{bmatrix} (A_q^1)_{2:n,2:n} & (B_q^1 M_1)_{2:n,1:\ell} \\ 0_{1:\ell,2:n} & E_{\ell\times\ell} \end{bmatrix}. \tag{5.23}$$

Then, $\tilde{B}_q$ and $\tilde{C}_q$ are given by

$$\tilde{B}_q = TB_q = \begin{bmatrix} \frac{h^n}{(n+\ell)!} & 0 & \cdots & 0 \end{bmatrix}^T \tag{5.24}$$

$$\tilde{C}_q = C_q T^{-1} = \begin{bmatrix} 1 & 0 & \cdots & 0 \end{bmatrix}. \tag{5.25}$$

Thus, the discrete-time model for an n-th order integrator is given by the following state-space representation:

$$w_{k+1} = \tilde{A}_q w_k + \tilde{B}_q u_k \tag{5.26a}$$

$$y_k = \tilde{C}_q w_k, \tag{5.26b}$$

To obtain the (sampling) zeros polynomial of (5.26), and therefore of (5.15), we compute the numerator polynomial as follows [2]:

$$N(z) = \det \begin{bmatrix} zI - \tilde{A}_q & -\tilde{B}_q \\ \tilde{C}_q & 0 \end{bmatrix} \tag{5.27}$$

$$= \left[\begin{array}{ccc|c} z - q_{11} & & -Q_{12} & -\frac{h^n}{(n+\ell)!} \\ & & & 0 \\ -Q_{21} & & zI - Q_{22} & \vdots \\ \hline 1 & 0 & \cdots & 0 \end{array}\right]. \tag{5.28}$$

The result follows computing the determinant along the last column ■

In what follows, we develop an approximate sampled-data model for the continuous-time system (5.2) when considering that a B-spline hold generates the system input and that the integration strategy is a truncated Taylor series expansion. Firstly, we need the following assumptions in order to obtain a (discrete-time) model that preserves the input affine property of the continuous-time system.

Assumption 5.6 *Let us assume that the nonlinear system in* (5.2) *satisfies:*

$$\frac{\partial b(\zeta_k, \eta_k)}{\partial \zeta_{r,k}} = 0 \tag{5.29a}$$

$$\frac{\partial^i a(\zeta_k, \eta_k)}{(\partial \zeta_{r,k})^i} = 0; \quad \forall\, i > 1. \tag{5.29b}$$

Theorem 5.7 *Consider the n-th order nonlinear system* (5.1)*, where the input is generated by an ℓ-th order B-spline hold. An approximate sampled-data model can be obtained applying a truncated Taylor series expansion having the following state space form:*

$$w_{k+1} = \left(\tilde{A}_q + \frac{h^{r+\ell}}{(r+\ell)!}\tilde{A}_2(w_k)\right) w_k + \frac{h^{r+\ell}}{(r+\ell)!}\tilde{A}_3(w_k) + \tilde{B}_q(w_k)u_k \tag{5.30a}$$

$$y_k = \tilde{C}_q\, w_k, \tag{5.30b}$$

where matrices $\tilde{A}_q$ and $\tilde{C}_q$ are defined in (5.21) *and* (5.25)*, respectively, and where $\tilde{A}_2(w_k)$, $\tilde{A}_3(w_k)$, $\tilde{B}_q(w_k)$ are given later in* (5.43), (5.44), (5.45).

Proof: Consider the nonlinear system (5.1) and that the input to the system in generated by an ℓ-th order hold. Also, consider that the $(\ell+1)$-th and higher order derivatives of the input are all equal to zero (see Lemma 3.1). Thus, applying the integration strategy shown in (2.154) up to order $r+\ell$, we obtain the following sampled-data model

$$\hat{\zeta}_1(kh+h) = \hat{\zeta}_1(kh) + h\hat{\zeta}_2(kh) + \cdots + \frac{h^r}{r!}\hat{\zeta}_r^{(1)}(kh) + \cdots + \frac{h^{r+\ell}}{(r+\ell)!}\hat{\zeta}_r^{(\ell+1)}(\alpha_1) \tag{5.31a}$$

$$\hat{\zeta}_2(kh+h) = \hat{\zeta}_2(kh) + \cdots + \frac{h^{r-1}}{(r-1)}\hat{\zeta}_r^{(1)}(kh) + \cdots + \frac{h^{r+\ell-1}}{(r+\ell-1)!}\hat{\zeta}_r^{(\ell+1)}(\alpha_2) \tag{5.31b}$$

$$\vdots \tag{5.31c}$$

$$\hat{\zeta}_r(kh+h) = \hat{\zeta}_r(kh) + h\zeta_r^{(1)}(kh) + \frac{h^2}{2}\hat{\zeta}_r^{(2)}(kh) + \cdots + \frac{h^{\ell+1}}{(\ell+1)!}\hat{\zeta}_r^{(\ell+1)}(\alpha_r) \tag{5.31d}$$

$$\hat{\eta}(kh+h) = \hat{\eta}(kh) + h\, q(\hat{\zeta},\hat{\eta})\Big|_{t=\alpha_{r+1}}. \tag{5.31e}$$

This model is exact for some unknown time instants $kh \leq \alpha_i < kh+h$; $i = 1, \ldots, r+1$. Replacing the time instants α_i by kh, we obtain an approximate discrete-time model given by

$$\zeta_1(kh+h) = \zeta_1(kh) + h\zeta_2(kh) + \cdots + \frac{h^r}{r!}\zeta_r^{(1)}(kh) + \cdots + \frac{h^{r+\ell}}{(r+\ell)!}\zeta_r^{(\ell+1)}(kh) \tag{5.32a}$$

$$\zeta_2(kh+h) = \zeta_2(kh) + \cdots + \frac{h^{r-1}}{(r-1)}\zeta_r^{(1)}(kh) + \cdots + \frac{h^{r+\ell-1}}{(r+\ell-1)!}\zeta_r^{(\ell+1)}(kh) \tag{5.32b}$$

$$\vdots \tag{5.32c}$$

$$\zeta_r(kh+h) = \zeta_r(kh) + h\zeta_r^{(1)}(kh) + \frac{h^2}{2}\zeta_r^{(2)}(kh) + \cdots + \frac{h^{\ell+1}}{(\ell+1)!}\zeta_r^{(\ell+1)}(kh) \tag{5.32d}$$

$$\eta(kh+h) = \eta(kh) + h\, q(\zeta,\eta)\big|_{t=kh} \tag{5.32e}$$

Based on Assumption 5.6, we have neglected the derivatives of $b(\zeta_k, \eta_k)$ and higher-order derivatives of $a(\zeta_k, \eta_k)$. In addition, considering that $\zeta(t)$ is close to the origin, we assume $a(\zeta_k, \eta_k) \approx 0$ (see Remark 5.3). This yields the following discrete-time state-space form that is affine in the input:

$$\zeta_{k+1} = A_q\zeta_k + A_3(\zeta_k, \eta_k) + B_2(\zeta_k, \eta_k)\bar{u}_k \tag{5.33a}$$

$$\eta_{k+1} = \eta_k(\zeta_k, \eta_k) + hq(\zeta_k, \eta_k), \tag{5.33b}$$

where $\bar{u}_k$ is given by (5.10) and

$$A_3(\zeta_k, \eta_k) = \begin{bmatrix} \frac{h^r}{r!} + \frac{h^{r+1}}{(r+1)!}\frac{\partial a}{\partial \zeta_r} + \cdots + \frac{h^{r+\ell}}{(r+\ell)!}\left(\frac{\partial a}{\partial \zeta_r}\right)^\ell \\ \vdots \\ h + \frac{h^2}{2}\frac{\partial a}{\partial \zeta_r} + \cdots + \frac{h^{\ell+1}}{(\ell+1)!}\left(\frac{\partial a}{\partial \zeta_r}\right)^\ell \end{bmatrix} a(\zeta_k, \eta_k). \tag{5.34}$$

$$B_2(\zeta_k, \eta_k) = b(\zeta_k, \eta_k) \quad \times$$
$$\begin{bmatrix} \frac{h^r}{r!} + \frac{h^{r+1}}{(r+1)!}\frac{\partial a}{\partial \zeta_r} + \cdots + \frac{h^{r+\ell}}{(r+\ell)!}\left(\frac{\partial a}{\partial \zeta_r}\right)^\ell & \frac{h^{r+1}}{(r+1)!} + \cdots + \frac{h^{r+\ell}}{(r+\ell)!}\left(\frac{\partial a}{\partial \zeta_r}\right)^{\ell-1} & \cdots & \frac{h^{r+\ell}}{(r+\ell)!} \\ \frac{h^{r-1}}{(r-1)!} + \frac{h^r}{r!}\frac{\partial a}{\partial \zeta_r} + \cdots + \frac{h^{r+\ell-1}}{(r+\ell-1)!}\left(\frac{\partial a}{\partial \zeta_r}\right)^\ell & \frac{h^r}{r!} + \cdots + \frac{h^{r+\ell-1}}{(r+\ell-1)!}\left(\frac{\partial a}{\partial \zeta_r}\right)^{\ell-1} & \cdots & \frac{h^{r+\ell-1}}{(r+\ell-1)!} \\ \vdots & \vdots & & \vdots \\ h + \frac{h^2}{2}\frac{\partial a}{\partial \zeta_r} + \cdots + \frac{h^{\ell+1}}{(\ell+1)!}\left(\frac{\partial a}{\partial \zeta_r}\right)^\ell & \frac{h^2}{2} + \frac{h^3}{3}\frac{\partial a}{\partial \zeta_r} + \cdots + \frac{h^{\ell+1}}{(\ell+1)!}\left(\frac{\partial a}{\partial \zeta_r}\right)^{\ell-1} & \cdots & \frac{h^{\ell+1}}{(\ell+1)!} \end{bmatrix}. \tag{5.35}$$

Remark 5.8 *Notice that, according to the integration strategy applied to each state component $\zeta_i(kh+h)$, the neglected terms appear in the $(r+i)$-th and higher-order derivatives. Moreover, the derivatives of $a(\zeta, \eta)$ that are not considered in the expansion are of order ℓ.*

Note that matrix (5.35) can be split into a linear part, given by B_q^1 in (5.9a), and a matrix with the nonlinearities factorized by $h^{(r+\ell)}/(r+\ell)!$, i.e.,

$$B_2(\zeta_k, \eta_k) = \underbrace{B_q^1 b_0}_{B_q^1} + \frac{h^{r+\ell}}{(r+\ell)!}B_q^2(\zeta_k, \eta_k). \tag{5.36}$$

Following the ideas presented in Theorem 5.4, $u(t)$ and its derivatives at the sampling instants can be included in the model as additional states (see (5.11)). Thus, we define $\bar{\zeta}_k = [\zeta_k;\ \xi_k]^T$ as the augmented state vector and then (5.33) can be written as follows:

$$\bar{\zeta}_{k+1} = \bar{A}_q(\zeta_k, \eta_k)\bar{\zeta}_k + \frac{h^{r+\ell}}{(r+\ell)!}\bar{A}_3(\zeta_k, \eta_k) + \bar{B}_q u_k \tag{5.37a}$$

$$\eta_{k+1} = \eta_k + hq(\zeta_k, \eta_k), \tag{5.37b}$$

where

$$\bar{A}_q(\zeta_k, \eta_k) = A_q + \frac{h^{r+\ell}}{(r+\ell)!} A_2(\zeta_k, \eta_k), \tag{5.38}$$

where A_q is given by (3.27) and

$$A_2(\zeta_k, \eta_k) = \begin{bmatrix} 0_{r\times r} & B_q^2(\zeta_k, \eta_k) M_1 \\ 0_{\ell\times r} & 0_{\ell\times\ell} \end{bmatrix}, \tag{5.39}$$

$$\bar{A}_3(\zeta_k, \eta_k) = \begin{bmatrix} A_3(\zeta_k, \eta_k) \\ 0_{\ell\times 1} \end{bmatrix}, \tag{5.40}$$

$$\bar{B}_q(\zeta_k, \eta_k) = \begin{bmatrix} B_2(\zeta_k, \eta_k) M_0 \\ 1 \\ 0 \\ \vdots \\ 0 \end{bmatrix}. \tag{5.41}$$

We apply now the similarity transformation $w_k = T\xi_k$, where T is defined in (5.18), and T_{21} is given by

$$T_{21} = -\frac{(B_q)_{2:r+\ell}}{B_q^1 M_0} = -\frac{(r+\ell)!}{b_0 h^r} (B_q)_{2:r+\ell}. \tag{5.42}$$

We are interested in obtaining a sampled-data model that can be defined in the neighborhood of the origin. Thus, using the results presented in (5.4), the new approximate sampled-data model is given by the sub-matrices of $\tilde{A}_q$ shown in (5.22)-(5.23) and

$$\begin{aligned} \tilde{A}_2(w_k) &= T A_2(T^{-1} w_k) \\ &= \tilde{Q}(w_k) = \begin{bmatrix} \tilde{q}_{11}(w_k) & \tilde{Q}_{12}(w_k) \\ \tilde{Q}_{21}(w_k) & \tilde{Q}_{22}(w_k) \end{bmatrix} && (5.43) \\ \tilde{A}_3(w_k) &= T\bar{A}_3(T^{-1} w_k) && (5.44) \\ \tilde{B}_q(w_k) &= T\bar{B}_q(T^{-1} w_k) \\ &= \begin{bmatrix} \frac{h^r}{(r+\ell)!} b(w_k) & 0 & \cdots & 0 \end{bmatrix}^T && (5.45) \end{aligned}$$

■

5.2 Local Vector Truncation Error

The integration strategy applied is a truncated Taylor series expansion, up to the order $r+\ell$. Thus, following the same arguments as in [42], this section analyzes the local truncation error between the exact and the approximate sampled-data model defined in (5.31) and (5.32), respectively.

Theorem 5.9 *Consider the continuous-time nonlinear system in* (5.1) *having an input generated by a B-spline generalized hold. Then, the approximate sampled-data model in* (5.32) *has a Local Vector Truncation Error of the order of* $(h^{r+2}, h^{r+1}, \cdots, h^2)$.

Proof: From the definition of Local Vector Truncation Error in [42], we have that the difference between the exact and the approximate discrete-time model is given by

$$\hat{e}_1 = \hat{\zeta}_1(kh+h) - \zeta_1(kh+h) = 0 \tag{5.46a}$$

$$\vdots$$

$$\hat{e}_r = \hat{\zeta}_r(kh+h) - \zeta_r(kh+h) = 0 \tag{5.46b}$$

$$\hat{e}_{r+1} = \hat{\eta}(kh+h) - \eta(kh+h) = 0. \tag{5.46c}$$

Then, considering Remark 5.8, the differences are given by

$$\hat{e}_1 = \frac{h^{r+1}}{(r+1)!}\frac{d^2}{dt^2}\left(\hat{\zeta}_r(kh) - \zeta_r(kh)\right) + \cdots + \frac{h^{r+\ell}}{(r+\ell)!}\frac{d^{r+\ell}}{dt^{r+\ell}}\left(\hat{\zeta}_r(\alpha_1) - \zeta_r(kh)\right) \tag{5.47a}$$

$$\hat{e}_2 = \frac{h^{r}}{r!}\frac{d^2}{dt^2}\left(\hat{\zeta}_r(kh) - \zeta_r(kh)\right) + \cdots + \frac{h^{r+\ell-1}}{(r+\ell-1)!}\frac{d^{r+\ell}}{dt^{r+\ell}}\left(\hat{\zeta}_r(\alpha_2) - \zeta_r(kh)\right) \tag{5.47b}$$

$$\vdots \tag{5.47c}$$

$$\hat{e}_r = \frac{h^{2}}{2}\frac{d^2}{dt^2}\left(\hat{\zeta}_r(kh) - \zeta_r(kh)\right) + \cdots + \frac{h^{r+\ell}}{(r+\ell)!}\frac{d^{\ell+1}}{dt^{\ell+1}}\left(\hat{\zeta}_r(\alpha_r) - \zeta(kh)\right)$$

$$\hat{e}_{r+1} = h\left(q(\hat{\zeta},\hat{\eta})\Big|_{t=\alpha_{r+1}} - q(\zeta,\eta)|_{t=kh}\right). \tag{5.47d}$$

Notice that $\hat{e}_i$ includes terms of the order of h^{r+2-i}, $i = 1, \ldots r+1$, and higher order. Thus, the error is of the order of h^{r+2-i}. According to the ideas presented in [42], the approximate sampled-data model (5.32) has a local vector truncation error of order $(h^{r+2}, h^{r+1}, \cdots, h^3, h^2)$. ■

From the above result, we can see that the (local) error between the output of model (5.32) and the output of the true system is of the order of h^{r+2} (see (2.152)). Moreover, it can be noticed that the approximate model based on B-spline functions is more accurate than the models considered in [42] and in [81], because the local truncation error in each state component $\zeta_i(kh+h)$ is of a higher order in the sampling period h. Thus, the assumption about the smoothness of the system input has been exploited to improve the accuracy of the obtained model.

5.3 Asymptotic Zero Dynamics

In what follows we characterize the zero dynamics of the corresponding nonlinear discrete-time model that appear due to the sampling process. In particular, Theorem

5.10 shows that these sampling zero dynamics asymptotically converge to the sampling zeros of an n-th order integrator (see (5.17)).

Theorem 5.10 *Consider the approximate discrete-time model* (5.30)*. The associated sampling zero dynamics can be asymptotically characterized, as the sampling period goes to zero, in terms of the eigenvalues of matrix Q_{22}, i.e.,*

$$\bar{\chi}_{k+1} = Q_{22}\bar{\chi}_k \tag{5.48a}$$
$$\eta_{k+1} = \eta_k, \tag{5.48b}$$

where $\bar{\chi}_k = (w_{2:r+\ell})_k$.

Proof: We impose the zero dynamics condition to the model (5.30), i.e., $y_k = (w_1)_k = 0$. Thus,

$$\begin{bmatrix} 0 \\ \hline w_2 \\ \vdots \\ w_{r+\ell} \end{bmatrix}_{k+1} = \left(Q + \frac{h^{r+\ell}}{(r+\ell)!}\tilde{Q}(w_k)\right)\begin{bmatrix} 0 \\ \hline w_2 \\ \vdots \\ w_{r+\ell} \end{bmatrix}_{k} + \frac{h^{r+\ell}}{(r+\ell)!}\tilde{A}_3(w_k) + \tilde{B}_q(w_k)(u^{zd})_k. \tag{5.49}$$

where, Q and $\tilde{Q}(w_k)$ are given by (5.20)-(5.21) and (5.43), respectively. Then, solving for the first row in (5.49), we have that

$$(u^{zd})_k = -\frac{(r+\ell)!}{h^r b(w_k)}\left[\left(Q_{12} + \frac{h^{r+\ell}}{(r+\ell)!}\tilde{Q}_{12}(w_k)\right)\bar{\chi}_k + \frac{h^{r+\ell}}{(r+\ell)!}(\tilde{A}_3(w_k))_{1,1}\right].$$

For the remaining equations and considering that $\bar{\zeta}_k(t)$ evolves close to the origin, we have that

$$\bar{\chi}_{k+1} = \left(Q_{22} + \frac{h^{r+\ell}}{(r+\ell)!}\tilde{Q}_{22}(w_k)\right)\bar{\chi}_k + \frac{h^{r+\ell}}{(r+\ell)!}\tilde{A}_3(w_k) \tag{5.50}$$
$$\eta_{k+1} = \eta_k + hq(\zeta_k, \eta_k). \tag{5.51}$$

Considering that $h \to 0$, then (5.48) is readily obtained. ■

Notice that the nonlinear zero dynamics of the discrete-time model (5.30) are partially linearized and can be split into two parts: a linear subsystem, which is given by Q_{22} and represents the asymptotic zero dynamics that appear due to the sampling process, and a nonlinear subsystem, which is the Euler's discretization of the continuous-time zero dynamics of (5.1). Moreover, we can notice that the eigenvalues of Q_{22} are the sampling zeros of an n-th order integrator (see Theorem 5.5).

We conclude this section with an example to illustrate how the proposed sampled-data model and the associated zero dynamics are obtained.

Example 7 *Consider an n-th order nonlinear continuous-time system* (5.1) *with relative degree $r = 2$. The latter can be expressed in normal form as in* (5.2). *Moreover, we assume that the input is generated by a B-spline first-order hold given by* (2.10) *and we obtain the proposed approximate dynamics sampled-data model applying the integration strategy* (5.7) *of order $r + \ell = 3$, i.e.,*

$$\zeta_{1,k+1} = \zeta_{1,k} + h\zeta_{2,k} + \frac{h^2}{2}\zeta_2^{(1)}(kh) + \frac{h^3}{3!}\zeta_2^{(2)}(kh) \tag{5.52a}$$

$$\zeta_{2,k+1} = \zeta_{2,k} + h\zeta_2^{(1)}(kh) + \frac{h^2}{2}\zeta_2^{(2)}(kh) \tag{5.52b}$$

$$\eta_{k+1} = \eta_k + hq(\zeta,\eta) \tag{5.52c}$$

$$y(t) = \zeta_{1,k}(t) \tag{5.52d}$$

Considering Assumption (5.6), *the first two equations in* (5.52) *can be expressed as follows,*

$$\zeta_{1,k+1} = \zeta_{1,k} + h\zeta_{2,k} + \left(\frac{h^2}{2} + \frac{h^3}{6}\frac{\partial a}{\partial \zeta_2}u(kh)\right)a(\zeta,\eta) + \\ \begin{bmatrix} \left(\frac{h^2}{2} + \frac{h^3}{6}\frac{\partial a}{\partial \zeta_2}\right)b(\zeta,\eta) & \frac{h^3}{6}b(\zeta,\eta) \end{bmatrix}\bar{u}(kh) \tag{5.53a}$$

$$\zeta_{2,k+1} = \zeta_{2,k} + \left(h + \frac{h^2}{2}\frac{\partial a}{\partial \zeta_2}\right)a(\zeta,\eta) + \begin{bmatrix} \left(h + \frac{h^2}{2}\frac{\partial a}{\partial \zeta_2}\right)b(\zeta,\eta) & \frac{h^2}{2}b(\zeta,\eta) \end{bmatrix}\bar{u}(kh), \tag{5.53b}$$

where $\bar{u}(kh)$

$$\bar{u}(kh) = \begin{bmatrix} u(kh) \\ \dot{u}(kh) \end{bmatrix} = \begin{bmatrix} 0 & 1 \\ \frac{1}{h} & -\frac{1}{h} \end{bmatrix}\begin{bmatrix} u_k \\ u_{k-1} \end{bmatrix}. \tag{5.54}$$

Notice that there is only one extra state given by $(\zeta_1)_k = u_{k-1}$. Then, the augmented state-space model is given by

$$\bar{\zeta}_{k+1} = \begin{bmatrix} 1 & h & \frac{h^2}{6}b(\zeta,\eta)\left(h\frac{\partial a(\zeta,\eta)}{\partial \zeta_2} + 2\right) \\ 0 & 1 & \frac{h}{2}b(\zeta,\eta)\left(h\frac{\partial a(\zeta,\eta)}{\partial \zeta_2} + 1\right) \\ 0 & 0 & 0 \end{bmatrix}\bar{\zeta}_k + \\ \begin{bmatrix} \left(\frac{h^2}{2} + \frac{h^3}{6}\frac{\partial a(\zeta,\eta)}{\partial \zeta_2}\right) \\ \left(h + \frac{h^2}{2}\frac{\partial a(\zeta,\eta)}{\partial \zeta_2}\right) \\ 0 \end{bmatrix} a(\zeta,\eta) + \begin{bmatrix} \frac{h^2}{6}b(\zeta,\eta) \\ \frac{h}{2}b(\zeta,\eta) \\ 1 \end{bmatrix} u_k \tag{5.55a}$$

$$\eta_{k+1} = \eta_k + hq(\zeta,\eta). \tag{5.55b}$$

The result in (5.4) *allows us to split model* (5.55) *into a linear and a nonlinear part. Then, applying the similarity transformation T in* (5.18) *and $T_{21} = -[3/h, \quad -6/(h^2 b_0)]^T$, based on Remark 5.3, and considering that $\bar{\zeta}_k(t)$ evolves close to the origin, the following state-space representation is obtained:*

$$w_{k+1} = \tilde{A}_1 w_k + \tilde{A}_2(w)w_k + \tilde{A}_3(w) + \tilde{B}(w)u_k \tag{5.56a}$$

$$\eta_{k+1} = \eta_k + hc(\zeta,\eta), \tag{5.56b}$$

$$\tilde{A}_1 = \begin{bmatrix} 6 & h & \frac{h^2}{3}b_0 \\ -\frac{12}{h} & -2 & -\frac{h}{2}b_0 \\ -\frac{36}{h^2 b_0} & -\frac{6}{hb_0} & -2 \end{bmatrix}, \qquad \tilde{A}_2(w) = \begin{bmatrix} 0 & 0 & \frac{h^3}{6}b(w)\frac{\partial a(w)}{\partial w_2} + \frac{h^2}{3}\bar{b}(w) \\ 0 & 0 & -\frac{h}{2}\bar{b}(w) \\ 0 & 0 & -h\frac{\partial a(w)}{\partial w_2} \end{bmatrix}, \tag{5.57}$$

$$\tilde{A}_3(w) = \begin{bmatrix} \frac{h^2}{6}\left(h\frac{\partial a(w)}{\partial w_2} + 3\right) \\ -\frac{h}{2} \\ 0 \end{bmatrix} a(w), \quad \tilde{B}(w) = \begin{bmatrix} \frac{h^2}{6}b(w) \\ 0 \\ 0 \end{bmatrix}. \tag{5.58}$$

Applying the condition for the zero dynamics, we obtain

$$\begin{aligned} \bar{\chi}_{k+1} &= \begin{bmatrix} -2 & -\frac{h}{2}b_0 \\ -\frac{6}{hb_0} & -2 \end{bmatrix}\bar{\chi}_k + \begin{bmatrix} 0 & -\frac{h}{2}\bar{b}(w) \\ 0 & -h\frac{\partial a(w)}{\partial w_2} \end{bmatrix}\bar{\chi}_k - \begin{bmatrix} \frac{h}{2} \\ 0 \end{bmatrix} a(w) \\ \eta_{k+1} &= \eta_k + hq\left(0, \chi_k, \eta_k\right) \end{aligned} \tag{5.59a}$$

Note that the eigenvalues of the first matrix in (5.59a) *correspond to the roots of the Euler-Frobenius polynomial* $B_3(z) = z^2 + 4z + 1$. *Thus, following* (5.17), *the system* (5.59a) *can be expressed as:*

$$\bar{\chi}_{k+1} = Q_{22}\bar{\chi}_k + \begin{bmatrix} 0 & -\frac{h}{2}\bar{b}(w) \\ 0 & -h\frac{\partial a(w)}{\partial w_2} \end{bmatrix}\bar{\chi}_k - \begin{bmatrix} \frac{h}{2} \\ 0 \end{bmatrix} a(w). \tag{5.60}$$

Considering $h \to 0$, *we notice that the zero dynamics converge to the asymptotic sampling zeros of the linear case.*

Notice that the asymptotic assumption, i.e. $h \to 0$, is applied once the matrix Q_{22} have been defined.

5.4 Summary

In this chapter, we have presented an approximate sampled-data model for a class of nonlinear systems affine in the input based on normal forms. The resulting model includes extra zero dynamics that depend on the applied numerical strategy, namely, the truncated Taylor series expansion, the continuous-time relative degree, and the order of the B-spline hold.

Moreover, it has been shown that these zero dynamics can be asymptotically characterized, as the sampling period goes to zero, in terms of the asymptotic zeros of the linear case. Besides, to analyze the accuracy of the approximate model, we have characterized the local error truncation of each element of the state vector.

6 | CONCLUSIONS

In this thesis, discrete-time representations for deterministic continuous-time systems for both linear and nonlinear cases have been developed. The resulting sampled-data models can be explained as a consequence of the continuous-time system's characteristics and the sampling process itself: how the applied integration strategy directly impacts the obtained sampled-data model and how the continuous-time input is generated. Therefore, we believe that the current thesis present novel contributions and provides further insights into the discretization process.

Thus, in this final chapter, we summarize the obtained contributions, and present future work directions.

6.1 Input Smoothness

We considered the case when the smoothness of the continuous-time system input is, in principle, unknown. However, there are different options to interpolate the input from the available discrete-time sequence to represent knowledge about this signal. Hence, in Chapter 3, a B-spline generalized hold has been expressed as a hybrid system composed by the interconnection of a digital filter followed by a zero-order hold and an ℓ-th order continuous-time integrator. Thus, such equivalence is useful since the hold device's smoothness can be chosen to be, for example, like a zero, first, or second-order hold only varying the parameter ℓ.

Besides, this hold is shown to be related to the well-known Euler-Frobenius polynomials, which characterizes the asymptotic sampling zeros of the linear case and, also, the asymptotic zero dynamics for nonlinear systems. Thus, Chapter 3 asymptotically characterizes the (sampling) zeros, showing that the sampling zero polynomial corresponding to a system having relative degree r is increased exactly by the order of the hold, ℓ. Therefore, for fast sampling rates, assuming different input smoothness only modifies the corresponding sampled-data model by changing the Euler-Frobenius polynomial.

6.2 Numerical Integration Strategies

For linear systems, the exact discrete-time model can be obtained. However, approximate descriptions may be preferred since they are related more directly to the continuous-time system's parameters. Moreover, approximate models may also be easier to obtain than the exact model, and the methods can also be applied to nonlinear systems. In this sense, the interest was to analyze the effect of such numerical methods in the resulting discrete-time model.

Thus, we explored the connections between the sampling zero polynomial and a Runge-Kutta method of order κ, exploiting also the smoothness of the system input. When the expansion order is greater than or equal to $r + \ell$, then the exact sampled-data model is obtained, and therefore, the sampling zeros are given by the Euler-Frobenius polynomial. On the other hand, when the expansion order is lower than the continuous-time system relative degree and the B-spline function, an approximate sampled-data model is developed. Hence, we characterized the corresponding sampling zeros with novel polynomials which are related to the Euler-Frobenius polynomials.

Since the simplest Runge-Kutta method is the Euler approximation, the proposed models are more accurate than the Euler method. Moreover, such representations are readily obtained. Besides, results regarding the convergence of sampling zeros have been extended: we have shown that the order of the applied numerical integration strategy directly impacts the location of the asymptotic sampling zeros, and we have obtained a direct characterization of poles and zeros for different types of holds.

On the other hand, we study a class of nonlinear systems affine in the input based on normal forms. In this case, the applied integration strategy is a truncated Taylor series expansion, which also takes into account the smoothness of the system input. Thus, Chapter 5 proposed a nonlinear sampled-data model considering that the input is generated by a B-spline generalized hold.

Therefore, the developed model was shown to depend on the continuous-time relative degree of the continuous-time system and the order of the hold device. The resulting model includes extra zero dynamics that are exactly equal to the asymptotic sampling zeros found in the linear case when the sampling period goes to zero. It is important to recall that even when the (asymptotic) connection with the linear case has been previously established, we have extended the results to a more general case since this characterization is valid for different types of holds. Besides, the approximate model's accuracy has been measured using the local truncation error of each element of the state vector showing that the model developed in this Thesis is more accurate than the models considered in [42] and in [81].

6.3 Applications of Linear Sampled-Data Models

In Chapter 4, we explored the use of linear sampled-data models in control applications. The core idea is that, at high frequencies, a continuous-time system of relative degree r behaves similarly to an r-th order integrator. Then, one should be able to propose a discrete-time high-gain controller for stably invertible systems that depend only on the relative degree and high-frequency gain. As a first attempt, a preliminary theoretical analysis based on Ostrowski's Theorem has been analyzed for a second-order continuous-time system to set ideas. Then, the results were extended to the discrete-time domain for fast sampling rates. In this case, the discrete-time controller is designed based on two approximate models: the first model covers the case where the closed-loop bandwidth is significantly less than the Nyquist frequency, while the second covers the case when the closed-loop bandwidth is near the Nyquist frequency, i.e., it includes the asymptotic sampling zero.

The robustness properties of these two models differ due to the presence of asymptotic sampling zeros. We note that for the closed-loop stability of the true system, when the nominal closed-loop poles approach the inverse of the sampling period, the control design must be based on an approximate model that includes the sampling zeros. Moreover, it has been shown that the results are only suitable for small sampling period.

Therefore, we designed a simple sampled-data control law for relative degree two that stabilizes the true system for the continuous and sampled-data cases. This chapter's contribution has been the robust stability analysis, for fast sampling rates, based on perturbation theory.

6.4 Future Work

Despite the results presented in this Thesis for the discretization process for nonlinear systems, there are still open problems for future research work.

Regarding linear sampled-data models, for example, in the manuscript we considered the Brunovsky form that gives the state-space description of the continuous-time system. However, such representation of the system is not unique. Thus, it could be of interest to analyze the effect of changing such description when applying the numerical integration strategy. In particular, the impact of the new representation in the nonlinear system, and therefore, in the asymptotic zero dynamics.

On the other hand, we have developed novel characterizations of the sampling zeros when considering a low-order Runge-Kutta method. However, a closed-form expression of such characterization is still needed for a more direct computation of the sampling zeros. In fact, a point of departure may be the change of the state-space representation.

In Chapter 3, we introduced the ideas of error quantification by numerical examples. Nevertheless, it could be interesting to measure the resulting sampled-data model's accuracy through the relative error in the frequency domain.

With respect to the control applications for linear systems, it is important to recall that the theoretical analysis was restricted to second-order systems with no zeros. The stably invertible continuous-time case is supported by numerical studies considering a third-order system with one zero. However, the proof of this conjecture is still needed.

An initial attempt is based on the Root Locus method, where it is assumed that the poles α_i and zeros β_i belong to a bounded region in the complex plane, such that the closed-loop poles are placed at $|\alpha_i, \beta_i| << \alpha^*$. Thus, considering a general continuous-time system having m zeros and n poles, we hypothesize that n roots are placed around α^* and the remaining are located at the origin. Then, the bounds can be obtained using the Ostrowski's Theorem. However, the later idea continues to be supported only by simulation studies.

Moreover, the obtained bounds for both, continuous and discrete-time cases are conservative compared with the actual value. Therefore, planned future work considers extending the theory to a more general higher-order systems and systems with an unstable inverse. In addition, one may expect to extend these results to the nonlinear case using, for example, Lyapunov ideas.

Continuing with the nonlinear case and following the ideas presented in Chapter 3, future work can consider extending the results of a Runge-Kutta method of order κ to the nonlinear model. On the other hand, the obtained sampled-data model is based on strong assumptions that guarantee the continuous-time system's input affine property. However, we have neglected terms containing nonlinear information that can be included in the truncated Taylor series expansion, leading to a different approximate model. In fact, Runge-Kutta methods can lead to a better discrete-time model, since under this method, the derivatives are not computed but approximated.

On the other hand, there has been ongoing research on port-Hamiltonian systems (PHS) because they allow the modeling, interconnection, and control of multi-physics systems. Hence, we believe that discretization methods can be applied to obtain an approximate model that preserves the Hamiltonian structure and properties [117]. In fact, PHS is also affine in the input. Therefore the corresponding discrete-time model can be obtained using a truncated Taylor series expansion.

Then, following the ideas presented in Chapter 5, the order of each state variable corresponds to the derivative that makes the input to explicitly appear. Once the expansion is made, the approximate model is obtained when computing the derivatives at time instants kh. Finally, the model's accuracy can be measure using the local error truncation of each element of the state vector. However, the derivatives may be challenging to solve due to the nonlinear nature of the approach. Moreover, assumptions such as those presented in Chapter 5 may lead to approximate models that do not preserve the Hamiltonian properties.

Bibliography

[1] A. Feuer and G.C. Goodwin. *Sampling in Digital Signal Processing and Control*. Birkhäuser, Boston, 1996.

[2] J.I. Yuz and G.C. Goodwin. *Sampled-data Models for Linear and Nonlinear Systems*. Springer, 2014.

[3] H. Garnier and L. Wang, editors. *Continuous-time Model Identification from Sampled Data*. Springer, 2008.

[4] T. Chen and B. Francis. *Optimal Sampled-Data Control Systems*. Springer, 1996.

[5] K.J. Åström and B. Wittenmark. *Computer Controlled Systems. Theory and Design*. Prentice Hall, Englewood Cliffs, N.J., 3er ed. edition, 1997.

[6] D. S. Laila, D. Nešić, and A. Astolfi. Sampled-data control of nonlinear systems. In *Advance Topics in Control Systems Theory.*, chapter 3. Springer-Verlag, London, 2006.

[7] W. S. Levine, editor. *The Control Handbook: Control System Fundamentals*. CRC Press, 2010.

[8] K.J. Åström and B. Wittenmark. *Computer Controlled Systems. Theory and Design*. Prentice Hall, Englewood Cliffs, N.J., 3rd edition, 1997.

[9] G.C. Kuo. *Automatic Control Systems*. Prentice Hall, 4 edition, 1982.

[10] J. Ackermann. *Sampled-Data Control Systems*. Springer-Verlag, 1985.

[11] T. Söderström. *Discrete-time stochastic systems*. Prentice Hall, first edition, 1994.

[12] K.J. Åström. *Introduction to Stochastic Control Theory*. Academic Press, New York, 1970.

[13] G.C. Goodwin, J.I. Yuz, J.C. Agüero, and M. Cea. Sampling and sampled-data models. In *American Control Conference*, Baltimore, USA, 2010.

[14] J.I. Yuz and G.C. Goodwin. Sampled-data models for stochastic nonlinear systems. In *14th IFAC Symposium on System Identification, SYSID*, Newcastle, Australia, 2006.

[15] B. Wahlberg. Limit results for sampled systems. *International Journal of Control*, 48(3):1267–1283, 1988.

[16] G.C. Goodwin, J.I. Yuz, and M.E. Salgado. Insights into the zero dynamics of sampled-data models for linear and nonlinear stochastic systems. In *European Control Conference, ECC*, Kos, Greece, 2007.

[17] G.C. Goodwin, J.C. Agüero, M.E. Cea, M Salgado, and J.I. Yuz. Sampling and sampled-data models: The interface between the continuous world and digital algorithms. *IEEE Control Systems Magazine*, 33, 2013.

[18] R.H. Middleton and G.C. Goodwin. *Digital Control and Estimation. A Unified Approach*. Prentice Hall, Englewood Cliffs, New Jersey, 1990.

[19] H. Yang, Y. Xia, P. Shi, and L. Zhao. *Analysis and Synthesis of Delta Operator Systems*. Springer-Verlag Berlin Heidelberg, 1st ed. edition, 2012.

[20] H. Yang, Y. Xia, and Q. Geng. *Analysis and Synthesis of Delta Operator Systems with Actuator Saturation*. Springer, 1st ed. edition, 2019.

[21] R.H. Middleton. Trade-offs in linear control systems design. *Automatica*, 27(2):281–292, 1991.

[22] G.C. Goodwin, R. L. Leal, D.Q. Mayne, and R.H. Middleton. Rapprochement between continuous and discrete model reference adaptive control. *Automatica*, 22(2):199 – 207, 1986.

[23] C. Sánchez, G. Goodwin, J.I Yuz, M. Serón, and D. Carrasco. Towards a simple sampled-data control law for stably invertible linear system. In *21st IFAC World Congress*, Berlin, Germany, 2020.

[24] J. Wu, G. Li, R.H. Istepanian, and J. Chu. Shift and delta operator realisations for digital controllers with finite word length considerations. *Control Theory and Applications, IEE Proceedings*, 147, 2000.

[25] R.H. Middleton and G.C. Goodwin. Improved finite word length characteristics in digital control using delta operators. *IEEE Transactions on Automatic Control*, 31(11):1015–1021, 1986.

[26] C.P. Neuman. Properties of the delta operator model of dynamic physical systems. *IEEE Transactions on Systems, Man, and Cybernetics*, 23(1):296–301, 1993.

[27] K. J. Åström, P. Hagander, and J. Sternby. Zeros of sampled systems. *Automatica*, 20(1):31–38, 1984.

[28] S. Hara, H. Katori, and R. Kondo. The relationship between real poles and real zeros in siso sampled data systems. *IEEE Transactions on Automatic Control*, 34(6):632–635, 1989.

[29] A. Braga, W. Caminhas, and C. Braga. A recursive algorithm for estimating multiple models continuous transfer function with non-uniform sampling. *International Journal of Systems Science*, 49 (6):1131–1145, 2019.

[30] J. Gillberg and L. Ljung. Frequency-domain identification of continuous-time output error models: Part II: Non-uniformly sampled data and B-spline output approximation. *Automatica*, 46(1):11 – 18, 2010.

[31] J. Gillberg and L. Ljung. Frequency-domain identification of continuous-time output error models from non-uniformly sampled data. In *14th IFAC Symposium on System Identification, SYSID*, Newcastle, Australia, 2006.

[32] N. Hori, R. Cornier, and K. Kanai. On matched pole-zero discrete-time models. *Control Theory and Applications, IEE Proceedings D*, 139:273 – 278, 06 1992.

[33] C.A. Rabbath and N. Hori. Structural interpretation of matched pole-zero discretisation. *Control Theory and Applications, IEE Proceedings*, 149:257 – 262, 08 2002.

[34] A. Mutambara. *Design and Analysis of Control Systems*. CRC Press, 1999.

[35] R. Golden. Digital filter synthesis by sampled-data transformation. *IEEE Transactions on Audio and Electroacoustics*, 16:321–329, 1968.

[36] M. J. Blachuta. On approximate pulse transfer functions. *IEEE Transactions on Automatic Control*, 44(11):2062–2067, 1999.

[37] G.C. Goodwin, J. I. Yuz, and J.C. Agüero. Relative error issues in sampled data models. In *17th IFAC World Congress*, Seoul, South Korea, 2008.

[38] E. Yucra and J.I. Yuz. Frequency domain accuracy of approximate sampled-data models. In *IFAC World Congress*, Milal, Italy, 2011.

[39] A. Isidori. *Nonlinear Control Systems*. Springer, 3rd edition, 1995.

[40] J.C. Butcher. *Numerical Methods for Ordinary Differential Equations*. John Wiley and Sons, 3er ed. edition, 2016.

[41] E. Hairer, S. Norsett, and G. Wanner. *Solving Ordinary Differential Equiations I. Nonstiff Problems*. Springer, 3er ed. edition, 2008.

[42] D. Carrasco, G. Goodwin, and J.I. Yuz. Vector measures of accuracy for sampled data models of nonlinear systems. *IEEE Transactions on Automatic Control*, 58:224–230, 2013.

[43] D. Carrasco, G.C. Goodwin, and J.I. Yuz. Sampled data models for nonlinear stochastic systems: Truncation errors and sampling zero dynamics. *IEEE Transactions on Automatic Control*, 61, 2016.

[44] R. Churchill and J. Brown. *Complex Variable and Applications*. McGraw Hill Book Company, 1984.

[45] D. G. Zill. *Differential Equations with Boundary-Value Problems*. Cengage Learning, 9th ed. edition, 2016.

[46] T. Hagiwara. Analytic study on the intrinsic zeros of sampled-data systems. *IEEE Transactions on Automatic Control*, 41(2):261–263, 1996.

[47] T. Hagiwara and M. Araki. On preservation of strong stabilizability under sampling. *IEEE Transactions on Automatic Control*, 33(11):1080–1082, 1988.

[48] W. Cleveland. First-order-hold interpolation digital-to-analog-converter with application to aircraft simulation. Technical report, National Aeronautics and Space Administration, November 1976.

[49] C. Sisemore and V. Babuška. *The Science and Engineering of Mechanical Shock*. Springer, 2019.

[50] R Bárcena, M. De la Sen, and I Sagastabeitia. Improving the stability properties of the zeros of sampled systems with fractional order hold. *Control Theory and Applications*, 147:456 – 464, 2000.

[51] M. Naumovic. A revisit to the fractional-order hold device. *Electrical Engineering*, 96:267–273, 2014.

[52] F. Hashemzadeh, A. Rezaei, and P. Jabehdar-Maralani. A new fractional order hold and its capability in frequency response and zero placement. *Journal of Applied Mathematics*, 1:1–7, 2013.

[53] M. Ou, S. Liang, T. Liu, and C. Zeng. A stability condition of zero dynamics of a discrete time systems with backward triangle sample and hold. In *2017 International Conference on Advanced Mechatronic Systems, ICAMechS*, Xiamen, China, 2017.

[54] M. Ou, S. Liang, and C. Zeng. A novel approach to stable zero dynamics of sampled-data models for nonlinear systems in backward triangle sample and hold case. *Applied Mathematics and Computation*, 355:47–60, 2019.

[55] A. Feuer and G.C. Goodwin. Generalized sample hold functions: Frequency domain analysis of robustness, sensitivity, and intersample difficulties. *IEEE Transactions on Automatic Control*, 39(5):1042–1047, 1994.

[56] P. Kabamba. Control of linear systems using generalized sampled-data hold functions. *IEEE Transactions on Automatic Control*, 32(9):772–783, 1987.

[57] J.I. Yuz, G.C. Goodwin, and H. Garnier. Generalised hold functions for fast sampling rates. In *43rd IEEE Conference on Decision and Control*, Nassau, Bahamas, 2004.

[58] I. Arriagada and J.I. Yuz. On the relationship between splines, sampling zeros and numerical integration in sampled-data models for linear systems. In *American Control Conference*, Washington, USA, 2008.

[59] J. Freudenberg, R. Middleton, and J. Braslavsky. Robustness of zero-shifting via generalized sampled-data hold functions. In *33rd IEEE Conference on Decision and Control, CDC*, Florida, USA, 1994.

[60] J. Back, J. Kim, C. Lee, G. Park, and H. Shim. Enhancement of security against zero dynamics attack via generalized hold. In *IEEE 56th Annual Conference on Decision and Control, CDC*, 2017.

[61] J. Ha and H. Shim. Study on realizable generalized hold functions as a countermeasure against zero dynamics attack. In *2019 IEEE 58th Conference on Decision and Control (CDC)*, pages 5362–5367, 2019.

[62] Z. Cai and S. Dasgupta. A note on generalized hold functions. *Systems and Control Letters*, 14:361–368, 04 1990.

[63] G. C. Goodwin and A. Feuer. Generalised sample hold functions: facts and fallacies. In *31st IEEE Conference on Decision and Control, CDC*, Tucson, USA, 1992.

[64] J. S. Freudenberg, R. H. Middleton, and J. H. Braslavsky. Robustness of zero shifting via generalized sampled-data hold functions. *IEEE Transactions on Automatic Control*, 42(12):1681–1692, 1997.

[65] C. Sánchez and J.I. Yuz. On the relationship between spline interpolation, sampling zeros and numerical integration in sampled-data models. *System & Control Letters*, 128:1–8, 2019.

[66] M.E. Salgado, J. I. Yuz, and R.A. Rojas. *Análisis de Sistemas Lineales*. Pearson Ed, 1st ed. edition, 2005.

[67] S.R. Weller, W. Moran, B. Ninness, and A.D. Pollington. Sampling zeros and the Euler-Frobenius polynomials. *IEEE Transactions on Automatic Control*, 46(2):340–343, 2001.

[68] I. J. Schoenberg. Cardinal interpolation and spline functions. *Journal of Approximation Theory*, 2:167–206, 1969.

[69] C. de Boor. *A Practical Guide to Splines*. Springer, 2001.

[70] C. de Boor. On calculating with B-splines. *Journal of Approximation Therory*, 6:50–62, 1970.

[71] M. Unser, A. Aldroubi, and M. Eden. B-spline signal processing. I. Theory. *IEEE Transactions on Signal Processing*, 41(2):821–833, 1993.

[72] H. Kano, E. Magnus, H. Nakata, and C.F. Martin. B-splines and control theory. *Applied Mathematics and Computation*, 145:263–288, 2003.

[73] J. Gillberg and L. Ljung. Frequency-domain identification of continuous-time output error models, Part I: Uniformly sampled data and frequency function approximation. *Automatica*, 46:1–10, 2010.

[74] B. Wahlberg. Limit results for sampled systems. *International Journal of Control*, 48(3):1267–1283, 1988.

[75] T. Hagiwara, T. Yuasa, and M. Araki. Stability of the limiting zeros of sampled-data systems with zero- and first- order holds. *International Journal of Control*, 58(6), 1993.

[76] M.J. Blachuta. On zeros of pulse transfer functions of systems with first-order hold. In *37th Conference on Decision and Control, CDC*, Tampa, USA, 1998.

[77] M Ishitobi. Stability of zeros of sampled system with fractional order hold. *IEE Proceedings-Control Theory and Applications*, 143(3):296–300, 1996.

[78] M.J. Blachuta. On fast sampling zeros of systems with fractional order hold. In *American Control Conference*, Arlington, USA, 2001.

[79] W. Kang. Bifurcation and normal form of nonlinear control systems, part I. *SIAM Journal on Control and Optimization*, 36:193–212, 1998.

[80] K Passino and P. Antsaklis. Inverse stable sampled low-pass systems. *International Journal of Control*, 47(6):1905–1913, 1988.

[81] J. I. Yuz and G. C. Goodwin. On sampled data models for nonlinear systems. *IEEE Transactions on Automatic Control*, 50(10):1477–1489, 2005.

[82] D. Griffiths and D.J. Higham. *Numerical Methods for Ordinary Differential Equations. Initial Value Problems.* Springer, 2010.

[83] A. Iserles. *A First Course in the Numerical Analysis of Differential Equations.* Cambridge University Press, 2nd ed. edition, 2008.

[84] R.J. LeVeque. *Finite Difference Methods for Ordinary and Partial Differential Equations: Steady-State and Time-Dependent Problems.* SIAM, 2007.

[85] K. W. Morton and D. F. Mayers. *Numerical Solution of Partial Differential Equations.* Cambridge University Press, 2nd ed. edition, 2005.

[86] Y. Jeon, S. Bu, and S. Bak. A comparison of multi-step and multi-stage methods. *International Journal of Circuits, Systems and Signal Processing*, 11:250–253, 2017.

[87] P. Moin. *Fundamentals of Engineering Numerical Analysis.* Cambridge University Press, 2nd ed. edition, 2010.

[88] M Vidyasagar. *Nonlinear System Analysis.* Prentice Hall, 2nd ed. edition, 1993.

[89] M. A. Henson and D. E. Seborg. *Nonlinear Process Control.* Prentice Hall, 1997.

[90] K.M. Hangos, J. Bokor, and G. Szederkényi. *Analysis and Control of Nonlinear Process Systems.* Springer, 1st ed. edition, 2004.

[91] D.S. Naidu, S.O., and K.L. Moore. *Modeling, Sensing and Control of Gas Metal Arc Welding*. Elsevier, 2013.

[92] H.K. Khalil. *Nonlinear Systems*. Pearson, 3rd ed. edition, 2002.

[93] Y.A. Kuznetsov. *Elements of Applied bifurcation Theory*. Springer, 1998.

[94] R. Marino, W. Respondek, and A. J. Van Der Schaft. Equivalence of nonlinear systems to input-output prime forms. *SIAM Journal on Control and Optimization*, 32:387–407, 1994.

[95] W. Kang. Bifurcation and normal form of nonlinear control systems, part II. *SIAM Journal on Control and Optimization*, 36:213–232, 1998.

[96] M. Mueller. Normal form for linear systems with respect to its vector relative degree. *Linear Albegra and its Applications*, 430:1292–1312, 2009.

[97] D. Nešić, A.R. Teel, and P.V. Kokotović. Sufficient conditions for stabilization of sampled-data nonlinear systems via discrete-time approximations. *Systems and Control Letters*, 38:259–270, 1999.

[98] L. Jezequiel and C. Lamarque. Analysis of nonlinear dynamical systems by the normal form theory. *Journal of Sound and Vibration*, 149:429–459, 1991.

[99] P.C. Kunstmann, B. Li, and C. Lubich. Runge-Kutta time discretization of nonlinear parabolic equations studied via discrete maximal parabolic regularity. *Foundations of Computational Mathematics*, pages 1–22, 2017.

[100] L. Grüne and D. Nešić. Optimization-based stabilization of sampled-data nonlinear systems via their approximate discrete-time models. *SIAM Journal on Control and Optimization*, 42:98 – 122, 2003.

[101] S. Monaco and D. Normand-Cyrot. Zero dynamics of sampled nonlinear systems. *Systems and Control Letters*, 11:229–234, 1988.

[102] N. Kazantzis and C. Kravaris. System theoretic properties of sampled-data representations of nonlinear systems obtained via Taylor-Lie series. *International Journal of Control*, 67:997 – 1020, 1997.

[103] M. Ishitobi and M. Nishi. Zero dynamics of sampled-data models for nonlinear systems. In *American Control Conference*, Washington, USA, 2008.

[104] S. Liang, C. Zeng, M. Ishitobi, and J. Zhong. The roles of sampling zero dynamics in the discrete-time models for linear and nonlinear systems. In *33rd Chinese Control Conference*, Nanjing, China, July 2014.

[105] C. Sánchez and J.I. Yuz. B-spline generalized hold for nonlinear sampled-data systems. In *IEEE Conference on Decision and Control*, Nice, France, December 2019.

[106] S. Monaco and D. Normand-Cyrot. A unified representation for nonlinear discrete-time and sampled dynamics. *Journal of Mathematics Systems, Estimation, and Control*, 7(4):477–503, 1997.

[107] C. Califano, S. Monaco, and D. Normand-Cyrot. On the discrete-time normal form. *IEEE Transactions on Automatic Control*, 43(11):1654–1658, 1998.

[108] C. Silva and J.I. Yuz. On sampled-data models for model predictive control. In *36th Annual Conference of the IEEE Industrial Electronics Society*, pages 2966–2971, Glendale, Arizona, USA, November 2010.

[109] G.C. Goodwin, S.F. Graebe, and M.E. Salgado. *Control System Design*. Prentice Hall, New Jersey, 2001.

[110] S. Gayaka, L. Lu, and B. Yao. Global stabilization of a chain of integrators with input saturation and disturbances: A new approach. *Automatica*, 48:1389–1396, 2012.

[111] B. Zhou and G.R. Duan. A novel nested non-linear feedback law for global stabilisation of linear systems with bounded controls. *International Journal of Control*, 81(9):1352–1363, 2008.

[112] R. Middleton. Trade-off in linear control systems. *Automatica*, 27:281–292, 1991.

[113] A.M Ostrowski. *Solution of Equations in Euclidean and Banach Spaces*. Academic Press, 1973.

[114] J.C. Doyle, B. A. Francis, and A.R. Tannenbaum. *Feedback Control Theory*. Macmillan Publishing Co, 1990.

[115] L. Elsner. On the variation of the spectra of matrices. *Linear Algebra and its Aplications*, 47:127–138, 1982.

[116] X. Yang. Necessary conditions of Hurwitz polynomials. *Linear Algebra and its Applications*, 359:21–27, 01 2003.

[117] A. van der Schaft and D. Jeltsema. *A Port Hamiltonian Systems Theory: An Introductory Overview*. Foundations and Trends in Systems and Control, 2014.

List of Figures

List of Tables